

**Polymer/Nano-Inorganic Composite Proton Exchange
Membranes for Direct Methanol Fuel Cell Application**

Hongze Luo

Submitted in fulfillment of the requirements for the degree of MSc in Chemistry
in the Department of Chemistry, University of the Western Cape

Supervisor: Prof. Vladimir M. Linkov

Dr. Ji Shan

April 2005

KEYWORDS

Fuel Cell

Direct Methanol Fuel Cell (DMFC)

Proton exchange membrane (PEM)

Proton conductivity

Water uptake

Phosphorized zirconium oxide nano-particles (ZP)

Sulfonated poly ether ether ketone (SPEEK)

Methanol permeability (methanol cross-over)

Degree of sulfonation (DS)

Membrane-electrode assembly (MEA)

Declaration

I declare that *Polymer/Nano-Inorganic Composite Proton Exchange Membranes for Direct Methanol Fuel Cell Application* is my own work, and that it has not been submitted for any degree or examination in any other university, and that all sources I have used or quoted have been indicated and acknowledged by complete references.

Hongze Luo

October, 2004

Signed:

Acknowledgements

I would like to express my sincere gratitude to all those who helped me with my study at UWC. I wish to thank the following people:

- ✧ Prof. Vladimir Linkov for affording me the opportunity to be part of his research group;
- ✧ Supervisor Dr. Ji Shan, for his friendship, guidance throughout and constant advice, and most especially for his assistance with the many technical aspects of membrane technology;
- ✧ Dr. G. Vaivars, for his guidance throughout and especially his assistance with ZP;
- ✧ Dr. Z. Wang, for his assistance with the DMFC testing and constant support;
- ✧ Dr. Y. Liu for her assistance with the FTIR measurements;
- ✧ Prof. Key, staff and members of the chemistry department of the University of Western Cape for their assistance;
- ✧ L. Patrick, Ilie, Barbara Rodgers and Amanda Foster for their assistance in the laboratory;
- ✧ The Inorganic Porous Media Group, especially Mmalewane Modibedi and Nicollete Hendricks for their encouragement;
- ✧ Nolan and Basil in the Physics Department for their assistance with the SEM measurements;
- ✧ My parents and younger brother, for their patience, unending support, love and understanding during the time of my studies.

LIST OF ABBREVIATIONS

AFC	Alkaline Fuel Cell
DMAc	N, N Dimethylacetamide
DMFC	Direct Methanol Fuel Cell
DS	Degree of Sulfonation
FTIR	Fourier Transform Infra-Red
GC	Gas Chromatograph
HHV	High Heat Value
H ₂ -PEMFC	H ₂ Proton Exchange Membrane Fuel Cell
I	Current density [A/cm ²]
ICE	Internal Combustion Engine
IEC	Ion Exchange Capacity
l	Membrane thickness [cm]
MCFC	Moltern Carbonate Fuel Cell
MEA	Membrane Electrode Assembly
Nafion/ZP	Nafion/ phosphorized zirconium oxide nano-particles
P	Methanol permeability [cm ² /s]
PAFC	Phosphoric Acid Fuel Cell
PBI	Polybenzimidazole
PEEK	Poly Ether Ether Ketone
PEM	Proton Exchange Membrane
PEMFC	Proton Exchange Membrane Fuel Cell
PSU	Polysulfone
PTFE	Polytetrafluoroethylene
R	Resistance [Ω]
S	Surface area [cm ²]
SEM	Scanning Electron Microscopy
SOFC	Solid Oxide Fuel Cell
SPEEK	Sulfonated Poly Ether Ether Ketone
SPEEK/ZP	Sulfonated Poly Ether Ether Ketone/ Phosphorized Zirconium oxide nano-particles
SPI	Sulfonated Polyimide
TEM	Transmission Electron Microscopy
TEOS	Tetraethyl Orthosilicate
TGA	Thermal Gravimetric Analysis
V	Voltage [V]
XRD	X-Ray Diffraction
ZP	Phosphorized Zirconium oxide nano-particles
σ	Proton conductivity [S/cm]

Abstract

The proton exchange membrane (PEM) is one key component of direct methanol fuel cells (DMFCs), which has double functions of conducting protons, separating fuels and oxidant. At present, the performance and price of sulfonic acid PEMs used in DMFCs are deeply concerned. In order to reduce membrane's cost and improve performance of Nafion membrane, three different kinds of membranes have been studied in this thesis.

Chapter 3, Chapter 4 and Chapter 5 present those three different but related types of membranes, respectively.

In Chapter 3, sulfonated poly(ether ether ketone) (SPEEK) was synthesized by sulfonating poly(ether ether ketone) with 98% sulfuric acid.

SPEEK membranes possess good thermal stability and mechanical properties, low methanol permeability ($P = 4.00 \times 10^{-9}$ cm²/s at DS = 0.30) and the proton conductivity ($\sigma = 2.5 \times 10^{-2}$ S/cm at DS = 0.82). The proton conductivity of the SPEEK membranes, water uptake and methanol permeability were increased with increasing DS and temperature.

In Chapter 4, SPEEK/phosphorized zirconium oxide nano-particles (ZP) composite membranes were prepared by incorporating various ratios of ZP into SPEEK. SPEEK/ZP membranes showed many improved properties. Key amongst these are

increased conductivity, reduced water uptake and the 28% methanol permeability reduction of a membrane with 5 wt% of ZP compared with that of SPEEK membrane, it is 12 times lower than that of Nafion[®] 117. A DMFC testing result showed a promising performance. SPEEK/ZP composite membrane with low incorporated ZP content is considered for DMFC application.

In Chapter5, a series of Nafion/ZP composite membranes were also prepared and investigated to overcome the shortcomings of Nafion[®]. The incorporated ZP increased the proton conductivity and maintained at high temperature. The conductivity of the composite membranes exceeded 2.2×10^{-2} S/cm at room temperature and reached a value of 8.3×10^{-2} S/cm at 100°C for Nafion/ZP (70% ZP) membrane. The composite membrane with low amount of ZP incorporated shown lower methanol crossover comparing to Nafion. Nafion/ZP membrane can be used as candidate proton exchange membranes for the high temperature operation of the DMFCs.

TABLE OF CONTENTS

TATLE PAGE.....	viii
KEYWORDS	ii
DECLARATION	viii
ACKNOWLEDGEMENTS	viii
LIST OF ABBREVIATIONS	viii
ABSTRACT	vi
TABLE OF CONTENTS	viii
LIST OF FIGURES	viii
LIST OF TABLES	viii
CHAPTER 1	
Introduction	
1.1 Background	1
1.2 Objectives.....	2
1.3 Steps towards attaining solutions	3
CHAPTER 2	
Literature review	
2.1. Background of Energy resources	5
2.2. History of Fuel Cell Technology.....	6
2.3. Advantages of Fuel Cells compared to conventional technologies	7
2.4. Types of fuel cells	8
2.5. Proton Exchange Membrane Fuel Cells (PEMFC).....	10
2.5.1. H ₂ -Proton Exchange Membrane Fuel Cell.....	11
2.5.2. Direct Methanol Fuel Cell (DMFC).....	12
2.5.2.1. Advantages and comparison of DMFC with H ₂ -PEMFC	12
2.5.2.2. Principle of Direct Methanol Fuel Cell.....	13
2.5.2.3. Components of a Direct Methanol Fuel Cell	14
2.5.2.4. Membrane electrode assembly (MEA)	15
2.6. Proton Exchange Membrane Families	18
2.6.1. Perfluorinated membranes and composites	19
2.6.1.1. Homogeneous perfluorinated membranes.....	19
2.6.1.2. Composites of perfluorinated ionomers with heteropolyacids ionomer	21
2.6.1.3. Micro-reinforced perfluorinated composite membranes	21
2.6.1.4. Partially fluorinated membranes	22
2.6.2. Non-Perfluorinated membranes	23

2.6.2.1. Sulfonated polymers.....	23
2.6.2.2. Polybenzimidazole-based membranes	28
2.6.2.3. Crosslinked membranes based on sulfonated polymer	29
2.7.3. Composite membranes	30
2.7. Membrane morphology	32
2.7.1. Nafion [®] (Sulfonated fluoropolymer membrane morphology)	32
2.7.2. Other membranes	36
2.8. The significance of the review	38

CHAPTER 3

Preparation and Characterization of SPEEK membranes

3.1. Introduction	39
3.2. Experimental	41
3.2.1. Chemical materials.....	41
3.2.2. Sulfonating PEEK	41
3.2.3. Preparation of SPEEK membranes	42
3.2.4. Characterization of the SPEEK membranes	43
3.2.4.1. FTIR study	43
3.2.4.2. Thermal-gravimetric analysis (TGA).....	43
3.2.4.3. Water uptake	44
3.2.4.4. Proton conductivity	45
3.2.4.5. Measurement of methanol permeability.....	46
3.3. Results and discussions	49
3.3.1. Thermal property and degree of sulfonation.....	49
3.3.2. Solubility of SPEEK	53
3.3.3. FTIR study	53
3.3.4. Methanol permeability (methanol cross-over)	56
3.3.5. Water uptake	57
3.3.6. Proton conductivity	58
3.4. Summary	61

CHAPTER 4

Preparation and Characterization of SPEEK/ZP composite membranes

4.1. Introduction	62
4.2. Experimental	64
4.2.1. Chemical materials.....	64
4.2.2. Preparation of composite membranes	64
4.2.2.1. Preparation of ZP	64
4.2.2.2. Pre-treatment of SPEEK	65

4.2.2.3. Membrane preparation	65
4.2.3. Characterization of SPEEK/ZP composite membranes	66
4.2.3.1. Fourier transform infrared (FTIR) study	66
4.2.3.2. X-ray diffraction (XRD)	67
4.2.3.3. Thermo-gravimetric analysis (TGA)	67
4.2.3.4. Water uptake	67
4.2.3.5. Measurement of methanol permeability.....	68
4.2.3.6. Scanning electron microscope (SEM) (Study of surface morphology) ...	68
4.2.3.7. Electrochemical measurements (Cyclic voltammetry: Electrochemical stability)	69
4.2.3.8. Measurement of proton conductivity	69
4.2.4. DMFC testing.....	69
4.2.4.1. Preparation of the membrane-electrode assembly (MEA)	69
4.2.4.2. Assembly of single cell and test.....	70
4.3. Results and discussions.....	72
4.3.1. Fourier transform infrared (FTIR) spectroscopy.....	72
4.3.2. X- ray diffraction (XRD)	74
4.3.3. Themo-stability study by thermo-gravimetric analysis (TGA)	75
4.3.4. Water uptake	76
4.3.5. Methanol permeability	77
4.3.6. Morphology.....	79
4.3.7. Electrochemical stability.....	82
4.3.8. Proton conductivity	83
4.3.9. DMFC performance	85
4.4. Summary	87

CHAPTER 5

Preparation and Characterization of Nafion/ZP composite membrane

5.1. Introduction	89
5.2. Experimental	91
5.2.1. Preparation of ZP	91
5.2.2. Preparation of composite membranes	91
5.2.3. Characterization of the membranes.....	92
5.2.3.1. X-ray diffraction (XRD)	92
5.2.3.2. Water uptake	92
5.2.3.3. Methanol permeability measurements	92
5.2.3.4. Thermo-gravimetry analysis (TGA)	92
5.2.3.5. Proton conductivity	92
5.2.3.6. Morphology by SEM.....	92

Table of contents

5.3. Results and discussion	93
5.3.1. Study by XRD	93
5.3.2. Scanning electron microscopy	94
5.3.3. Water uptake	96
5.3.4. Proton conductivity	97
5.3.5. Methanol permeability	100
5.4. Summary	104
 CHAPTER 6	
Conclusions and recommendations	
6.1. Conclusions	105
6.2. recommendations	107
 REFERENCES	 108

LIST OF FIGURES

Chapter 2	
Figure 2.1:	Basic description of a DMFC operation 14
Figure 2.2:	A view of a DMFC stack and an exploded view of a single cell 15
Figure 2.3:	Chemical structure of Nafion [®] membrane 19
Figure 2.4:	Chemical structure of Dow ionomer membrane..... 20
Figure 2.5:	Chemical structure of sulfonated polyetherketone 25
Figure 2.6:	Poly[2,20-(m-phenylene)-5,50-benzimidazole], PBI 28
Figure 2.7:	Cluster-network model for Nafion [®] membrane 33
Figure 2.8:	A: Three region structural model for Nafion [®] B: Schematic representation of microstructure of Nafion [®] 34
Figure 2.9:	Schematic of membrane showing the interconnecting channel swollen 35
Figure 2.10:	Schematic of a membrane showing the collapsed interconnecting channel 35
Figure 2.11:	Schematic representation of the microstructure of Nafion [®] and a sulfonated polyetherketone membrane 37
Chapter 3	
Figure 3.1:	Schematic representation of the cell for measuring conductivity..... 45
Figure 3.2:	Schematic diagram of methanol permeability measurement..... 47
Figure 3.3:	Chemical structure of PEEK 49
Figure 3.4:	TGA curves of PEEK 50
Figure 3.5:	TGA curves of SPEEK..... 51
Figure 3.6:	Degree of sulfonation (DS) of SPEEK with the sulfonation time..... 53
Figure 3.7:	Comparative FTIR spectra of PEEK and sulfonated PEEK..... 54
Figure 3.8:	Structure and atom numbering of SPEEK..... 56
Figure 3.9:	Influence of DS on methanol permeability..... 57
Figure 3.10:	Water uptake as a function of DS at room temperature and 80°C 58
Figure 3.11:	Conductivity of the membranes with different DS..... 59
Chapter 4	
Figure 4.1:	The procedures of membrane-electrode assembly 70
Figure 4.2:	Lynntech endplates 71
Figure 4.3:	Schematic overview of the experimental setup for DMFC testing 71
Figure 4.4:	FTIR of ZrO ₂ and ZP 73
Figure 4.5:	FTIR of SPEEK, ZP and composite membrane 73

List of figures

Figure 4.6: The XRD patterns of nano-sized ZrO ₂ and ZP	74
Figure 4.7: Thermo-gravimetric curves of PEEK, SPEEK and SPEEK/ZP	75
Figure 4.8: Water uptake of the membranes with different ZP content.....	77
Figure 4.9: Effect of incorporated ZP content on methanol permeability	78
Figure 4.10: SEM micrographs of membranes	81
Figure 4.11: Cyclic voltammetry of SPEEK/ZP composite membrane.....	82
Figure 4.12: Proton conductivity of SPEEK/ZP composite membranes as a function of temperature	83
Figure 4.13: Effect of ZP content on proton conductivity at room temperature.....	84
Figure 4.14: Effect of ZP content on proton conductivity at 100 °C	84
Figure 4.15: Discharge curve of a single DMFC	86
Figure 4.16: SEM cross-section of MEA.....	87
Chapter 5	
Figure 5.1: XRD patterns of ZrO ₂ and various Nafion/ZP composite membranes	94
Figure 5.2: SEM of composite membranes.....	95
Figure 5.3: Water uptake of Nafion/ZP composite membranes as a function of temperature.....	97
Figure 5.4: Conductivity of Nafion/ZP membranes at room temperature and 100% humidity	98
Figure 5.5: Effect of different ZP content on the conductivity as a function of temperature.....	99
Figure 5.6: The methanol permeability of Nafion and Nafion/ZP composite membranes	101
Figure 5.7: TEM of nano-sized ZrO ₂ and ZP.....	103

List of tables

Table 2.1: Types of Fuel Cells	9
Table 3.1: Chemical materials.....	41
Table 3.2: HP 5890 parameters.....	48
Table 3.3: The properties of SPEEK membranes	52
Table 4.1: Chemical materials.....	64
Table 4.2: The specifications and working parameters of XRD.....	67
Table 4.3: Operating parameters of SEM	68
Table 4.4: present properties of the membranes	77

CHAPTER 1

Introduction

1.1. Background

Fuel cells are electrochemical energy converters, transforming chemical energy directly into electricity. Due to their many benefits, they are forming an attractive new technology of electricity generation. In the next few years, strides in fuel cell technology will forever change our concept of alternative energy systems and will become the driver of the next growth wave of the world's economy ^[1]. As well as offering a high theoretical efficiency, especially at low temperatures, fuel cells emit low or zero levels of pollutants. They can run on a wide range of fuels –from the gaseous, such as hydrogen and natural gas to the liquid fuels such as methanol and gasoline ^[2].

DMFCs use methanol as the fuel. Methanol is a low-cost liquid fuel having high electrochemical activity. It has a high energy density with respect to its volume, which allows for greater efficiency over traditional combustion engines. Presently, DMFCs are becoming very attractive for transportation and portable applications as they offer important advantages such as elimination of fuel reforming, ease of refueling, and simplified system design ^[3].

Proton exchange membranes play the major role in DMFCs. They effect the performance and the cost of DMFCs. Since, the proton exchange membranes based on perfluorinated polymer, such as Nafion[®] membranes, exhibit high proton conductivity and stability^[4], they are widely used as the electrolyte.

However, the high methanol permeability (crossover) is the major drawback of Nafion[®]. The methanol crossover or diffusion across the polymer exchange membrane from the anode to the cathode in the DMFC causes loss of fuel, reduced cathode voltage and excess thermal load in the cell. It strictly limits the performance of the DMFC^[5-9]. Furthermore, the high price of fluorine-based Nafion[®] is the major factor influencing the cost of the DMFC system. The commercialization of DMFCs is thus limited by the high cost of available perfluorinated membranes^[10, 11]. Therefore, an important task is the development of cheap membranes with low methanol crossover.

1.2. Objectives

The main objective of this project is to develop an inexpensive proton exchange membrane with low methanol crossover and high conductivity. The main focus of this study includes:

1. A search for cheaper membrane non-perfluorinated materials.
2. Preparation of membranes, and developing effective membrane synthesis methods.
3. Modification of the membrane structure to improve the properties of the membrane.
4. Characterizing the properties of the prepared membrane using different techniques.
5. Assembling the single cell of a DMFC using synthesized membrane, and evaluating its performance and its commercial potential.
6. To modify the existing Nafion[®] membrane to overcome its shortcomings.

1.3. Steps towards attaining solutions

1. According to the literature review, the basic starting material identified is SPEEK.
2. Sulfonating PEEK to various levels and casting the membranes with the prepared SPEEK. Chapter 3 introduces a detailed preparation of SPEEK, preparation of SPEEK membranes, their characterizations, results and discussions.
3. Incorporating phosphorized zirconium oxide nano-particles (which are nano-sized inorganic proton conductors) into SPEEK for improving the properties of SPEEK membranes. Chapter 4 presents a detailed synthesis of SPEEK/ZP membranes

including preparation of ZP, characterization of SPEEK/ZP composite membranes, the testing of a DMFC using prepared SPEEK/ZP membrane, results and discussion.

4. Incorporating various ratio of ZP into Nafion to prepare a series of Nafion/ZP composite membranes which are expected to overcome the technical shortcomings of Nafion membrane. Chapter 5 gives a detailed preparation of Nafion/ZP composite membranes, characterization of Nafion/ZP membrane, results and discussions.

CHAPTER 2 Literature Review

2.1. Background of Energy resources

The increase in energy usage (especially coal, crude oil, natural gas) for every citizen in the world has increased rapidly. Fossil energy resources will be used up within just a few generations if present usage levels are sustained and the availability of energy resources globally is becoming a key issue for the future.

Pollution arising from the current techniques of energy use is a major problem and newer more efficient and clean techniques are required.

Fuel cells have gained popular recognition and are under serious consideration as an economically and technically viable power source. They are considered a prime candidate for the future — being clean, quiet, and efficient.

According to President George Bush, speaking from the White House Lawn, February 25, 2002, *“We happen to believe that fuel cells are the wave of the future... we need to have a focused effort to bring fuel cells to market, and that’s exactly what my administration is dedicated to do.”* ^[12]

2.2. History of Fuel Cell Technology

The origin of fuel cell technology in 1839, is credited to William Robert Grove (1811-1896) who was a British jurist and amateur physicist ^[13, 14]. Ludwig Mond (1839-1909) with assistant Carl Langer conducted experiments with a hydrogen fuel cell in 1888 that produced 6 amps per square foot at 0.73 volts ^[15]. Francis Thomas Bacon invented the first alkaline fuel cell (AFC) in 1932 ^[16]. 27 years later, he made a 5 kw fuel cell for practical application.

From 1839, it took 120 years until NASA demonstrated some potential applications in providing power during space flight. During that time, the first PEMFC was invented and developed ^[17, 18]. As a result of these successes, industry recognized the commercial potential of fuel cells in the 1960s, but encountered technical barriers and high investment costs. Since 1984, the Office of Transportation Technologies at the U.S. Department of Energy has been supporting research and development of fuel cell technology ^[19]. Hundreds of companies around the world are working towards making fuel cell technology pay off. In 1993, Ballard Corporation made the first fuel cell car in Canada. Just as in the commercialization of the electric light bulb nearly one hundred years ago, today's companies are being driven by technical, economic, and social forces such as high performance characteristics, reliability, durability, low cost, and environmental benefits ^[20].

2.3. Advantages of Fuel Cells compared to conventional technologies

Fuel cells are not Carnot cycle (thermal energy based) engines ^[21]. Since the fuel is converted directly to electricity, a fuel cell has the potential to operate at much higher efficiencies than in conventional energy conversion processes, thereby extracting more electricity from the same amount of fuel, while providing the heat of condensation of the water vapour in the products. Fuel cells have low emission profiles. If a hydrogen fuel is used, the only waste product is water. Fuel cells are mechanically ideal because these devices have no moving parts thereby making them quiet and reliable sources of power.

In principle, a fuel cell operates like a battery ^[22, 23]. Unlike a battery, a fuel cell does not run down or require recharging. A fuel cell will be able to continually generate energy as long as fuel and the oxidant are provided to the cell. This is distinctly different from typical batteries, which are merely energy storage devices. Since it is a storage appliance, the battery is dead (or discharged) when the stored reactants are exhausted. The fuel for fuel cells is stored external to the actual device, and therefore, can not become internally depleted ^[24, 25].

2.4. Types of fuel cells

Fuel cell types are generally classified by different electrolyte material. The electrolyte is the substance between the positive and negative electrode, acting as the conductor (but it does not conduct electrons) for the ion exchange that produces electrical current ^[26]. There are five kinds of fuel cell undergoing study (Table 2.1), development and demonstration, in various stages of commercial availability. These five types of fuel cell are significantly different from each other in many respects that the key distinguishing feature is the electrolyte material. All fuel cells have the same basic operating principle.

Table 2.1: Types of Fuel Cells^[27, 28]

Type	Alkaline Fuel Cell (AFC)	Molten Carbonate fuel cells (MCFC)	Phosphoric Acid Fuel Cells (PAFC)	Solid Oxide fuel cells (SOFC)	Proton Exchange Membrane Fuel Cells (PEMFC)
Type of electrolyte	Typically aqueous KOH solution	Typically, molten $\text{Li}_2\text{CO}_3/\text{K}_2\text{CO}_3$ eutectics	H_3PO_4 solutions	Stabilized ceramic matrix with free oxide ions	Proton exchange membrane
Typical construction	Plastic, metal	High temp metals, porous ceramic	Carbon, porous ceramics	Ceramic, high temp metals	Plastic, metal, or carbon
Operational temperature	(60-260°C)	(650-700°C)	(150-210°C)	(650-1000°C)	(60-120°C)
Primary contaminate sensitivities	CO, CO_2 , and Sulfur	Sulfur	CO < 1%, Sulfur	Sulfur	CO, Sulfur, and NH_3
Applications	Military space	Electric utility	Electric utility, transportation	Electric utility	Electric utility, portable power, transportation
Advantages	Cathode reaction faster in alkaline electrolyte — therefore high performance	High temperature advantages	Up to 85 % efficiency in co-generation of electricity and heat. Impure H_2 as fuel	High temperature advantages. Solid electrolyte advantages	Solid electrolyte reduces corrosion & management problems. Low temperature. Quick start-up
Disadvantages	Expensive removal of CO_2 from fuel and air streams required	High temperature enhances corrosion and breakdown of cell components	Pt catalyst. Low current and power. Large size.	High temperature enhances breakdown of cell components	Low temperature requires expensive catalysts. High sensitivity to fuel impurities

2.5. Proton Exchange Membrane Fuel Cells (PEMFC)

PEMFCs offer high energy conversion efficiency, at operating temperatures $< 100^{\circ}\text{C}$, which can aid rapid start-up^[29]. These traits and the ability to rapidly change power output are some of the characteristics that make the PEMFCs the most promising fuel cell technique for large scale application in, for example, portable electronics, automobiles or stationary power supplies^[30]. H_2 -PEMFC and DMFC are classified as PEMFC because they all use a solid proton exchange membrane as the electrolyte. The membrane is an excellent proton conductor when it is saturated with water, but it does not conduct electrons. To achieve high efficiency in PEMFCs, the following membrane properties are required: (a) chemical and electrochemical stability under operating conditions^[31]; (b) mechanical strength and stability; (c) compatibility with and good adhesion to the components of the PEMFC; (d) extremely low permeability to the reactants (H_2 , methanol, O_2) to maximize coulombic efficiency; (e) high electrolyte transport to maintain uniform electrolyte content and to prevent local drying; (f) high proton conductivity to support high currents with minimal resistive losses and zero electronic conductivity; (g) production costs compatible with the intended application.

The main difference between the DMFC and the H_2 -PEMFC is the type of fuel used for the production of electrical power: methanol in the case of DMFC and H_2 in

the case of H₂-PEMFC.

2.5.1. H₂-Proton Exchange Membrane Fuel Cell

The first H₂-PEMFC device was developed in the 1960's by the General Electric Company for use as auxiliary power sources in the Gemini space missions^[17, 18, 32]. It emits no environmental pollutants. The H₂-PEMFC uses Platinum (Pt) catalyst and hydrogen fuel for the anode electrode and Pt and air or O₂ for the cathode electrode. Pt is extremely sensitive to CO poisoning^[33-36]. So, their fuels must be purified. Pure hydrogen fuel cells give the best performance in H₂-PEMFCs. But, because of hydrogen storage and transportation problems, alternate fuels have been sought.

According to Dr. Ferdinand Panik (DaimlerChrysler Fuel Cell Project Head) following the Cross-Country Trek of Methanol-Fueled NECAR 5, June 4, 2002;

“Hydrogen is an ideal fuel for fuel cell applications, but the problem with hydrogen is storing it on-board the vehicle. I don't believe we will find a solution in the next few years, so in my opinion, hydrogen will be limited to fleets with limited range. For individual transportation, I believe we need a liquid fuel and methanol is an excellent hydrogen carrier.”^[37]

2.5.2. Direct Methanol Fuel Cell (DMFC)

2.5.2.1. Advantages and comparison of DMFC with H₂-PEMFC

The alternative PEMFC is DMFC. DMFC technology has become widely accepted as a viable fuel cell technology^[38], and DMFCs have been successfully demonstrated in powering cars, mobile phones and laptop computers^[39]. DMFCs will be widely used in future years. In a DMFC system, liquid methanol is fed directly into the fuel cell without the intermediate step of reforming the fuel into hydrogen. Methanol is a cheap liquid at room temperature, easy to store, has high energy density and can be generated from a variety of sources such as natural gas, coal and even biomass. It also is biodegradable. Furthermore, it is not corrosive for the frame of the DMFC. DMFC offers to many applications a technology with endless possibilities.

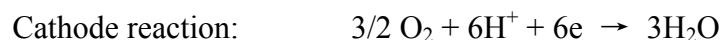
Comparing with the catalyst of H₂-PEMFC, in addition to platinum, other catalysts like ruthenium (Ru) have to be added to break methanol bond in the anodic reaction. The electrolyte and the operating temperature in DMFCs are basically the same as those used in H₂-PEMFCs, which would typically operate in a temperature range of 50 - 100 °C^[40]. Higher efficiencies are achieved at higher temperatures. The main difference is the anode reaction where methanol is oxidized instead of hydrogen as in the H₂-PEMFC. DMFC uses catalysts and a methanol solution (typically 1-2 M) at the anode electrode, Pt catalyst and air or O₂ at the cathode electrode^[41]. The

electrochemical oxidation reaction of methanol is more complicated than the oxidation reaction of hydrogen.

2.5.2.2. Principle of operating of the Direct Methanol Fuel Cell

A DMFC is comprised of an anode (which is negative electrode that repels electrons) on one side of an electrolyte (membrane) in the center with a cathode on the other side. A methanol and water mixture is fed to the anode catalyst where the catalyst particles present in the anode help to separate the methanol molecule into hydrogen atoms and carbon dioxide (CO₂) (See Figure 2.1). The separated hydrogen atoms are then typically stripped of their electrons to form protons, and passed through the membrane to the cathode side of the cell ^[42]. At the cathode catalyst, the protons react with the oxygen in air to form water minus an electron ^[43]. By connecting a conductive wire from the anode to the cathode side, the electrons stripped from the hydrogen atoms on the anode side can travel to the cathode side and combine with the electron deficient species.

The reaction of the DMFC:



For the formation of the final product - CO_2 - water is required. The six electrons are passing the load resistance of the outer circuit and are consumed at the cathode together with six protons.

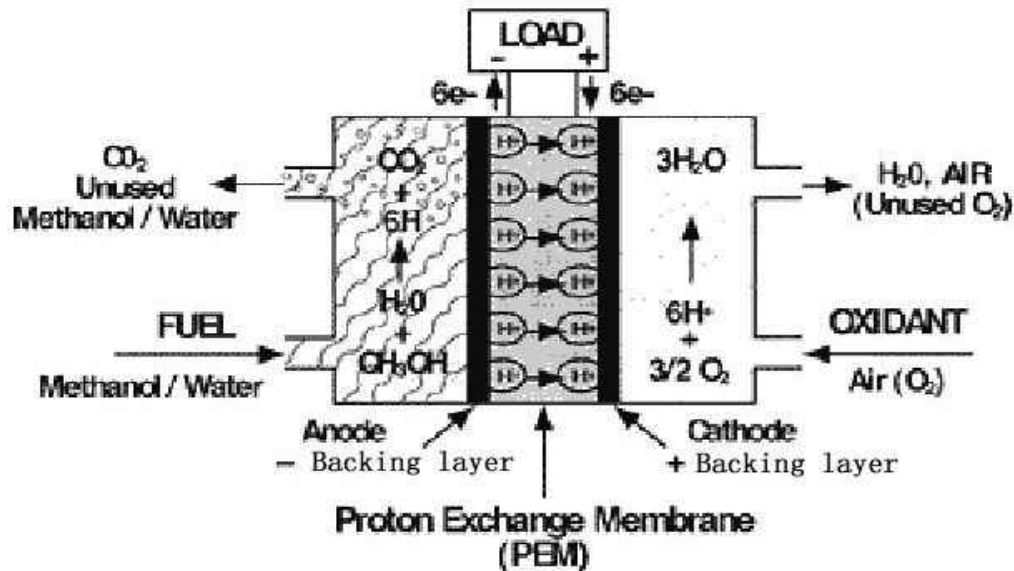


Figure 2.1: Basic description of a Direct Methanol Fuel Cell operation ^[44]

2.5.2.3. Components of a Direct Methanol Fuel Cell

An exploded view of a DMFC stack is presented in Figure 2.2. A single cell is the basic unit of a DMFC stack which consists of many individual cells to produce electricity. The MEA together with the plates make up a single DMFC cell which consists of a proton exchange membrane and two electrodes ^[45]. A single cell only produces about 1 volt ^[44]. A stack electrically connects many single cells in series or parallel to produce the overall voltage and current levels desired. The plates serve as

the electrical connections between individual cells and serve as the channels through which fuel and oxidant can flow. The number of fuel cells connected in series in the stack determines the stack voltage. The total surface area of the cells determines the total current produced. Additional components are required for electrical connections and/or insulation and the flow of methanol, water, CO₂, oxidant.

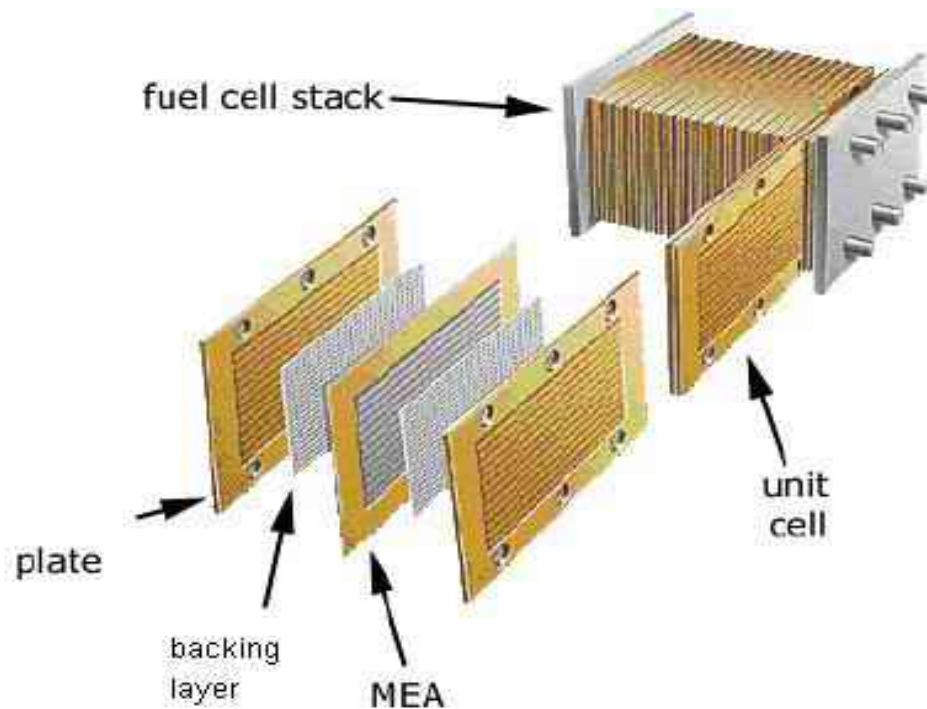


Figure 2.2: A view of a DMFC stack and an exploded view of a single cell ^[46].

2.5.2.4. Membrane Electrode Assembly (MEA)

MEA consists of two electrodes and Proton Exchange Membrane (electrolyte). A

major disadvantage of DMFC is the high cost of the system resulting from the high price of catalysts and that of membranes ^[43]. That means the high cost of DMFC system resulting from the high price of the MEA. The MEA is the heart of a single DMFC.

1. Electrodes (Electrode-Catalyst Layer)

In intimate contact with the membrane and the backing layer is a catalyst layer. The

catalyst layer with its binder forms the electrode. The catalyst and binder electrode structure is either applied to the membrane or else applied to the backing layer ^[3].

The performance of a DMFC is mainly influenced by catalytic activity, utilisation and active surface of the catalyst, the mass transport of methanol/CO₂ and the electrical (i.e. ionic/electronic) conductivity ^[47].

Excepting catalytic activity, these properties are influenced by both the catalyst loading and the ionomer content. Since the active surface of the catalyst increases with increasing catalyst loading but the thickness of the catalyst layer which increases with catalyst loading cause a mass transport limitation to methanol and CO₂ ^[48, 49]. However a thicker anode catalyst layer can be advantageous for cell performance, because a part of the methanol is consumed in the outer part of the layer and the

permeation of methanol to the cathode is reduced.

The DMFC usually operates at temperatures less than 100 °C, typically in the 50 – 80°C range. The low operating temperature of DMFCs has both advantages and disadvantages. Low temperature operation is advantageous because the cell can start from ambient conditions quickly. It is a disadvantage in CO-containing fuel streams – produced as a by-product or intermediate – in the methanol electro-oxidation reaction [50] because CO will attack the platinum catalyst sites, and by limiting catalytic activity will reduce cell performance [51, 52].

2. Proton Exchange Membrane (electrolyte)

The function of the proton exchange membrane is to provide a conductive path while at the same time separating the reactants. However, the membrane material is an electrical insulator. It is also a film barrier that separates fuel and oxidant in the anode and cathode compartments of the fuel cell. It acts as the separating layer in a fuel cell. The proton exchange membrane is the key component of a fuel cell system [40, 44] because only highly stable membranes can withstand the harsh chemical and physical environment in a fuel cell which includes: chemically active noble metal catalysts in the fuel cell electrodes, optionally chemically aggressive fuels like methanol and its partial oxidation products, aggressive oxidants like oxygen, the

formation of reactive radicals at the electrodes –especially at the cathode, and process temperatures which can exceed 100°C.

The largest current problem with the DMFC is Methanol permeability which is the undesirable transport of fuel from the anode side through the membrane to the cathode side where it is oxidized by chemical reaction with the oxidant present without any contribution to power generation, resulting in poor cell performance. Methanol permeability also deactivates the cathode electro-catalyst resulting in further efficiency losses, limits the applicable working temperature and decreases the cell potential.

Proton exchange membranes with low methanol permeation may allow the use of fuels with high methanol concentration and thereby increase the energy density, which is particularly attractive for portable electronic applications.

Furthermore, the cost of existing membranes is one of the key issues influencing the cost of the DMFC system.

2.6. Proton Exchange Membrane Families

Membranes can be either inorganic or organic. Many membranes have been developed, and many membranes are still ongoing research. Some representative membranes are discussed below.

2.6.1. Perfluorinated membranes and composites

2.6.1.1. Homogeneous perfluorinated membranes

Perfluorinated membranes are based on a polytetrafluoroethylene (PTFE) backbone that is sulfonated. The best known materials of this class are the DuPont Nafion[®] membranes^[4]. Nafion[®] is by far the leading membrane in all types of PEMFCs. It was first conceived during the space programme in the 1960's^[17, 18]. A side chain ending in a sulfonic acid group (-SO₃H) is added to the PTFE backbone by the sulfonation process. Generally used in fuel cells, Nafion[®] has become the most widely used and studied H₂-PEMFC and DMFC membrane due to its commercial availability, stability in the operating environment of the fuel cell, and mechanical strength^[53, 54]. The macro-molecule of Nafion[®], shown in Figure 2.3 below, is both hydrophobic and hydrophilic.

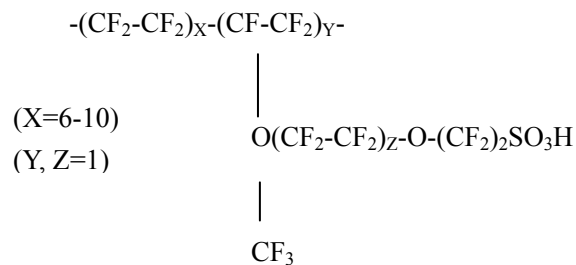


Figure 2.3: Chemical Structure of Nafion[®] Membrane^[55]

The sulfonate head is hydrophilic and has a strong affinity for water. It is generally

believed that a hydrated fluoropolymer membrane forms a bi-phasic system; one phase containing water and the dissociated ions, the other made up of the polymer matrix [4, 56, 57]. All sulfonated fluoropolymers have a hydrophobic backbone and hydrophilic sulfonate head groups on a side chain, they all form two-phase systems when hydrated. Changing the length of the chains, and location of the side chain on the backbone, makes the different membranes. The family of sulfonated fluoropolymers includes and the Dow product Dow[®] membranes (Figure 2.4) and a Japanese membrane (produced by Chlorine Engineers, Japan) [58]. The difference between these membrane types and Nafion[®] is that the side chain of the Dow[®] membrane is shorter than the side chain of Nafion[®] [59].

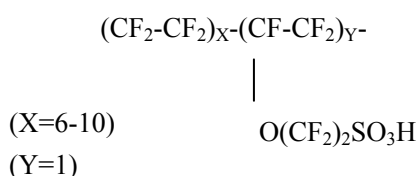


Figure 2.4: Chemical structure of Dow ionomer membrane [60]

The Flemion (Asahi Glass) and Aciplex (Asahi Chemical) membranes, which are also members of the perfluorinated membrane family, have also been investigated for use in H₂-PEMFC and DMFCs [61, 62]. Both the Aciplex and the Flemion membranes have a bi-layer structure that is comprised of sulfonic acid functional groups on the anode side and carboxylic acid functional groups on the cathode side [57][61]. Flemion

and Aciplex membranes can be made thinner while still providing the same acid activity and thus a higher cation exchange capacity, and therefore a better conductivity^[57].

The main drawbacks of these polymers are their high price (about \$ 800/m²) and the production process which includes strongly toxic and environment-unfriendly intermediates^[63]. A shortcoming of the perfluorinated ionomers especially related to their application in DMFC is their high methanol permeability which drastically reduces the performance of DMFCs^[64].

2.6.1.2. Composites of perfluorinated ionomers with heteropolyacids ionomer

Other Nafion[®] composite membranes contain polythiophene or different heteropolyacids like phosphomolybdenic acid, phosphotungstic acid or phosphotitanic acid^[65]. The conductivity is significantly increased via the addition of these materials. The application of such composite membranes in fuel cells is still under active research.

2.6.1.3. Micro-reinforced perfluorinated composite membranes

The Gore Corporation has developed micro-reinforced composite membranes with the trade name Gore-Select[®], which consist of a microporous stretched PTFE

membrane whose pores are filled with perfluorinated ionomer ^[66, 67]. Compared to Nafion[®], these membranes could be reduced in thickness to 5 μm , leading to a proton conductivity of the Gore-Select[®] membranes which is a factor 10 higher than the proton conductivity of Nafion[®].

2.6.1.4. Partially fluorinated membranes

Partially fluorinated membranes are still the subject of ongoing research, for example, the Paul Scherrer Institute, Villigen, Switzerland ^[68, 69]. These proton exchange membranes showed good performance when being applied in H₂-PEMFC and DMFCs. Grafted ionomer membranes based on poly (vinylidene fluoride) have been developed by Sundholm ^[70].

A shortcoming of these membranes is the use of styrene and divinylbenzene monomers from where it known that their oxidation stability is limited this is due to the presence of tertiary C–H bonds in the styrene/divinylbenzene graft chains which are sensitive to O₂ and hydrogen peroxide attack.

The Canadian Ballard Corporation has developed a number of partially fluorinated proton exchange membranes which consist of sulfonated ^[71] or phosphonated ^[72] polymerisates of unmodified a,b,b-trifluorostyrene and a,b,b-trifluorostyrene modified with radicals R. Disadvantages of these membrane types include the

complicated production process for the monomer a,b,b-trifluorostyrene ^[73] and the difficult sulfonation ^[71] and phosphonation ^[72] procedures for poly(a, b, b-trifluorostyrene) -homopolymers and copolymers.

2.6.2. Non-Perfluorinated Membranes

2.6.2.1. Sulfonated polymers

1. Sulfonated Poly(arylene ether)s

Poly(arylene ether)s such as poly(ether sulfone)s, poly(ether ketone)s or poly(ether ether ketone)s are well known engineering plastics that display excellent thermal and mechanical properties as well as resistance to oxidation and acid catalyzed hydrolysis. The favourable properties displayed by this class of polymers now form the focus of attention as promising candidates for fuel cell membranes.

(i). Sulfonated Poly(arylethersulfone) membranes

Polysulfone (PSU) has very good chemical stability, and it is cheap. The synthesis and characterization of sulfonated polysulfone (SPSU) has been achieved by Johnson *et al.* ^[74] and Nolte *et al.* ^[75]. The shortcomings identified were that membranes cast from SPSU (Udel™ P-1700) solutions were completely water soluble ^[75-77] and

become very brittle when drying out which can happen in the fuel cell application under intermittent conditions ^[78].

Kerres and co-workers developed promising alternative composite membranes which have been crosslinked by S-alkylation of PSU sulfonate groups with di-halogenoalkanes. These membranes show very good performance in H₂-PEMFC and DMFC ^[79-81]. These membranes also show markedly reduced methanol permeability ^[79, 82, 83].

(ii). Sulfonated Poly(aryletherketone) membranes

Poly(arylether ketone)s consist of sequences of ether and carbonyl linkages between phenyl rings, that can either “ether-rich” like PEEK and PEEKK, or “ketone-rich” like PEK and PEKEKK. The most common materials are polyetherketone (PEK), and polyetheretherketone (PEEK) which is commercially available under the name Victrex™ PEEK from Imperial Chemical Industries Ltd. A number of groups are developing proton exchange polymer materials based on this classification of materials.

Sulfonated polyetherketone membranes have been investigated for use in PEMFCs and DMFCs ^[84, 85] in the last decade. The motivation for these developments was that these polymer families have chemical and mechanical stabilities closest to the fluorinated polymer classes ^[86, 87]. Sulfonated polyetherketone membranes consist of a

polyetherketone backbone that has a sulfonic acid functional group attached to it (see Figure 2.5).

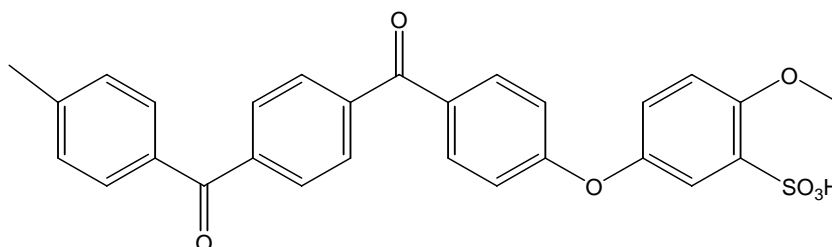


Figure 2.5: Chemical structure of sulfonated polyetherketone.

The backbone is hydrophobic and the sulfonate head is hydrophilic. However, the backbone is less hydrophobic than the PTFE backbone and the sulfonic acid group is less acidic and therefore less hydrophilic^[88]. The polyetherketone backbone is less flexible than the PTFE backbone of the sulfonated fluoropolymer family of membranes^[88]. As a result of these differences between the two membranes, the sulfonated polyetherketone membranes are not separated into a two-phase system as distinctly as the sulfonated fluoropolymer family of membranes. The polyaromatic membranes are easier to manufacture than the sulfonated fluoropolymer membranes, and they are significantly cheaper^[88].

Sulfonation of polyetherketones can be carried out directly in concentrated sulfonic acid or oleum, the extent of sulfonation being controlled by the reaction time and temperature^[89, 90].

Sulfonated polyaryls have been demonstrated to suffer from hydroxyl radical initiated

degradation ^[91]. In contrast to this, SPEEK was found to be durable under fuel cell conditions extending over several thousand hours by Kreuer ^[92]. The brittleness of SPEEK makes their handling difficult and may lead to mechanical membrane failure during operation. These types of membranes become very brittle when drying out.

2. Sulfonated polyaramides membranes

Aromatic polyamides such as Nomex[®] and Kevlar[®] are known as polymers of high mechanical strength and high chemical resistance. The preparation of sulfonated and carboxylated copolyaramides with high ion exchange capacities has been described by Sherman ^[93] and Konagaya and Tokai ^[94]. These materials were used for the preparation of reverse osmosis membranes with enhanced rejection properties and chlorine resistance. So far, sulfonated polyaramides have not been mentioned as potential membrane materials in fuel cell applications.

3. Sulfonated Polyimide membranes

Gunduz and McGrath ^[95] recently described the synthesis of sulfonated polyimides using 2, 5-diaminobenzene sulfonic acid sodium salt as the source of the sulfonated subunits. In addition, 4, 4-diaminodiphenyl sulfone and 4, 4-(9-fluorenylidene dianiline) were used as amine monomers. Two different tetracarboxylic acid

anhydrides, namely biphenyl-3,3,4,4-tetracarboxylic acid dianhydride and 4,4-(hexafluoroisopropylidene)-bis-phthalic acid anhydride have been employed as monomers. Polymers with high molecular weights and narrow molecular weight distributions were obtained by the ester–acid procedure in aprotic solvents. Films prepared from polyimides with a DS of 50 and 75% were tough and creased. A higher DS yielded brittle films, especially when completely dried. As expected, the hydrophilicity increased with increasing DS.

Woo et al. ^[96] have studied the properties of sulfonated polyimides derived from the reaction of 3,3,4,4-benzophenonetetracarboxylic acid dianhydride with 4,4-diaminobiphenyl-2,2-disulfonic acid and 4,4-oxydianiline. The water uptake was found to be five times lower than that of Nafion® 117 at comparable IEC, and which was related to the rigid structure of the polyimides leading to a lesser swelling. A sudden increase in water uptake, methanol permeability as well as proton conductivity was observed at $DS \geq 35$ mol%. However, data from fuel cell tests were not available.

S. Faure and G. Gebel ^[97, 98] claimed that the sulfonated polyimide membranes were 3 times less permeable to hydrogen gas than Nafion® membranes. The lifetime measurements were performed on a 175 μm thick phthalic polyimide and a 70 μm thick naphthalenic sulfonated polyimide film at 60°C, at 3 bar pressure for H₂ and O₂

and at a constant current density. It was found that the membrane based on the phthalic structure broke after 70 hours whereas the membrane based on the naphthalic polyimide was stable for over 3000 hours ^[98].

2.6.2.2. Polybenzimidazole-based membranes

Polybenzimidazoles are synthesised from aromatic bis-*o*-diamines and dicarboxylates (acids, esters, amides), either in the molten state or in solution. The repeating unit, benzimidazole, has rather remarkable thermal properties when compared to its carbon congener indene, as illustrated by melting and boiling point data ^[99]. The commercially available polybenzimidazole is poly-[2,20-(*m*-phenylene)-5,50-benzimidazole] shown in Figure 2.6 which is synthesized from diphenyl-*iso*-phthalate and tetra-aminobiphenyl, and will be referred to hereafter simply as “PBI”. It has excellent thermal and mechanical stability.

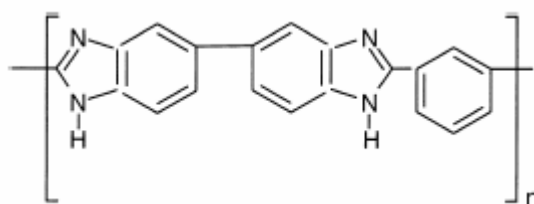


Figure 2.6: Poly[2,20-(*m*-phenylene)-5,50-benzimidazole] (PBI)

PBI is a suitable basic polymer which can readily be complexed with strong acids ^[100-109]. The immersion of PBI film in aqueous phosphoric acid leads to an increase in both its conductivity and thermal stability ^[110].

Early reports of the proton conductivity of PBI are conflicting. Thus, whereas

values in the range 2×10^{-4} – $8 \times 10^{-4} \text{ Scm}^{-1}$ at relative humidities between 0 and 100% were published [103], other authors [99, 111] observed proton conductivity some two to three orders of magnitude lower. These latter values are those generally accepted for non-modified PBI, and are clearly too low for any use of PBI membranes in fuel cell applications. Two principal routes have been developed to improve the proton conduction properties, and these repose upon the particular reactivity of PBI – which is twofold – and arises from the $-\text{N}=\text{}$ and $-\text{NH}-$ groups of the imidazole ring. Due to its basic character ($\text{p}K$ value of ~ 5.5) PBI complexes with inorganic and organic acids [112, 113]. In addition however, the $-\text{NH}-$ group is reactive; hydrogen can be abstracted, and functional groups then grafted onto the anionic PBI polymer backbone [114, 115]. It should also be mentioned that unlike other polyaromatic polymers, the direct sulfonation of PBI using sulfuric or sulfonic acid is not appropriate for the preparation of proton conducting polymers for fuel cell membranes, since it tends to lead to a polymer with a low degree of sulfonation and increased brittleness [116].

2.6.2.3. Crosslinked membranes based on sulfonated polymer

The most representative crosslinked membranes were developed in developed in Stuttgart University (Germany). Kerres and co-workers investigated crosslinked sulfonated polymer membrane based on sulfonated polymer via crosslinking reactions

^[117-119]. Chemically crosslinked membranes were developed to reduce membrane swelling and increase mechanical strength. Materials prepared by crosslinking are comparable to commercial Nafion[®] in terms of their mechanical strength and proton conductivity ^[120]. Although the crosslinked membrane exhibits very good properties, the processes are complex.

2.7.3. Composite membranes

The organic/inorganic composite proton exchange membranes are developed to overcome the disadvantages of the actual state-of-the-art membranes which require increasing the operating temperature above 100°C and/or reducing methanol permeability (methanol crossover). In addition, as in many proton conductors with conductivity suitable for electrochemical applications, the proton transfer process takes place on the surface of the inorganic particles; and an increase in surface area (small particle size) increases the conductivity ^[121]. The method of inclusion of inorganic particles involves a bulk powder dispersed in a polymer solution. These methods include intercalation/exfoliation, sol-gel chemistry, and ion-exchange ^[121,122].

Incorporating highly porous SiO₂ into Nafion[®] membranes up to concentrations of 3% has been reported ^[123]. The SiO₂ works as a water storage medium, enabling good

proton conductivities even at temperatures of 145°C. Nafion[®] membranes containing no SiO₂ have only very low proton conductivity at this temperature. The application of such membranes to DMFCs yielded good performance. A maximum power density of 240 mW/cm² at 0.6 A/cm² and 0.4V was obtained.

Mauritz has done pioneering work in preparing ionomer/inorganic oxide “nano-composites” via sol–gel techniques, where the inorganic compound is molecularly dispersed in the ionomer matrix ^[124].

Systems of this type are as follows:

ionomer: Nafion[®]; precursor: TEOS; inorganic network: SiO₂/OH ^[125];

ionomer: Nafion; precursor: Zr(OBu)₄; inorganic network: ZrO₂/OH ^[126];

ionomer: Surlyn[®]; precursor: TEOS; inorganic network: SiO₂/OH ^[127].

A disadvantage of the above-mentioned nano-composite membranes is that the sol–gel reaction takes place in a preformed membrane, and therefore the inorganic content in the composite membrane cannot be varied over a broad range. Nevertheless the nano-composite ionomer membranes could be interesting candidates for fuel cell application, especially in DMFCs at temperatures of > 100°C.

Another class of membranes considered for fuel cell application are the so-called “ormolytes” (organically-modified silane electrolyte), for example, poly(benzy-sulfonic acid siloxane) ^[128], which are produced by the sol–gel process, followed by sulfonation in ClSO₃H/dichloromethane. These inorganic/organic hybrid polymer

membranes can be crosslinked via hydrosilylation. The poly(benzylsulfonic acid siloxane) membrane shows an ionic conductivity of 1.6×10^{-2} (S/cm) ^[128] at room temperature. Fuel cell data on these membranes has not yet been published.

2.7. Membrane Morphology

2.7.1. Nafion[®] (Sulfonated Fluoropolymer Membrane Morphology)

The hydrated membrane forms a two-phase system consisting of a water-ion phase distributed throughout a partially crystallized perfluorinated matrix phase ^[60, 56, 88, 129]. The crystallized portion of the membrane crosslinks the polymer chains, preventing complete dissolution of the polymer at temperatures below which the crystalline portion of the polymer network is affected ^[60]. The glass transition temperature of Nafion[®] is reported to be about 152 °C ^[132].

Two models have been developed to explain the resulting morphology of the hydrated Nafion[®] membrane. They are the cluster network model by Gierke, Hsu et al. (hereafter referred to as GH) ^[130–133], and the model of Yeager and Steck (hereafter referred to as YS ^[90]).

According to the cluster network model of GH, the ion exchange sites form clusters within the membrane. This model is supported by evidence developed from numerous experimental techniques ^[131]. Through transmission electron micrographs

of ultra-microtomed Nafion[®] sections, GH was able to show that the clusters are approximately spherical [131]. As the membrane is hydrated, the sorbed water molecules are attracted to the hydrophilic sulfonate heads, which aggregate into clusters. As more water is sorbed, the clusters grow, and eventually short narrow channels form and connect the clusters [131, 132]. The polymeric charges are located close to the cluster surface, at the phase interface between the liquid and polymer phases [131]. The spherical clusters measured were approximately 4 nm in diameter [57].

Figure 2.7 shows the proposed morphology of the membrane.

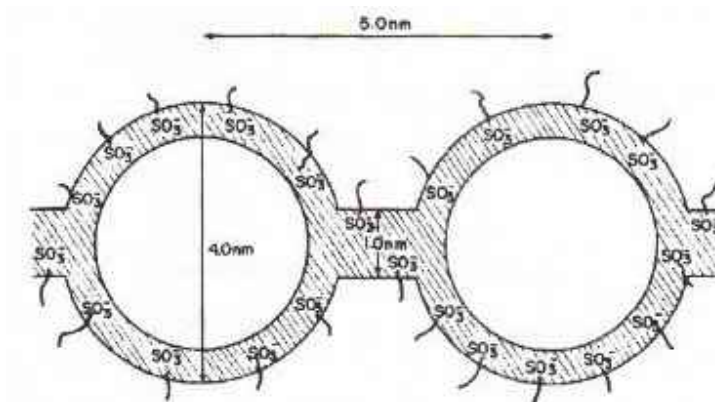


Figure 2.7: Cluster-network model for Nafion[®] Membrane [131]

In the second model, YS claim that the ionic clusters are not spherical. YS identify three regions that comprise the membrane morphology. Region A is the fluorocarbon phase, made up of the hydrophobic backbone where it is energetically unfavorable for water to be. Region C is comprised of the ionic clusters; it also incorporates the sulfonate heads. Region B is an interfacial region between region A and C and

contains few sorbed water, sulfonate heads that have not yet been incorporated into the clusters, and a portion of the counterions^[90]. In Figure 2.8, A is a schematic of the morphology described by YS. Figure 2.8 B is a schematic of the morphology of Nafion[®] discussed by Kreuer et al. in several of their papers^[132].

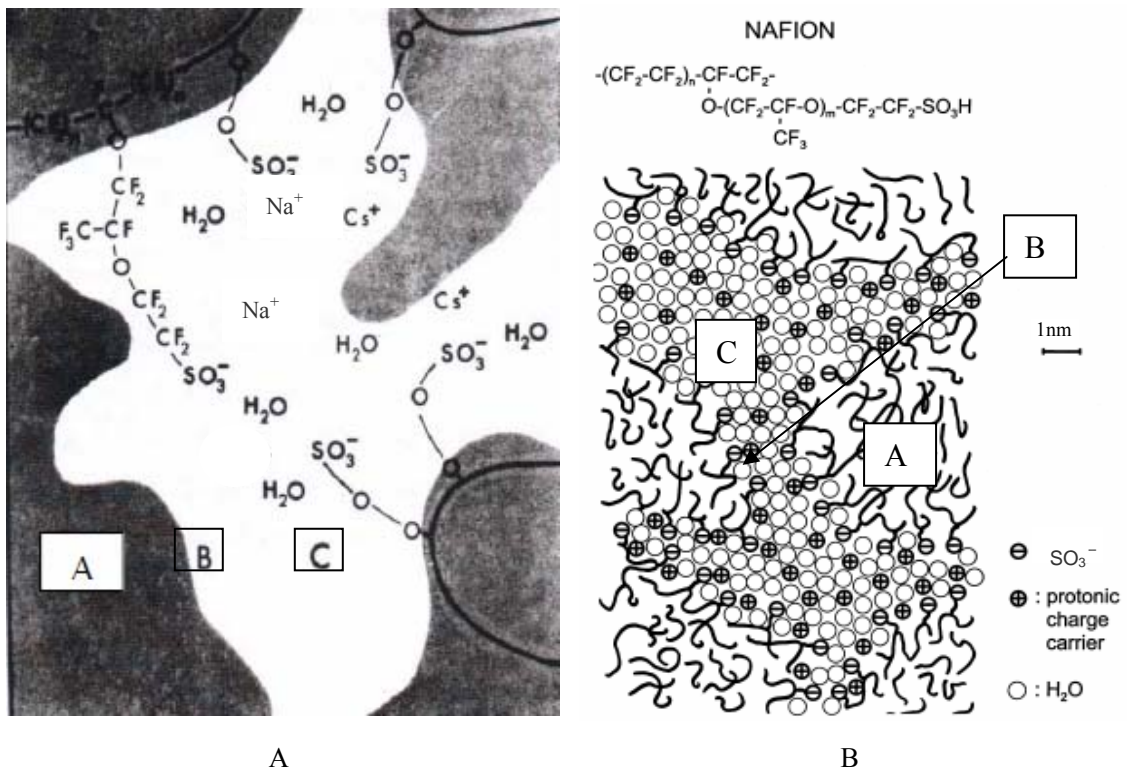


Figure 2.8:

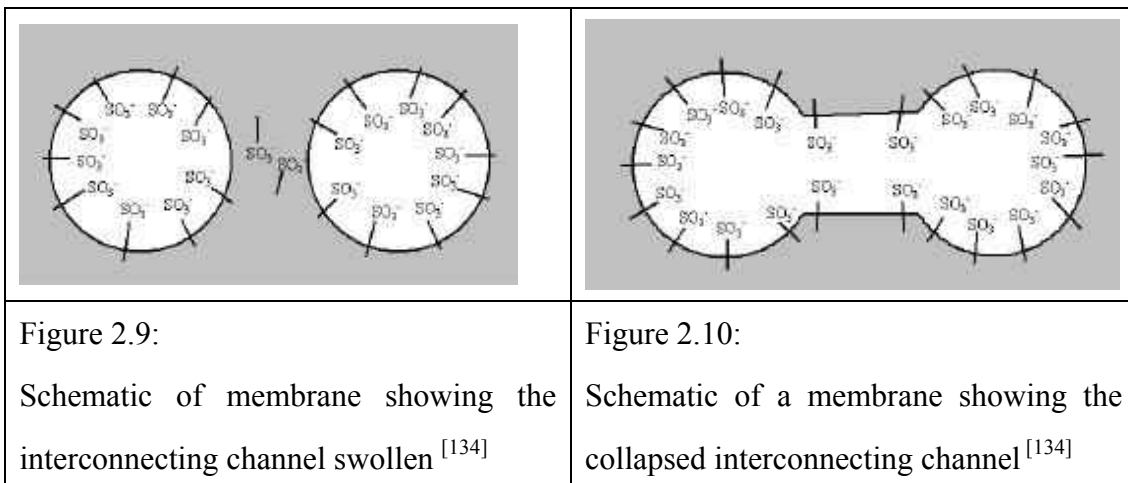
A: Three region structural model for Nafion[®]^[132].

B: Schematic representation of microstructure of Nafion[®]^[132].

Weber and Newman in Ref.^[57] (hereafter referred to as WN) consider the model of GH to be an idealization of the model of YS. The ideas of WN provide the best

insight into the structure of the membrane, allowing us to unify our view of the morphology of the membrane. That is within the membrane, ionic clusters form where there is a high density of sulfonate heads. These clusters are approximately spherical in shape. The interfacial regions introduced by YS are what GH consider to be the channels that connect the ionic clusters ^[57].

We can consider the interfacial region as collapsed channels that can fill with water to form a liquid channel, but note that even in their collapsed form they allow for conductivity, since sorbed water can dissociate from the sulfonate heads located in the collapsed channels; however, not enough water is sorbed to form a continuous liquid pathway ^[57]. The collapsed channels form in membrane regions with lower sulfonate head concentrations. Figure 2.9 and 2.10 below show how the morphology can be described in terms of collapsed channels with ionic clusters.



2.7.2. Other Membranes

The Dow family of membranes has a structure similar to Nafion[®] except with a shorter side chain. As WN predict, the clusters formed within the Dow membranes will be smaller due to the higher elastic deformation energy^[57].

WN also considered Flemion and Aciplex. They predict a microstructure with clusters that are closer together and also predict that the network is more hydrophilic and also better interlinked^[57].

It has already been established that the backbone of the sulfonated polyetherketone membranes is stiffer than that of Nafion[®], and that the sulfonate heads are less hydrophilic and the backbone less hydrophobic than Nafion[®]. Because the hydrophobic/hydrophilic difference is smaller than for Nafion[®] and the backbone is stiffer, the separation into two domains, one hydrophobic and one hydrophilic, is not as well defined as in Nafion[®]^[132]. The structure of the sulfonated polyetherketone membranes is, as a result, one with narrower channels and the clusters are not as well connected as in Nafion[®]^[57, 132]. Figure 2.11 below is a schematic of the microstructure of Nafion[®] and a sulfonated polyetherketone membrane illustrating the effected the less pronounced phase separation.

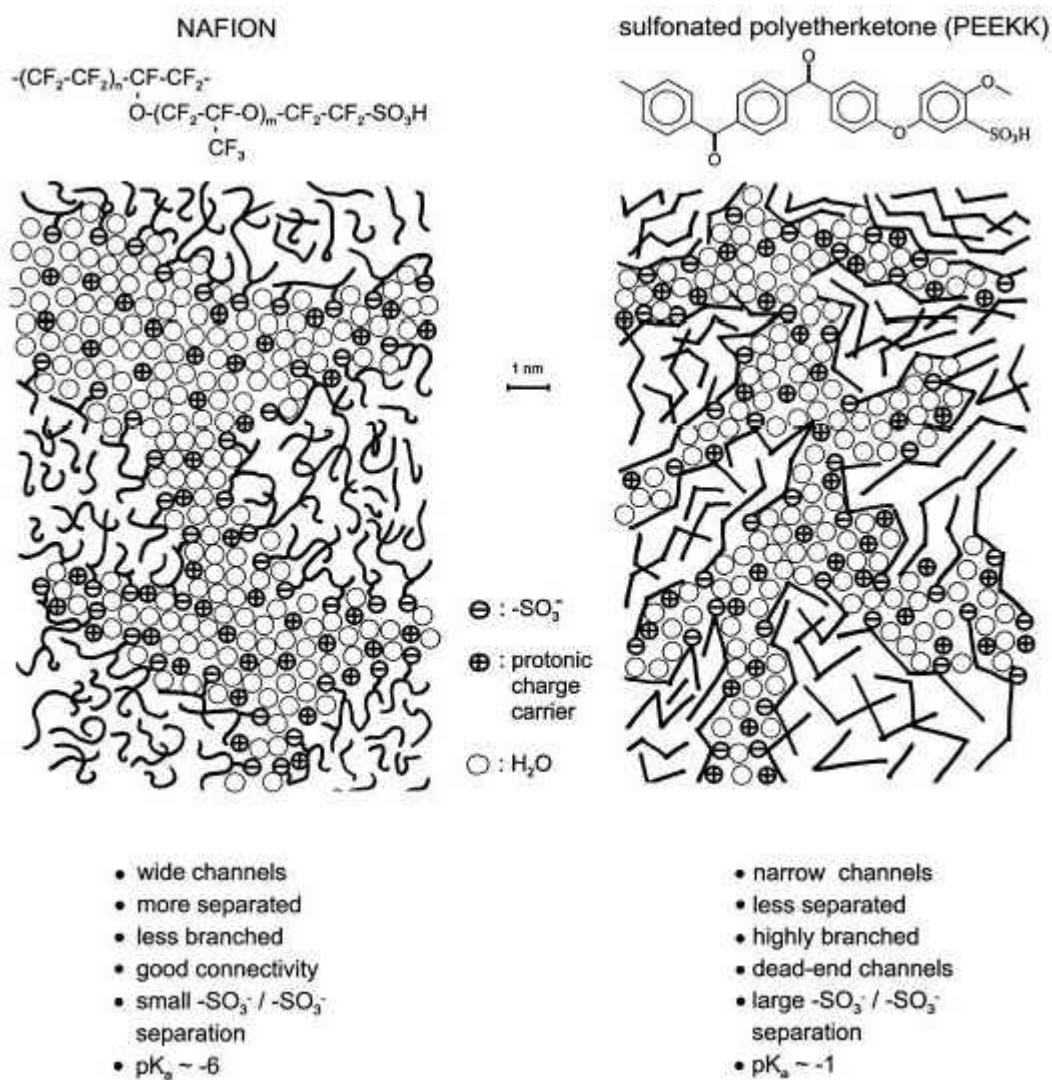


Figure 2.11:

Schematic representation of the microstructure of Nafion[®] (left) and a sulfonated polyetherketone membrane^[132] (right)

2.8. The significance of the review

The DMFC has become the most promising type of fuel cell due to its many advantages. First it is an emerging technology that needs to be better understood. Which is being performed world wide aimed at solving the engineering problems that currently prevent fuel cells from becoming commercially available. The need is to reduce the cost of producing fuel cells. The existing problems of high price and high methanol permeability of the proton exchange membrane results in the high initial cost of DMFC manufacturing and its performance. Furthermore, the available proton exchange membranes are very limited and expensive. Developing new proton exchange membranes which possess better properties at lower cost is crucial. It is believed that the opportunity to develop new membranes is attractive and will be extremely advantageous for us.

CHAPTER 3

Preparation and characterization of SPEEK membranes

3.1 Introduction

Fuel cell technology is expected to become one of the key technologies of the 21st century both for stationary applications (like block power stations) and portable applications (like vehicles, laptops and cellphones). The proton exchange membrane is the key component of a fuel cell system, because only highly stable membranes can withstand the harsh chemical and physical environment in a fuel cell, which includes chemically active noble metal catalysts in the full cell electrodes, chemically aggressive fuels like methanol and its partial oxidation products, and process temperatures which can exceed 100 °C.

At present, the solid polymer proton conductivity electrolytes used in DMFCs are exclusively perfluorinated polymer, such as Nafion[®]. The perfluorinated ionomers have an outstanding chemical stability, and excellent performance can be achieved when these membranes are applied in membrane fuel cells, especially in hydrogen fuel cells. The main shortcomings of these materials are their high price and the production process which includes strongly toxic and environment-unfriendly intermediates. A shortcoming of the perfluorinated ionomers especially related to their application in DMFCs is their high methanol permeability which drastically

reduces DMFC performance.

Therefore, developing alternatives to perfluorinated ionomers have become active projects. In the last decade, numerous types of arylene main chain polymers have been developed. The motivation for these developments was that this polymer family shows the best chemical and mechanical stability next to that of the perfluorinated polymer classes. A huge number of these polymers have also been sulfonated in order to obtain proton conducting membranes. Among the arylene polymers which have been sulfonated are the following polymer families: polysulfone^[135, 136], polyimides^[137, 138], polyetheretherketone (PEEK)^[139–145]. According to the literatures, it has been shown that SPEEK possesses many of the required properties as a proton conductive membrane for fuel cell application (such as good thermal stability, chemical inertness, good mechanical properties, low cost and adequate conductivity) which make it a promising alternative material for fuel cell application.

In this chapter, the focus is on synthesizing membrane based on sulfonated polymer. To this end, a series of SPEEK polymers were prepared and investigated. The polyether ether ketone (PEEK) was purchased from Aldrich. The sulfonation of PEEK was performed using concentrated sulfuric acid (95-98%) at room temperature. SPEEK with various DS were obtained by controlling the reaction time. The results showed that DS increased with sulfonation time. The conductivity of the membranes and the water uptake were also increased with the increase in DS. SPEEK membrane with various DS ranging from 0.3 up to 0.82 have shown conductivity values ranging from 5.6×10^{-3} to 2.5×10^{-2} S/cm at room temperature, while the methanol permeability remains considerably smaller than that of Nafion[®] membrane.

3.2 Experimental

3.2.1 Chemical materials

The chemical materials employed are shown in Table 3.1

Table 3.1: Chemical materials

Chemicals	Specifications	Supplier
Poly(oxy-1,4-phenyleneoxy-1,4-phenylenecarbonyl-1,4-phenylene)	Typical M_n 10,300; Typical M_w 20,800	Aldrich Chemical Corp
N, N Dimethylacetamide (DMAc)	99%	Aldrich Chemical Corp
Sulfuric acid	98%	KIMIX
Methanol	99.5%	KIMIX

3.2.2. Sulfonating PEEK

In this study, sulfonated PEEK was prepared via sulfonation reaction using concentrated sulfuric acid at room temperature in this study. PEEK was sulfonated according to the procedure as described in [146, 147].

PEEK pellets were dried in a vacuum oven at 100 °C overnight. 10 g of PEEK pellets were added slowly to 200 ml concentrated sulfuric acid (98%) under vigorous magnetic stirring to dissolve the PEEK. Then the container was sealed and kept stirring at room temperature for the desired time. After the prescribed time, the

sulfonated polymer was recovered by precipitating the acid polymer solution into a large excess of ice water under mechanical agitation. The polymer suspension was left to settle in ice water for two days. The polymer precipitate was filtered, washed several times with deionized water until the pH was neutral, and dried under vacuum in an oven for one week at 60 °C. By changing the sulfonation time, SPEEK with various DS were obtained.

3.2.3 Preparation of SPEEK membranes

Membranes were prepared by dissolving 1.0 g of SPEEK in N, N-dimethylacetamide (DMAc) to give a 5 wt% solution. After dissolving, the resulting SPEEK mixture solutions were filtered. Subsequently, the polymer solution was cast onto a flat glass plate to give a thin film. The cast membrane was allowed to evaporate the DMAc solvent and dried in a vacuum oven at 60 °C for 48 hours, followed by 120 °C for 24 hours. After the evaporation of the solvent, and cooling to room temperature, the resultant membrane was peeled from the glass in deionized water. After drying, the thickness of the dried SPEEK membranes was about 0.05-0.2 mm.

3.2.4. Characterizations of the SPEEK membranes

3.2.4.1. FTIR study

The chemical structure of the prepared SPEEK and PEEK were analyzed by FTIR spectroscopy. Analysis was performed using a Perkin Elmer Paragon 1000 FTIR Spectrophotometer. The analysis of SPEEKs were used the dried prepared membrane as the testing samples. For PEEK testing sample, the PEEK powder and KBr were mixed and prepared into a film. The SPEEK membranes and prepared PEEK film were tested after drying in an oven at 110 °C overnight. The measurement of PEEK was carried out by using the KBr background, for SPEEK testing sample was used air as the background. For both absorbance spectra were recorded.

3.2.4.2. Thermal Gravimetric Analysis (TGA)

Thermal stability and DS of the SPEEK were investigated and determined using TGA. The approximately 10 mg samples were placed in a Thermal Analyzer STA 1500 (CCI-3, *Rheometric Scientific*), and then programmed to record the mass loss from room temperature to 800 °C at a rate of 10 °C/min in a N₂ atmosphere. The DS of the SPEEK was determined according to the method of S.M.J. Zaidi ^[86]. This method is based on the assumption that the second weight loss step is entirely caused by splitting of sulfonic acid group.

3.2.4.3. Water uptake

The water uptake of a membrane was determined in the following way: The water uptake measurements were conducted by measuring the weight differences between the fully-hydrated membranes and the dried membranes. Before measurement, at first the weighed membranes with area 10mm×50mm were immersed in deionized water at room temperature for one day. The membranes were saturated with water until no further weight gain was observed. The water uptake also measured at 80°C condition. The membranes were immersed in water at 80°C for one hour before the measuring. The liquid water on the surface of the wetted membranes was quickly removed using tissue paper, and immediately weighed to determine the swollen membranes' wet mass. Subsequently, the membranes were dried in the drying oven at 100°C for 6 hours and reweighed. The percentage weight gain with respect to the dried membrane weight was taken as water uptake. The water uptake was determined by the following formula:

$$\text{Water uptake} = \frac{G_w - G_d}{G_d} \times 100\%$$

G_w is the weight of the wet membranes and G_d the weight of the dry membranes.

3.2.4.4. Proton conductivity

The proton conductivities of membranes in the traverse direction were measured in a conductivity cell by milliohmmeter. Figure 3.1 shows a schematic representation of the cell for electron and proton conductivity measurements.

Two stainless steel electrodes with a contacting area of 0.28 cm^2 , were connected to a milliohmmeter and horizontally pressed onto the membrane surface to be tested. Conductivity measurements were only performed on flat membranes. During the measurements, the membranes were sandwiched between the two steel plates under a 2 kg pressure as shown in the diagram below. For conductivity testing, the membrane was immersed in 1M sulfuric acid solution for 6 hours at room temperature at $80 \text{ }^\circ\text{C}$. The membrane was then rinsed with deioned water several times to remove any excess H_2SO_4 and then immersed in deioned water for 6 hours at $60 \text{ }^\circ\text{C}$. All the membranes were kept in deioned water at room temperature before conductivity testing measurement.

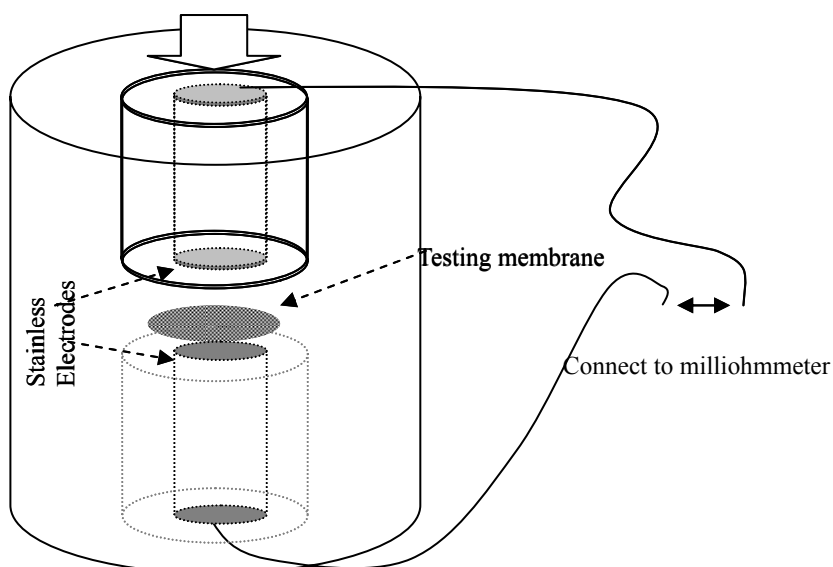


Figure 3.1: Schematic representation of the cell for measuring conductivity

The conductivity σ of the membranes in the transverse direction was calculated from the resistance data, using the relationship:

$$\sigma = d/RS$$

d, R and S are the thickness, resistance and face area of the membranes respectively.

3.2.4.5 Measurement of Methanol permeability

Methanol permeability (crossover) of the membranes was examined by using a diaphragm diffusion cell. A plastic cell containing solutions A and B (see Figure 3.2) in two identical compartments separated by the test membranes was utilized for methanol permeability tests. Compartment A was filled with 1M methanol-water solution while compartment B was filled with deionized water. The membranes were placed between the two compartments by a screw clamp and both compartments were under ultrasonic vibrations during the permeation experiments (all the methanol permeability measurements were used a constant vibration speed in this study). The concentration of methanol in solution B was estimated using a GC (Hewlett Packard 5890). The GC is highly sensitive to methanol, and can be continuously measured during the test. The methanol concentration of the receiving compartment was measured with time. The methanol permeability P was calculated from the slope of the straight line plot of methanol concentration versus permeation time. The measurements were taken at room temperature.

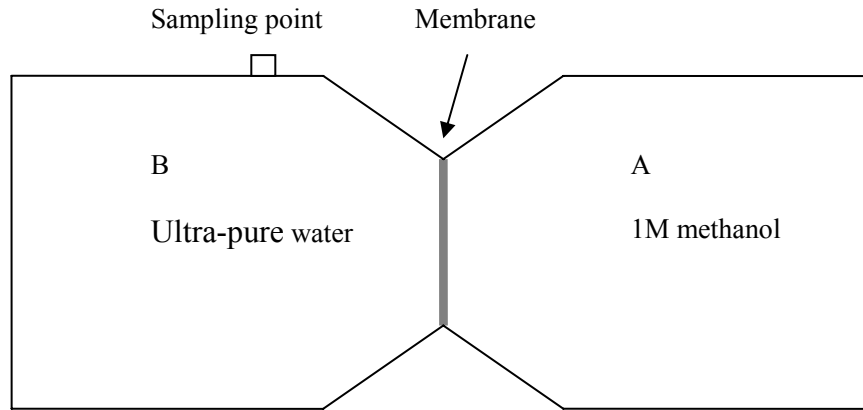


Figure 3.2: Schematic diagram of methanol permeability measurement

Methanol permeability was calculated according to the equation described in [148, 149] and expressed as follows:

$$C_B(t) = \frac{A}{V_B} \frac{DK}{L} C_A(t - t_0)$$

A: membrane area available for diffusion

C_A : initial concentration

C_B : final concentration

L: membrane thickness

P: membrane permeability ($P = DK$)

T: time ($t - t_0$)

V_B : volume of the receiving compartment

Methanol permeability was calculated using the following equation:

$$P = \frac{L}{A} \times \frac{V_B}{C_A} \times \frac{\Delta C}{\Delta t}$$

Gas Chromatography (GC):

The gas chromatograph used for methanol permeability determination was a Hewlett Packard 5890 series II model. The column was used a Porapak Q with the following specifications:

Length 6 feet

Inside diameter 2.2 mm

Outside diameter 1/8 inches

The GC parameters and settings are shown in Table 3.2.

Table 3.2: HP 5890 parameters

GC parameters	Settings
Helium flow rate	30 ml/min
Hydrogen flow rate	25 ml/min
Air flow rate	450 ml/min
Column temperature	175 °C
Injector temperature	150 °C
Detector temperature	250 °C
Sampling loop volume	1 µl

3.3 Results and discussions

The full name of PEEK is polymer poly (oxy-1,4-phenylene-oxy-1,4-phenylene-carbonyl-1,4-phenylene), which is a semi crystalline polymer possessing excellent thermal and chemical stability, and electrical and mechanical properties^[89, 150]. Figure 3.3 shows the chemical structure of PEEK. It does not dissolve in organic solvents but in strong acids. Presumably, the difficulty in dissolving PEEK lies in overcoming the strong inter-crystalline forces. The solubility of PEEK in strong acids can be attributed to protonation, in some cases, to chemical modification (e.g. sulfonation) of the polymer^[150, 151].

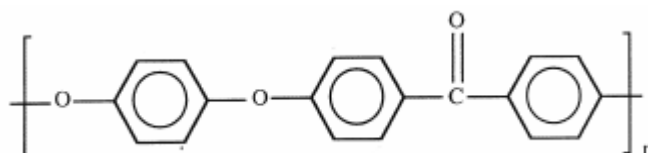


Figure 3.3: Chemical structure of PEEK

3.3.1 Thermal properties and degree of sulfonation

All the sulfonated PEEK and neat PEEK powder were analyzed by TGA in order to characterize their thermal stability.

The onset of weight loss for PEEK began at about 550 °C. This weight loss is due to main chain decomposition, which results in the formation of phenols and benzene (see Figure 3.4). Compared to PEEK which exhibits a single step thermal degradation,

SPEEK has three distinct weight loss steps (see Figure 3.5). The first loss step is the loss of water physically absorbed in the sample. The second weight loss is mainly associated with the splitting off of sulfonic acid groups in the temperature range of 300–400 °C. The third weight loss step is related to the decomposition of the main chain of SPEEK when the temperature is over 500 °C. The main chain decomposition temperature of SPEEK is lower than that of PEEK because of the catalytic decomposition of the polymer chain caused by SO_3H .

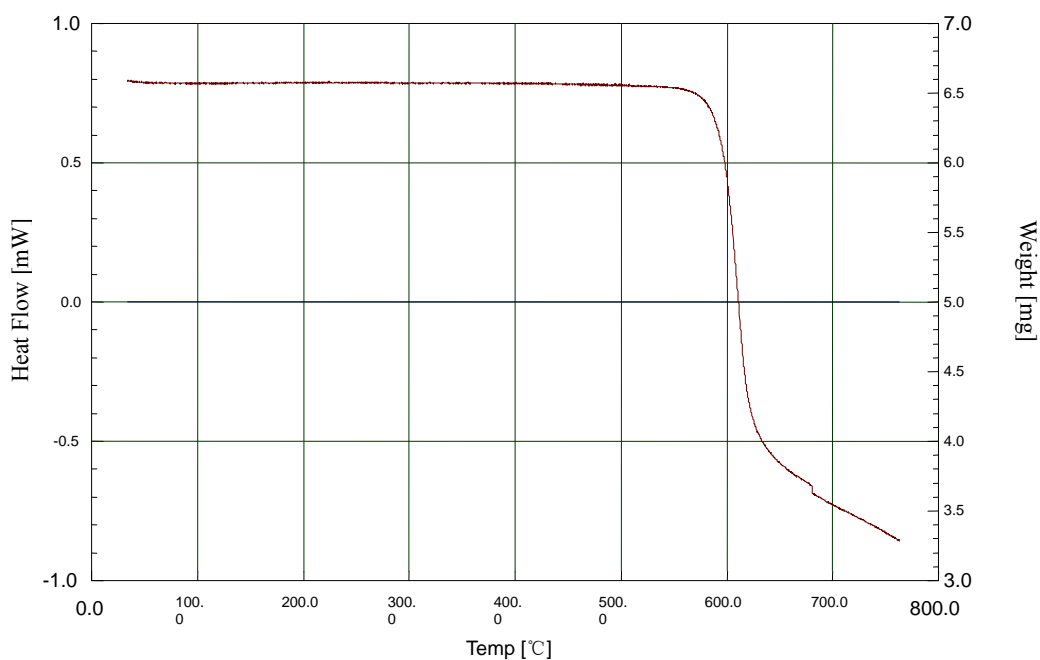


Figure 3.4: TGA curves of PEEK

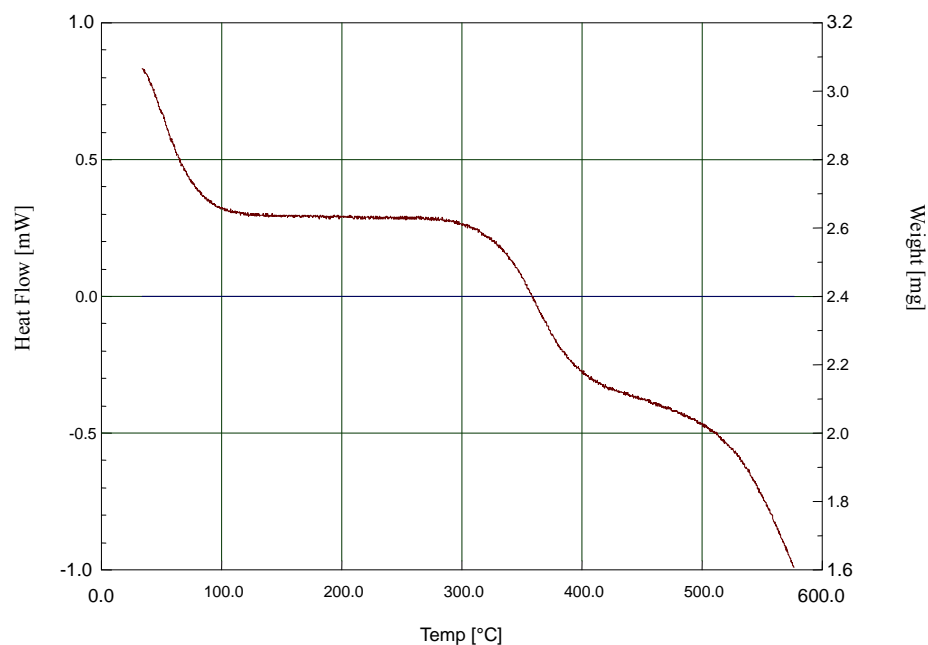


Figure 3.5: TGA curves of SPEEK

TGA analysis has been used to determine the DS of SPEEK according to the method of S.M.J. Zaidi ^[86] which attributes the second weight loss step entirely to SO_3 release. The results in Table 3.3 show that the DS values obtained from TGA. The PEEK was sulfonated for different reaction times ranging from 14 to 163 h to produce SPEEK polymers with various DS. It is known that the DS of SPEEK can be controlled by changing reaction time, acid concentration and temperature ^[152]. In this study, the DS was controlled by changing reaction time due to its easy to control.

Table 3.3: The properties of SPEEK membranes

Polymer designation	DS (from TGA)	Methanol permeability (cm ² /s)	Proton conductivity at 20 °C (S/cm)	Water uptake (wt%) at room temperature	Water uptake (wt%) at 80 °C	Sulfonation time (hour)
SPEEK18	0.18		Insoluble in DMAc			13
SPEEK30	0.30	4.00×10^{-9}	5.6×10^{-3}	16	20	24
SPEEK63	0.63	9.00×10^{-8}	0.9×10^{-2}	18	25	40
SPEEK75	0.75	1.50×10^{-7}	1.3×10^{-2}	20	40	56
SPEEK79	0.79	1.58×10^{-7}	1.9×10^{-2}	24	60	63
SPEEK82	0.82	1.80×10^{-7}	2.5×10^{-2}	32	95	72
SPEEK92	0.92		Soluble or gel	Soluble or gel		163

The DS of SPEEK polymers is presented in Figure 3.6 as a function of sulfonation time. On the whole, it is consistent with the reported methods, such as described in [89, 153-156].

The results (see Figure 3.6) show that the sulfonation of SPEEK proceeded rapidly before 60 hours, but progressed slowly after 60 hours.

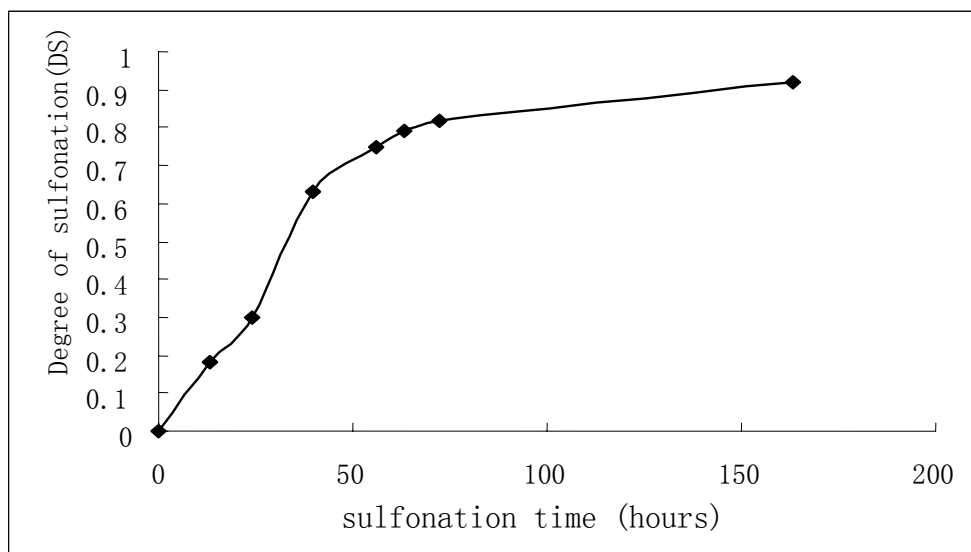


Figure 3.6: Degree of sulfonation (DS) of SPEEK with the sulfonation time

3.3.2. Solubility of SPEEK

Sulfonation modifies the chemical properties of PEEK, which reduces the crystallinity and affects the solubility of the polymer. The SPEEK with DS = 0.18 is soluble only in concentrated H₂SO₄. When DS = 0.3 the SPEEK polymers are soluble in hot DMAc. When DS = 0.63, 0.75 or 0.82, the SPEEKs are soluble in the DMAc solvents at room temperature but insoluble in water; when DS \geq 0.92, the polymer is soluble in hot water.

3.3.3. FTIR study

Fourier transform infrared spectroscopy is a powerful tool used to characterize the functional groups in a material. FTIR has been successfully utilized to characterize

many sulfonated polymers.

The chemical structure of the SPEEK membranes was analyzed by FTIR spectra. The FTIR spectra of PEEK and SPEEK samples with different DS are shown in Figure 3.7. The broadband in SPEEK samples appearing at 3480cm^{-1} was assigned to O-H vibration from sulfonic acid groups interacting with molecular water. The aromatic C-C band at 1490cm^{-1} for PEEK was observed to split due to new substitution upon sulfonation. A new absorption band at 1080cm^{-1} which appeared upon sulfonation was assigned to sulfur-oxygen symmetric vibration O=S=O. The new absorptions at 1255 , 1080 , and 1020cm^{-1} which appeared in sulfonated samples were assigned to the sulfonic acid group in SPEEK^[156].

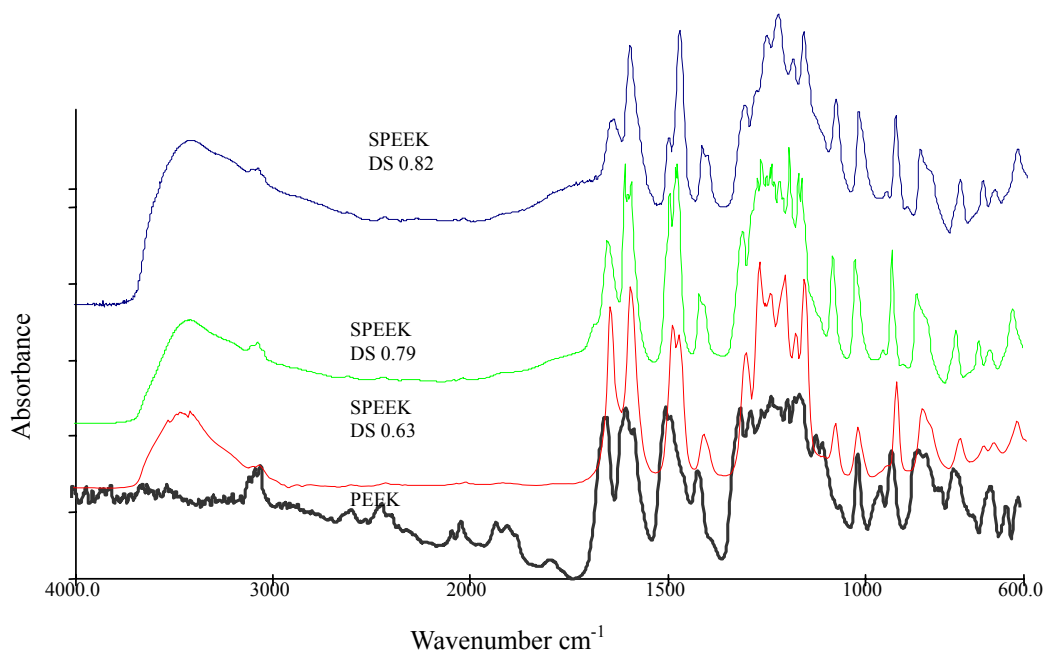


Figure 3.7: Comparative FTIR spectra of PEEK and sulfonated PEEK

It can be conformed from FTIR data that PEEK is sulfonated at one position of the phenylene ring between the ether groups as the intensity of the absorption band of SPEEK at 1080 cm^{-1} assigned to the monosubstituted benzene ring decreased with increasing DS; while the intensities of the absorption bands at 1020 cm^{-1} and 730 cm^{-1} are attributed to a para-substituted benzene ring and the S-O stretching vibration increased with increasing DS ^[156] respectively. The FTIR spectral data thus indicate that sulfonation of PEEK in sulfuric acid only takes place at the para position of the terminal phenoxy group.

These results are consistent with the reports of Jin et al. ^[150] that the maximal DS = 1.0 and which only occurs on the four chemically equivalent positions of the hydroquinone segment ^[153]. Sulfonated PEEK was prepared via the sulfonation reaction using concentrated sulfuric acid at room temperature. Sulfonation on this ring does not exceed DS = 1.0 under ambient condition, due to the sulfonation of PEEK at room temperature in concentrated sulfuric acid places less than one sulfonic group per repeat unit ^[154, 157, 158]. They confirmed (Figure 3.8) that sulfonation occurred exclusively on the hydroquinone segment, which is consistent with the results of Jin et al. ^[150]. The electron-withdrawing deactivating effect of the $-\text{SO}_3\text{H}$ group once it is introduced in that ring. The other two phenyl rings connected through ether linkages are therefore deactivated for electrophilic sulfonation by the electron-withdrawing effect of the carbonyl group.

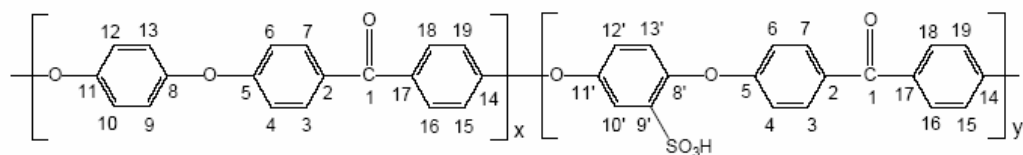


Figure 3.8: Structure and atom numbering of SPEEK, $x + y = n$, $y/(x + y) = DS$ ^[150]

3.3.4 Methanol permeability (methanol cross-over)

Before methanol permeability measurement, all the membrane samples were soaked in water for hydration. Figure 3.9 shows the resulting methanol permeability of these SPEEK membranes at room temperature.

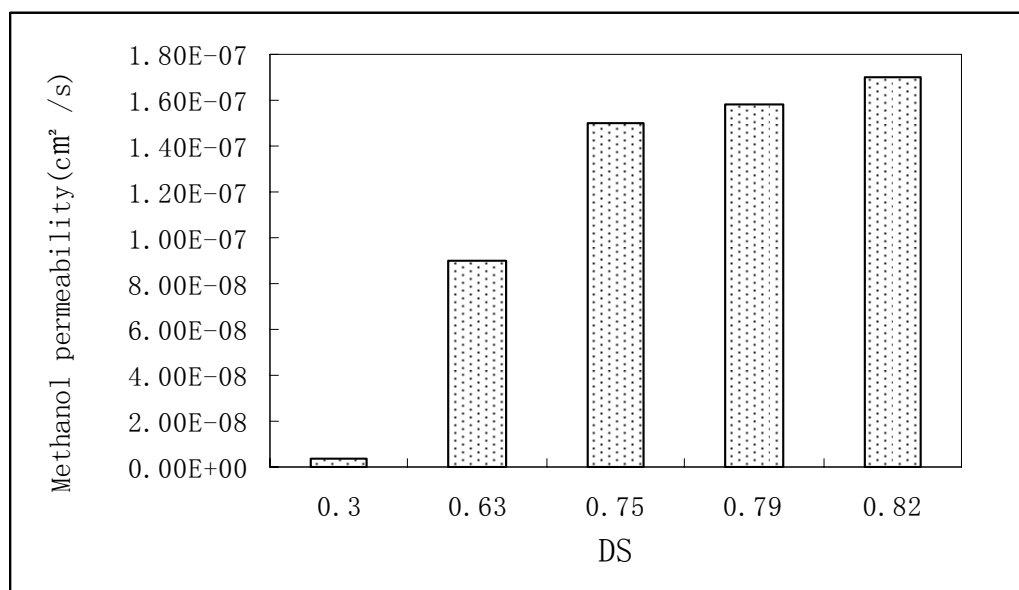


Figure 3.9: Influence of DS on methanol permeability

The methanol permeability of SPEEK membranes increases with incremental DS. The measured methanol permeability of Nafion[®] 117 membrane is $1.39 \times 10^{-6} \text{ cm}^2/\text{s}$ at

room temperature, which corresponds with the literature result of $1.41 \times 10^{-6} \text{ cm}^2/\text{s}$ [159]. It is noticeable that the methanol permeability of SPEEK membranes is considerably smaller than that of Nafion[®] 117 membrane, which is consistent with the references [86, 87, 150, 155, 156]. The highest methanol permeability with DS = 0.82 is only $1.80 \times 10^{-7} \text{ cm}^2/\text{s}$.

3.3.5. Water uptake

The water uptake of SPEEK membrane as a function of DS measured at room temperature and at 80 °C is presented in Figure 3.10. It can be seen that water uptake is enhanced with increasing DS and temperature.

The main purpose of sulfonating PEEK is to enhance acidity and hydrophilicity, as it is known that the presence of water facilitates proton transfer and increases the conductivity of solid electrolytes.

It has been reported that the proton conductivity of SPEEK depends on DS, pre-treatment of the membrane, hydration state, temperature and ambient relative humidity [160]. The proton conductivity of the ionomeric membranes depends on the number of available acid groups and their dissociation capability in water, which is accompanied by the generation of protons. As water molecules dissociate acid functionality and facilitate proton transport, water uptake is an important parameter in studying proton exchange membranes.

Excessively high levels of water uptake can result in membrane dimensional

change leading to failures in mechanical properties and, in extreme cases, solubility in water at elevated temperatures, so it is important to know the relationship between DS and water uptake for membranes.

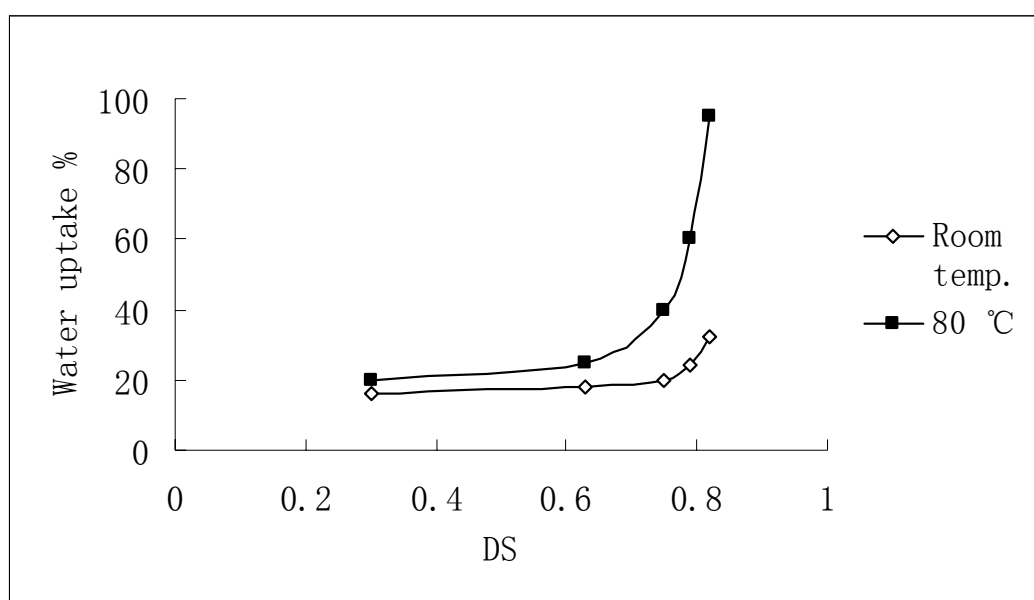


Figure 3.10: Water uptake as a function of DS at room temperature and at 80°C

3.3.6. Conductivity

The conductivities of the membranes were measured in a fully hydrated condition at room temperature. The effect of DS on the conductivity of SPEEK membranes at room temperature is shown in Figure 3.11. It shows that conductivity increases with the degree of sulfonation of the SPEEK.

The conductivity was found to increase with DS and reached a value of 2.5×10^{-2}

S/cm at DS = 0.82. This is explained by the SPEEK membrane becoming more hydrophilic and absorbing more water (see Figure 3.10), which facilitates proton transport. Therefore, sulfonation raises the conductivity of the PEEK not only by increasing the number of protonated sites (SO_3H), but also through formation of water mediated pathways for protons.

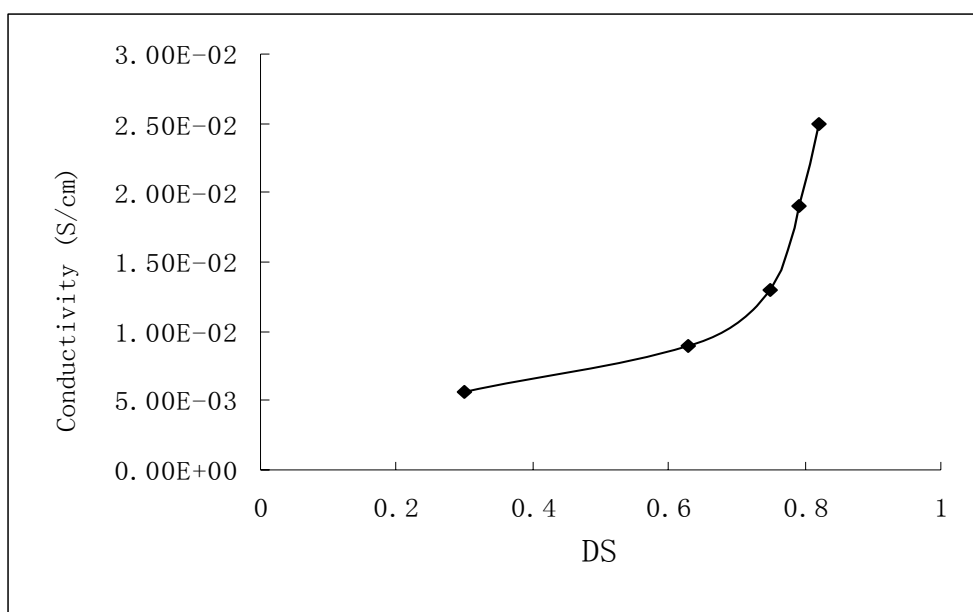


Figure 3.11: Conductivity of the membranes with different DS

The proton conductivity at DS = 0.82 is the highest measured among these SPEEK membrane in this study, but, the water uptake value is also extremely high at 80 °C. As excessively high levels of water uptake can result in membrane dimensional change leading to failures in mechanical properties, it is considered an unsuitable membrane. Table 3.3 shows that SPEEK membranes with DS close to 1.0 could be

dissolved when immersed in water at room temperature. The SPEEK membrane with $DS = 0.79$ which possesses high conductivity and suitable water uptake was chosen for further study.

3.4. Summary

In this study, a relatively cheap and high proton conductive material has been obtained by sulfonating PEEK. A series of SPEEKs were prepared and investigated.

TGA analysis shows that SPEEK was thermally stable over the temperature range of fuel cell application and that the DS of SPEEK increases with sulfonating time. FTIR spectral data indicate that the sulfonation of PEEK in sulfuric acid only takes place at the para position of the terminal phenoxy group. It was also mean that water uptake increased with increasing DS and temperature but that with DS close to 1.0, SPEEK membrane is soluble in water. The proton conductivities at room temperature were measured and found to increase with increasing DS and temperatures.

SPEEK membranes with DS values ranging from 0.3 up to 0.82 show conductivity values from 5.6×10^{-3} to 2.5×10^{-2} S/cm at room temperature.

The prepared SPEEK membranes with DS = 0.6 – 0.79, possess reasonable conductivities and thermal stability, properties which are considered apply to DMFC. For the purpose of improving the properties of the SPEEK membranes, especially increasing conductivity and reducing the extremely high water uptake, SPEEK with DS = 0.79 is chosen as the material for further investigation.

CHAPTER 4

Preparation and Characterization of SPEEK/ZP composite membranes

4.1. Introduction

In this chapter, new organic–inorganic SPEEK/ZP composite membranes based on SPEEK with incorporation of phosphorized zirconium oxide nano-particles (ZP) for application in DMFCs were prepared and investigated.

SPEEK membranes exhibit reasonable conductivity, thermal and chemical stability, depending on DS. Zirconium phosphate could be the material of choice for large scale application due to its stability, low cost and low toxicity, and which is also promoted as environmentally friendly. Zirconium phosphate has the features of increasing conductivity by using high proton mobility on the surface of the particles, and good water retention. The reduced methanol permeability of the polymer membrane while maintaining high power density is obtained by impregnating it with zirconium phosphate^[161-163].

This approach of impregnating polymer membrane with zirconium phosphate was adopted in order to improve proton conductivity and reduced the methanol crossover and in the present work consists of synthesizing composite membranes by incorporating inorganic proton conductive material into sulphonated PEEK polymer. In this study an alternatively inorganic material, phosphorized zirconium oxide nanoparticles (ZP) is chosen because of the following properties:

1. It has high proton conductivity when humidified (approaching 10^{-2} S/cm) and high surface area as V. Guntars reported in [164].
2. It can reduce the methanol permeability as reported by Nobanathi Wendy Maxakato in [169].
3. It is a high hydrophilic material.
4. It is easily synthesized.
5. It is a cheap material.

When appropriately embedded in a hydrophilic polymer matrix, the phosphorized zirconium oxide nano-particles (ZP) particles are expected to endow the composite membrane with their high proton conductivity and reduced methanol permeability, while retaining the desirable mechanical properties of the polymer film. The binder matrix was SPEEK. The sulfonated form of PEEK was used in order to provide the polymer matrix with some hydrophilicity. This chapter reports on the electrical and thermal properties of these new SPEEK/ZP composite membranes as a potential alternative to perfluorinated membranes in DMFCs.

4.2. Experimental

4.2.1. Chemical materials

The chemical materials used are presented in Table 4.1.

Table 4.1: Chemical materials

Chemicals	Specifications	Supplier
N, N Dimethylacetamide (DMAc)	99.8%	Aldrich Chemical Corp
Sulfonated PEEK with DS value of 0.79		Prepared in our Lab. The detailed procedure was shown in Chapter 3
Zirconium oxide nono-particles	Nano-sized	Degussa
Acetic acid	99.8%	KIMIX
Phosphoric acid	85%	KIMIX
Nafion solution	5 wt% in a mixture of lower aliphatic alcohols and water	Aldrich
Sulfuric acid (95–98 wt%)	98%	KIMIX
Methanol	99.5%	KIMIX
Feul cell anodic catalyst on carbon black	Pt 19.20 wt%, Ru 10.30 wt., 2.1 nm size	Alfa Aesar; Johnson Matthey
Feul cell cathodal catalyst on carbon black	Pt 38.530 wt%, 3.8 nm size	Alfa Aesar; Johnson Matthey
Carbon cloth		DTEK

4.2.2. Preparation of composite membranes

4.2.2.1. Preparation of ZP

ZP was prepared according to the method described in [164, 165]. Treatment of ZrO_2 with phosphoric acid solution is called phosphorization.

At first, a ZrO₂ nano-particles suspension was prepared by mixing 3 g of ZrO₂ nano-particles powder with 2.08 M acetic acid solution. The mixture was stirred with a magnetic stirrer and under ultrasonic vibration to disperse the ZrO₂ particles. 50 ml of phosphoric acid solution (5 wt% in water) was added into the ZrO₂ nano-particles suspension to phosphorize the ZrO₂. After 1 hour of magnetic stirring and further 1 hour ultrasonic vibration, the mixture was heated up to 90 °C in an oven, allowed to cool down to room temperature, then the resultant precipitate was filtered and dried.

4.2.2.2. Pre-treatment of SPEEK

According to the results presented in the Chapter 3, prepared SPEEK with DS = 0.79 was chosen as the basic polymer for synthesizing composite SPEEK/ZP membrane.

The SPEEK (DS = 0.79) was placed in 1 M methanol solution. After heating to boiling, the SPEEK was filtered, washed with deionized water, and dried.

The SPEEK solution was prepared by dissolving the pre-treated SPEEK in N, N-dimethylacetamide (DMAc) to give a 5 wt% solution. The solution was filtered, and kept for later use.

4.2.2.3. Membrane preparation

The SPEEK solution was mixed with different weight of ZP. The mixture was magnetically stirred and heated up to 60 °C for 2 hours, followed by ultrasonic vibrations for 1 hour to disperse the particles of the ZP fully into the mixture.

After further magnetic stirring for 1 hour, the mixture was cast onto a flat plate. The solvent (DMAc) of the casting membrane was elaborately heating in a vacuum oven at 60 °C for 48 hours, then up to 120 °C for 24 hours. After cooling down to room temperature, the resultant membranes were peeled from the glass after immersion in deionized water for 30 minutes.

A series of composite membranes with different ratios of SPEEK/ZP were synthesized. Before testing the conductivity and fuel cell testing, the membranes were activated with 1M sulfuric acid solution at 80°C for 24 hours. All the composite membranes were kept in deionized water before testing. The thickness of the dried composite membranes was at the range of 0.09-0.2 mm.

4.2.3. Characterization of SPEEK/ZP composite membranes

4.2.3.1. *Fourier Transform Infrared (FTIR) study*

The chemical structure of the prepared ZP was studied and compared with ZrO₂ by FTIR analysis.

ZP and ZrO₂ were ground into fine powders with mortar and pestle and dried in an oven at 110 °C overnight to remove water. After 24 hours, the samples were mixed with dried KBr (ZP or ZrO₂/KBr = 1 wt%/99 wt%). The powdered mixture was placed in a sample holder. A spectrum was first obtained using blank KBr powder before the samples were run. The sample was tested and absorbance spectra were recorded in scanning range of 400-4000 cm⁻¹.

The infrared spectra of SPEEK/ZP membrane were also carried out in this study. The method is the same as described in Chapter 3 (see page 43).

4.2.3.2. X-Ray Diffraction (XRD)

The chemical composition and crystalline structure of the prepared ZP and ZrO₂ were determined by XRD. The XRD was performed using Philips equipment. The specifications and the working parameters are given in Table 4.2.

Table 4.2: The specifications and working parameters of XRD

Goniometer	PW1050
Detector	PW3011
XRay tube	PW2233 Cu NF
Automatic divergence slit	12mm
Anti scatter slit	4 degrees
Receiving slit	0.1mm
The software used	Philips X'Pert software
Working angle	between 0 and 90°

4.2.3.3. Thermal gravimetric analysis (TGA)

The procedure is the same as described in Chapter 3 (see page 43).

4.2.3.4. Water uptake

The method of water uptake measurement is the same as described in Chapter 3 (see page 44).

4.2.3.5. Measurement of methanol permeability

The procedure of measurement of methanol permeability is the same as described in Chapter 3 (see page 46).

4.2.3.6. Scanning Electron Microscope (SEM) (Study of surface morphology)

The morphological studies were performed using a Hitachi x650 Scanning Electron Microscope (SEM).

Specimens for the SEM were prepared by freezing the dry membrane samples in liquid nitrogen and then breaking the membranes into small pieces. Thereafter, pieces of the fractured membranes were mounted on aluminum stubs and vacuum sputtered with a thin layer of gold for 4 minutes to facilitate conduction. Table 4.3 describes the SEM operating parameters.

The cross section of the MEA was also examined by the same instrument.

Table 4.3: Operating parameters of SEM

Equipment	Hitachi x650			
Accelerating voltage	Aperture	Tilt Angle	Resolution	Working distance
25 kV	0.4 mm	0°	6 nm	15 mm

4.2.3.7. *Electrochemical measurements (Cyclic voltammetry: Electrochemical stability)*

The redox behavior of the SPEEK/ZP composite membrane was investigated by cyclic voltammetry on the Pt/electrolyte interface, and performed on an Autolab PGSTAT30 (Eco Chemie, Netherlands) at room temperature. For this study, the membrane was placed between a platinum counter electrode and a working platinum microelectrode, and performed at a scan rate of 5mv/s. The reference electrode was the Ag/AgCl electrode ^[166].

4.2.3.8. *Measurement of proton conductivity*

The conductivities were measured from room temperature up to 100 °C. The procedure of the measurement is the same as described in Chapter 3 (see page 45).

4.2.4. DMFC testing

4.2.4.1. *Preparation of the membrane-electrode assembly (MEA)*

Pt catalyst for the cathode and Pt-Ru for the anode supported on commercial carbon cloths were used in this study. The catalyst loading for all electrodes (anode and cathode) used in the experiments was 2 mg/cm².

The catalyst ink, for both anode and cathode, was prepared by mixing the alcoholic Nafion[®] solution with the catalyst powders, and dispersing the powder by magnetic stirring and ultrasonic vibration to form the catalyst ink. The electrodes were prepared by brushing the prepared catalyst ink on carbon cloth

backings. On each electrode, approximately 2 mg/cm^2 of catalyst was coated. The loading was determined by weighing the dried electrode.

The membrane-electrode assembly (MEA) was manufactured by hot-pressing the electrode onto the membrane at $130 \text{ }^\circ\text{C}$ and 140 bar for 2 min. The geometrical area of both electrodes was 4 cm^2 . Figure 4.1 shows the procedures.

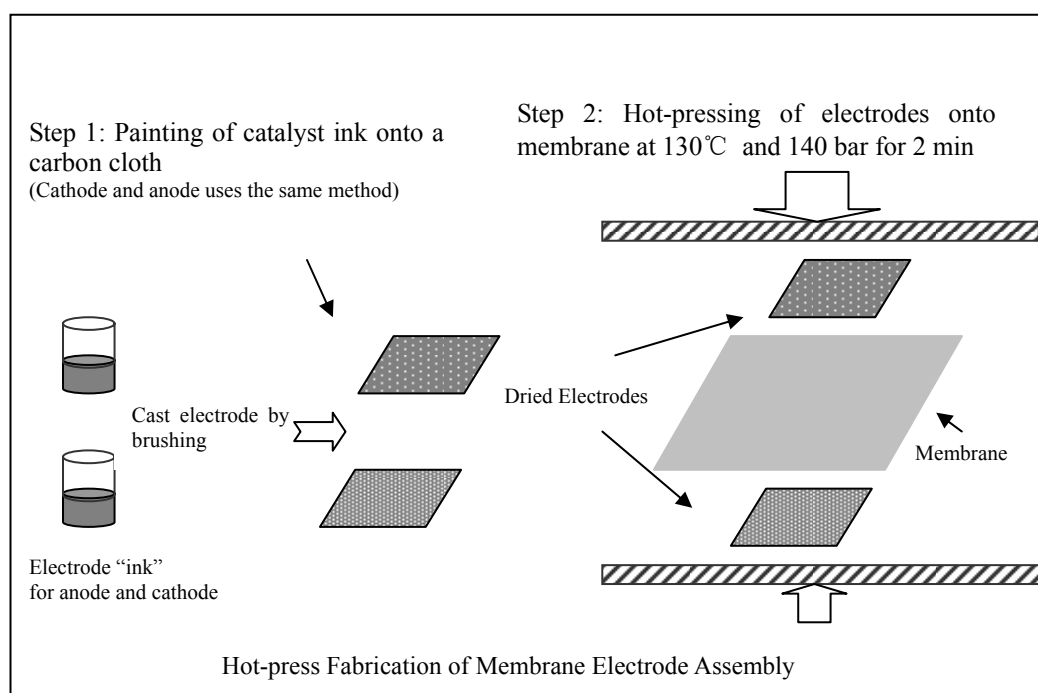


Figure 4.1: The procedures of membrane-electrode assembly

4.2.4.2. Assembly of Single cell and testing

The single cell was assembled by mounting the MEA into cell endplates. The endplates used were purchased from Lynntech (see Figure 4.2). The flow fields for the reactants used were of serpentine configuration with three serpentines connected in parallel. The endplates are also fitted with holes to accommodate a heating cartridge and a thermocouple for the temperature controller.

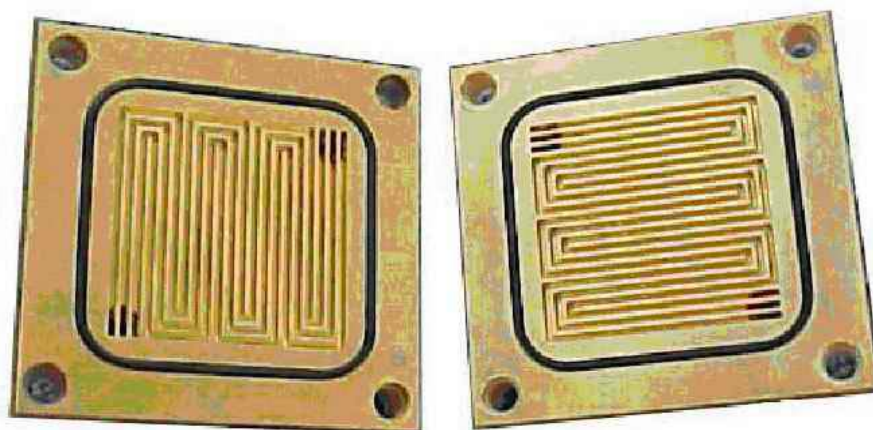


Figure 4.2: Lynntech endplates

The operating temperature of the cell was 80 °C. 1 M methanol solution was pumped through the DMFC anode at a flow rate of 1 ml/min, and air was fed to the cathode at 0.5 L/min at a pressure of 2 bars.

An experimental set-up for DMFC testing is shown in Figure 4.3. The MEA was tested by a Fuel Cell testing station which was controlled by a LYNNTTECH controller. The data was collected by Auto Lab.

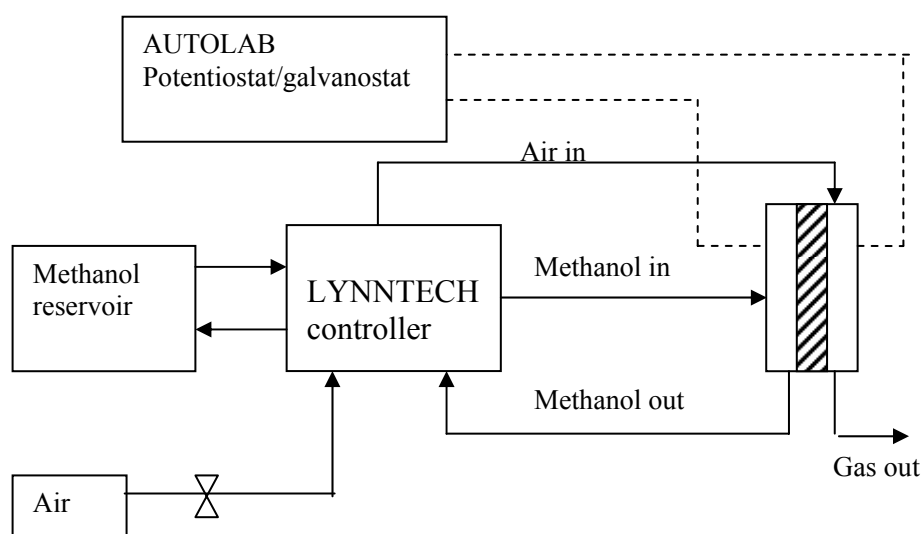


Figure 4.3: Schematic overview of the experimental setup for DMFC testing

4.3. Results and discussions

4.3.1. Fourier Transform Infrared (FTIR) spectroscopy

The FTIR technique proved to be a useful tool to show the conversion of zirconium oxide nano-particles (ZrO_2) to ZP via phosphorization. Figure 4.4 shows the infrared spectra of ZP and zirconium oxide nano-particles. The new peak at $\sim 1050\text{ cm}^{-1}$ is characteristic of the P-O stretching mode of the phosphate group ^[167], and the weak band at 1680 cm^{-1} results from the P=O vibration. It proves that a new chemical structure has been formed by the phosphorization. Water peaks were observed in the region between 2500 cm^{-1} and 3600 cm^{-1} . Figure 4.5 shows the infrared spectra of SPEEK/ZP composite membrane, SPEEK membrane and ZP. However, the infrared spectrum of SPEEK/ZP did not show the peaks assigned to the sulfonic acid group and P-O stretching vibration. It might be due to the fact that their individual vibration bands are in the same wave number region of 1000 cm^{-1} to 1700 cm^{-1} . It is noticeable that the water peaks of SPEEK/ZP and that of ZP were intense. Without doubt, ZP quickly absorbed moisture from the atmosphere before testing the dried samples by FTIR. These results confirm that ZP is a strongly hygroscopic and hydrophilic material.

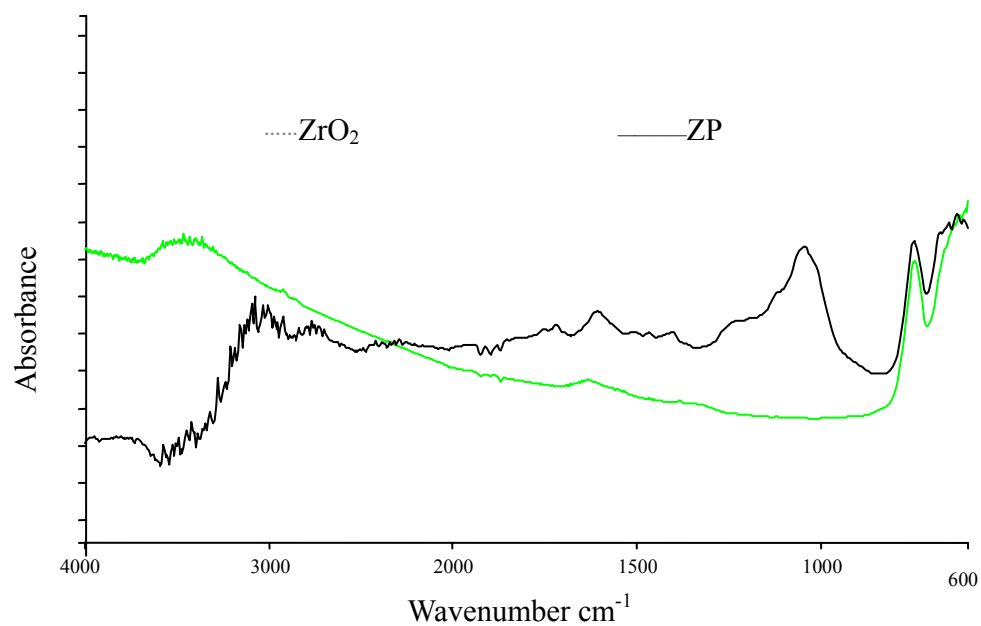
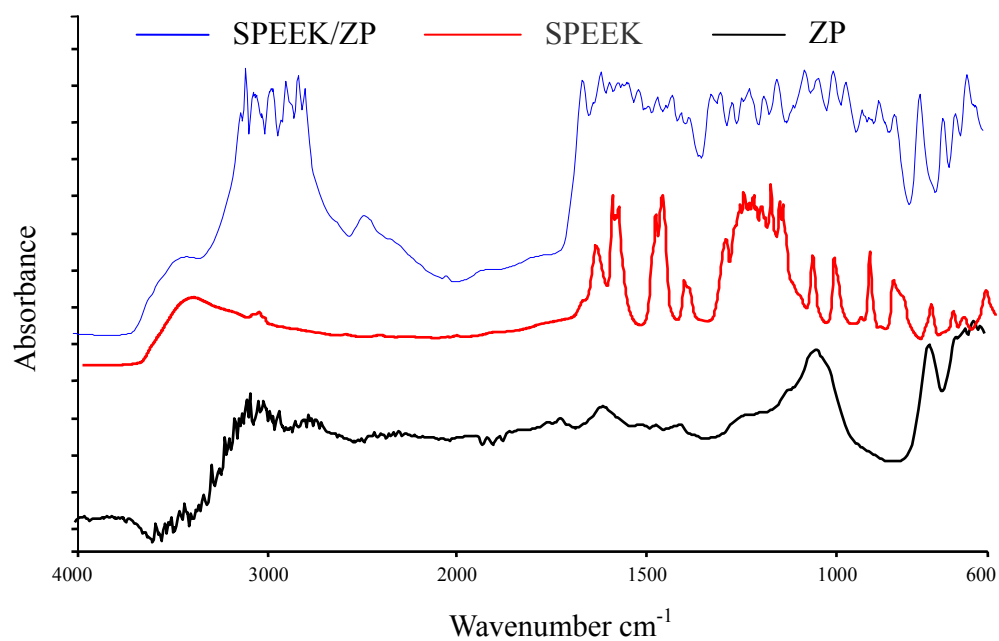
Figure 4.4: FTIR of ZrO_2 and ZP

Figure 4.5: FTIR of SPEEK, ZP and composite membrane

4.3.2. X- Ray Diffraction (XRD)

The X-ray diffraction pattern of ZrO_2 and ZP are shown in Figure 4.6. The X-ray diffraction analysis of ZrO_2 revealed the presence of both monoclinic and tetragonal structures. The Bragg angles (2θ) of the monoclinic structure appears at 24.4° , 28.2° , 31.5° , 34.5° and 62.3° , whereas the angles for the tetragonal structure are 30.2° , 50.2° , 50.7° , 59.3° and 60.2° [168]. X-ray diffraction analysis of ZP is almost the same as that of ZrO_2 . This shows that crystalline zirconium phosphate does not exist in the ZP sample. It means that the bulk structure of the nano-sized ZrO_2 did not change after phosphorization by phosphoric acid solution. However, FTIR analysis of phosphated ZrO_2 shows that there is zirconium phosphate existing in phosphated ZrO_2 . Combining the results of XRD and FTIR, it suggests that the bulk structure of ZrO_2 was not changed and that phosphorization only occurred on the surface of the nano-sized ZrO_2 . The reason why the XRD of ZP doesn't show the characteristic peaks of ZP, is because the ZP is amorphous and only a single layer of ZP is formed on the surface of nano-sized ZrO_2 .

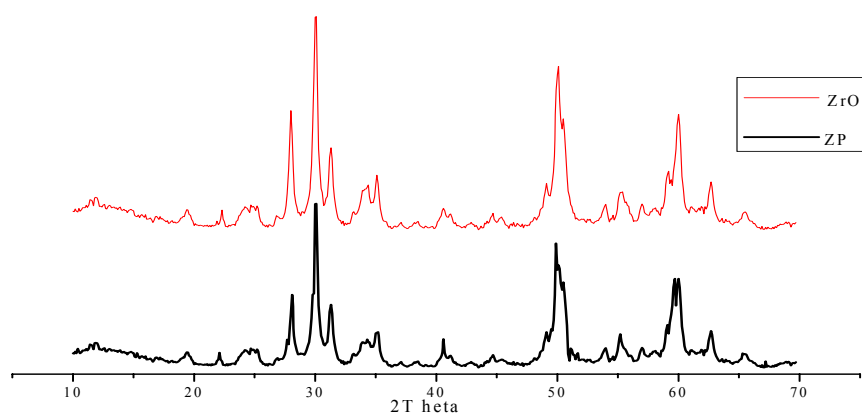


Figure 4.6: The XRD patterns of nano-sized ZrO_2 and ZP

4.3.3. Thermo-stability study by Thermo-gravimetric Analysis (TGA)

The thermal stability of the membranes was studied by TGA analysis. The resulting data for the PEEK, SPEEK and SPEEK/ZP composite membranes are displayed in Figure 4.7. The PEEK polymer powder displays thermal stability up to 550 °C. There are three weight losses for the SPEEK and SPEEK/ZP composite membranes samples. They are physically absorbed water, the splitting off of the sulfonic acid group ^[100], and the decomposition of the main chain of PEEK, respectively. However, by reason of the ZP incorporation, the trend of the last weight loss (decomposition of the main chain of PEEK) of the composite is slower than pure SPEEK's. From the TGA analysis, it is shown that the thermo-stability of the composite membranes is quite similar to that of pure SPEEK membrane. Both of them are stable at temperatures lower than 300 °C. The results suggest that these composite membranes have adequate thermal properties for application in fuel cells.

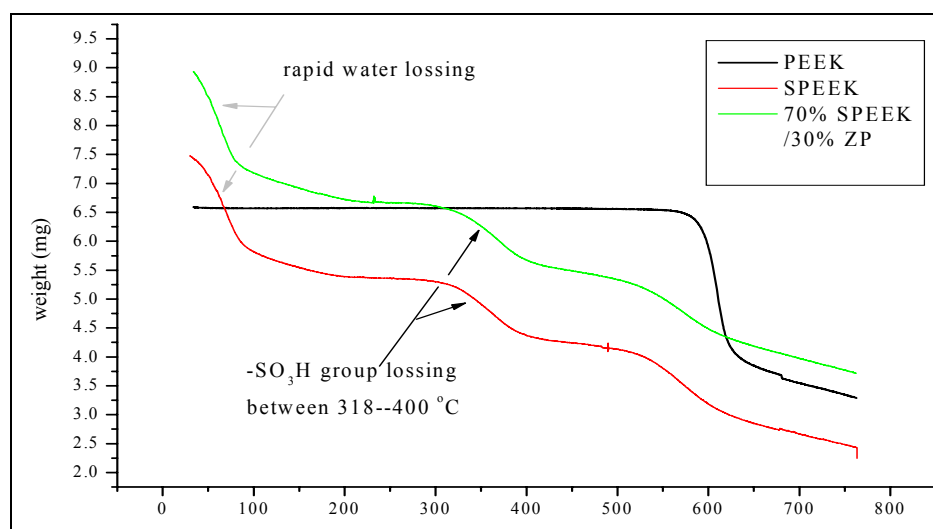


Figure 4.7: Thermo-gravimetric curves of PEEK, SPEEK and SPEEK/ZP

4.3.4. Water uptake

From Figure 4.8 it is observed that, for the composite membranes, water uptake was slightly decreased with the incorporated ZP content at room temperature. The water uptake of the composite membranes was obviously reduced with the incorporated ZP at 80 °C compared to at room temperature. For pure SPEEK membranes (ie. 0wt% ZP), water uptake was obviously increased at 80 °C compared to at room temperature. It is the ratiocination that the major reason for the increasing water uptake is caused by SPEEK absorbing more and more water with the temperature rise. Another reason might be suggested that there are many empty spaces within the SPEEK membrane, which accounts portion of the water uptake. However, the incorporation of nano-sized ZP into the polymer matrix could fill the free spaces within the membrane, thereby reducing the extent of the water uptake. Therefore, according to this thinking the incorporated ZP can retard the water uptake of the modified SPEEK-based membrane in particularly at higher temperature.

For each membrane (pure SPEEK membrane and SPEEK/ZP membrane), water uptake was increased from room temperature up to 80 °C. Comparing with this result and the corresponding proton conductivity in Figures 4.12 (see page 83), it can also be observed that higher water uptake is associated with higher proton conductivity, thus showing the importance of sorbed water in the proton conductivity of membranes, which is in agreement with previous studies^[140].

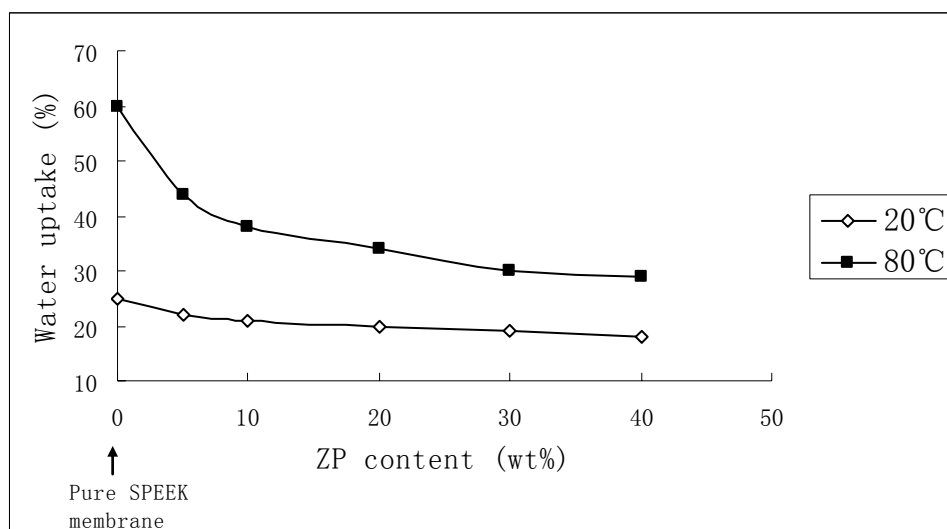


Figure 4.8: Water uptake of the membranes with different ZP content

4.3.5. Methanol permeability

The values of methanol permeability of the membranes are shown in Table 4.4.

Table 4.4: Present properties of the membranes

Membrane type	Conductivity (S/cm) at room temperature (20 °C)	Conductivity (S/cm) (80 °C)	Water uptake (wt%) room temperature (20 °C)	Water uptake (wt%) (80 °C)	Methanol Permeability (cm ² /s)	tretching capability
Pure SPEEK	0.0185	0.0324	25	60	1.58×10^{-7}	↓
SPEEK/ZP5 (5 wt% ZP)	0.0186	0.0400	22	44	1.13×10^{-7}	
SPEEK/ZP10 (10 wt% ZP)	0.0186	0.0410	21	38	1.50×10^{-7}	
SPEEK/ZP20 (20 wt% ZP)	0.0188	0.0425	20	34	4.30×10^{-7}	
SPEEK/ZP30 (30 wt% ZP)	0.0190	0.0435	19	30	5.80×10^{-7}	
SPEEK/ZP40 (40 wt% ZP)	0.0197	0.0460	18	29	6.380×10^{-7}	

The permeability of the pure SPEEK is $1.58 \times 10^{-7} \text{ cm}^2/\text{s}$, it is much lower than that of Nafion[®] ($1.39 \times 10^{-6} \text{ cm}^2/\text{s}$). However, the composite membrane (containing 5 wt% of ZP) exhibited a 28.5% reduction of methanol permeability compared to the pure SPEEK membrane. It is remarkable that this value is 12 times lower than that of Nafion[®] 117 ($1.39 \times 10^{-6} \text{ cm}^2/\text{s}$) measured at room temperature, which corresponds with the literature result of $1.41 \times 10^{-6} \text{ cm}^2/\text{s}$ [159]. However, the methanol permeability compared with that of SPEEK membrane was slightly increased when the incorporated ZP content exceeded 10 wt%. Figure 4.9 shows the influence of incorporated ZP content on methanol permeability.

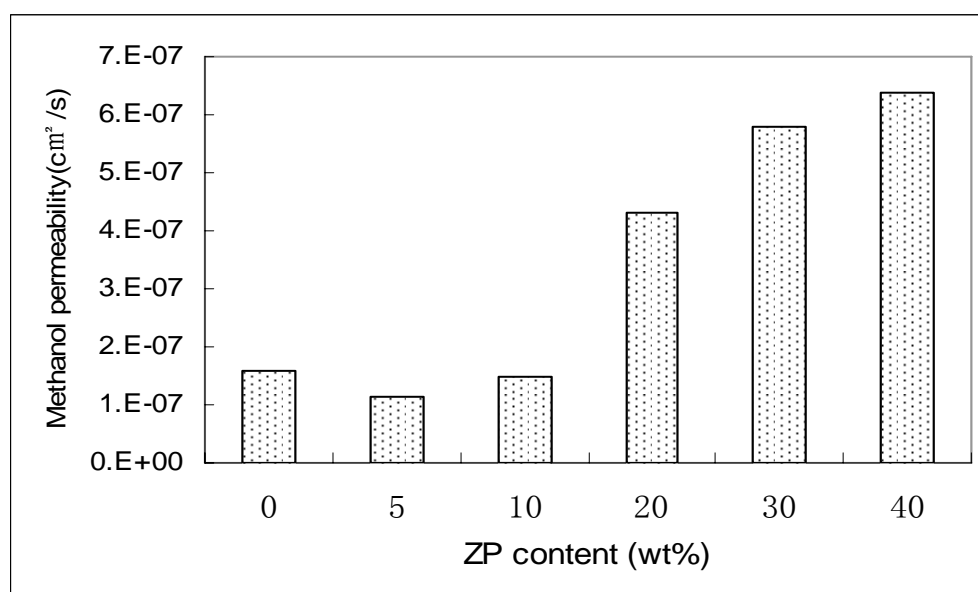


Figure 4.9: Effect of incorporated ZP content on methanol permeability

The decrease of the methanol permeability is believed to derive mainly from the enhanced barrier properties of the membranes due to the incorporation of

small size ZP nano-particles as the fillers. The incorporated nano-sized inorganic particles blocked the channels to methanol passing. It is believed that with rising ZP content, there is not enough SPEEK polymers surrounding and bonding all the ZP particles. It is also believed that on a random area of the surface, sufficient number of empty spaces between the incorporated ZP particles could form several inorganic physical channels (ZP channels). The number of the channels formed increases with increasing ZP content. These ZP channels could possibly transport methanol across the membrane. The methanol permeability increases with the amount of the incorporated ZP because more channels are formed. The low incorporated ZP nano-particles could highly dispersed within the membrane by polymer bonding and the nano-particles acted as the barriers, but incorporating high ZP content into the composite membrane, the ZP channels could formed and as transporting channel for methanol.

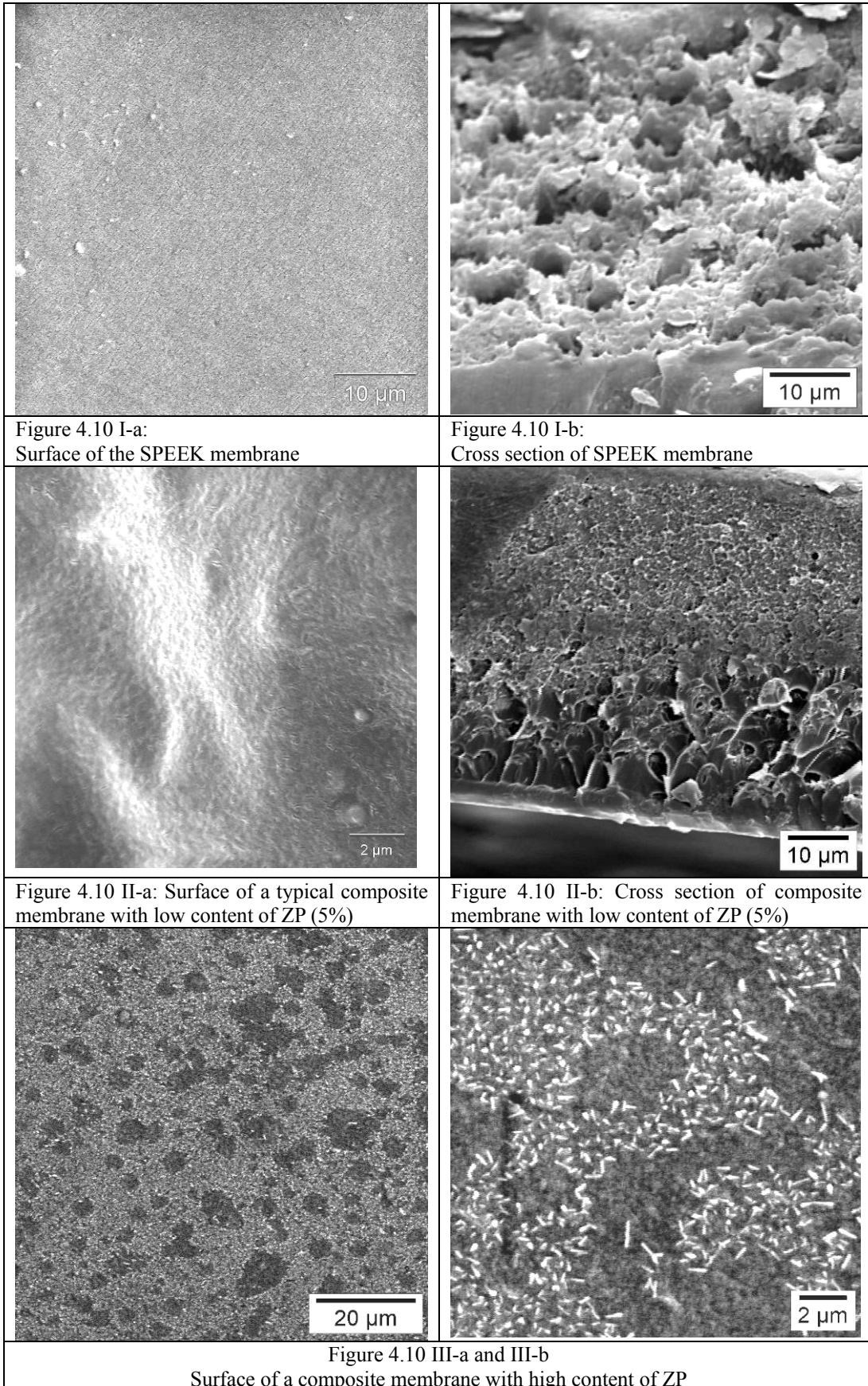
4.3.6. Morphology

The morphology of the membranes was studied by scanning electron microscopy. SEM micrographs of pure SPEEK membrane and typical examples of the composite membrane are presented in Figure 4.10. The micrographs show that the solid ZP is well mixed with SPEEK and shows no agglomeration after membrane preparation within the low ZP content SPEEK/ZP composite membrane –the nano-sized ZP particles are observed to be homogeneously distributed. Figures 4.10 I-a and 4.10 I-b are micrographs of the surface and the cross-section of the pure SPEEK membrane. The typical micrographs show in

Figure 4.10 II-a and 4.10 II-b the surface and the cross section resp. of the SPEEK/ZP composite membrane, show that the SPEEK/ZP composite membrane with low ZP incorporation (5 wt%), is denser than pure SPEEK membrane.

Figures 4.10 III-a and 4.10 III-b are micrographs of the membrane with high ZP content (30 wt%). It is observed that there are many ZP particles within the membrane. Some ZP without surrounding polymers can form “ZP channels”. The number of “ZP channels” can be increased with rising ZP content.

The cross-section’s SEM micrographs of the membranes show that the inner of the pure SPEEK membrane is incompact compared with other SPEEK/ZP composite membranes. It has noted that incorporated ZP influenced the physical structure of the membranes. The structure of the SPEEK/ZP composite membrane is markedly enhanced with low ZP incorporation (5 wt%). It is the densest among these membranes. It has been pointed that properly incorporating ZP can improve the structure of the membrane. However, high ZP incorporation results to form “ZP channels”. It impairs the structure of the membrane again.



4.3.7. Electrochemical stability

The redox behavior of the electrolytic membrane was investigated by cyclic voltammetry on the Pt/electrolyte interface. The electrochemical stability window, defined as a potential region where no appreciative faradic current flows, is limited to its cathodic and anodic parts, where the reduction or oxidation of the polymer or H^+ ion can take place. A broad stability window during the reduction and oxidation cycles is important for the practical use of these materials in contact with the electrolyte^[166]. Fig 4.11 gives the first (red) and 50th circle (black) of the cyclic voltammogram of the Pt electrode using the SPEEK/ZP (10 wt%) composite membrane. The cyclic voltammogram is just a little modified after 50 cycles as shown in Fig. 4.11. It demonstrates that the composite SPEEK/ZP membrane is very stable in the potential range between -0.75 and 1.25 V.

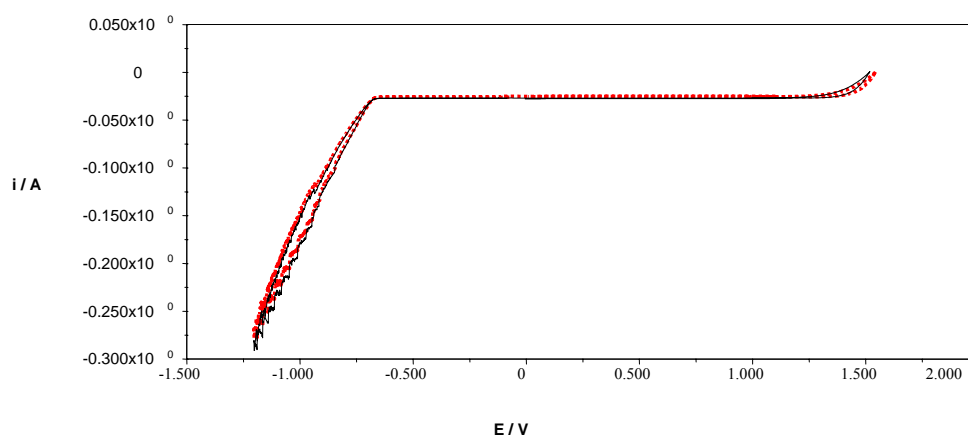


Figure 4.11: Cyclic voltammetry of SPEEK/ZP composite membrane, obtained at the symmetrical Pt| electrolyte| Pt cell at room temperature and a scan rate: 5 mv/s. Black curve: the first circle, Red curve: the 50th circle (both circles are almost superposed)

4.3.8. Proton conductivity

The conductivities of composite membranes with various ZP content were measured from room temperature up to 100 °C. The effect of temperature and ZP content on proton conductivity is presented in Figure 4.12 and which shows that conductivities increase with increasing temperature. SPEEK membrane losses the conductivity very quickly from 100 °C due to dehydration. However, the composite membranes show very good stability in maintaining conductivity when the temperature is 100 °C because the ZP can increase the capability of water retention. The conductivity of SPEEK/ZP composite membrane with 40 wt% of ZP is up to 0.045 S/cm at 100 °C.

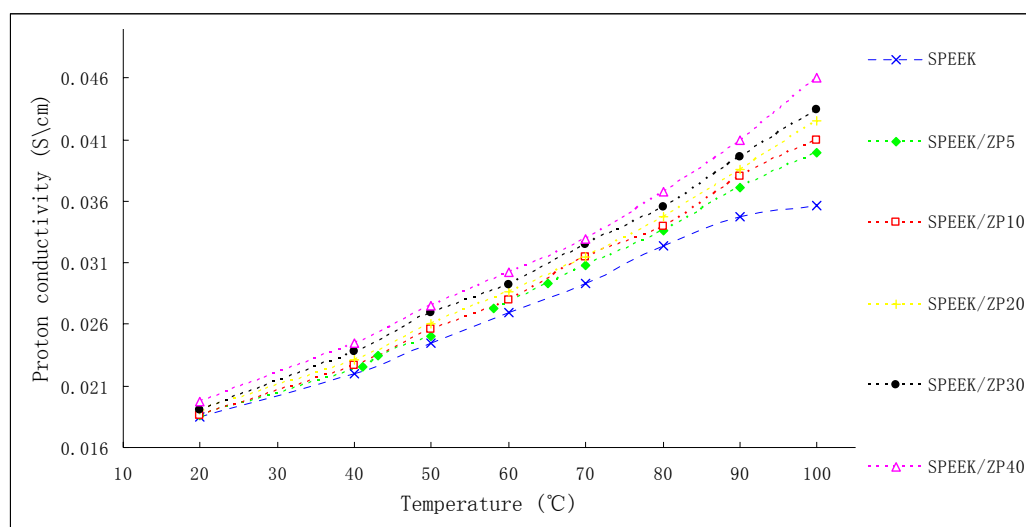


Figure 4.12: Proton conductivity of SPEEK/ZP composite membranes as a function of temperature

Figure 4.13 and Figure 4.14 show the proton conductivity of the composite membranes increases with the ZP content. Figure 4.13 shows that the proton

conductivity of these SPEEK/ZP composite membranes just slightly increases with incorporated ZP content at room temperature. However, the enhancement of conductivity of the composite membranes as function of the incorporated ZP content is obvious at 100 °C (see Figure 4.14). The conductivities of SPEEK/ZP composite membranes are higher than that of SPEEK.

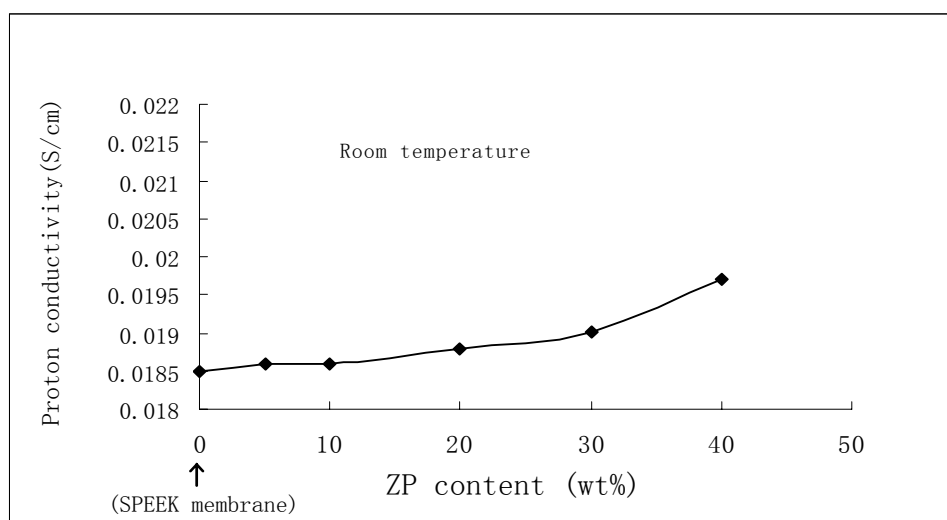


Figure 4.13: Effect of ZP content on proton conductivity at room temperature

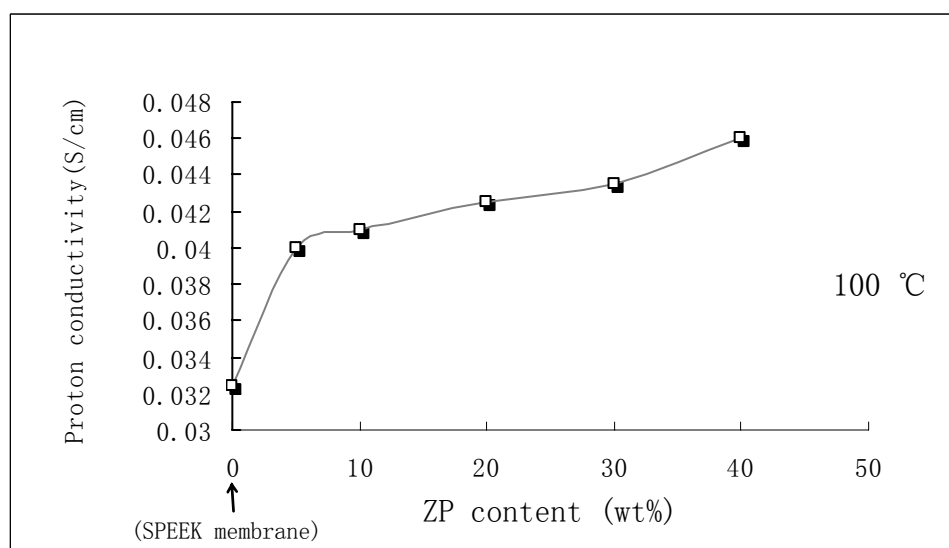


Figure 4.14: Effect of ZP content on proton conductivity at 100 °C.

From the above results, it is concluded that the water uptake reduces with the incorporation of ZP, but the conductivity of the composite membranes increases. The incorporated ZP nano-particles serve as conductors and fillers within the composite membranes. While ZP increases the proton conductivity, incorporated a small ZP content can also reduce water uptake and methanol permeability.

4.3.9. DMFC performance

A discharge curve of a single DMFC using a SPEEK/ZP composite membrane is shown in Figure 4.15. The curve was established after 100 hours of operation in the DMFC testing station. The operating temperature of the cell was 80 °C. 1 M methanol solution was pumped through the DMFC anode at a flow rate of 1 ml/min, and air was fed to the cathode at 0.5 L/min at a pressure of 2 bars. The open circuit potential is 0.65 V. A power density of about 15 mW/cm² was obtained with a current density of 50 mA/cm² at 0.3 V. From these results, the application of a SPEEK/ZP composite membrane with low wt% incorporated ZP in a single DMFC, shows promising performance. It is suggested that the low ZP content SPEEK/ZP composite membrane is a promising alternative proton exchange membrane for DMFC application.

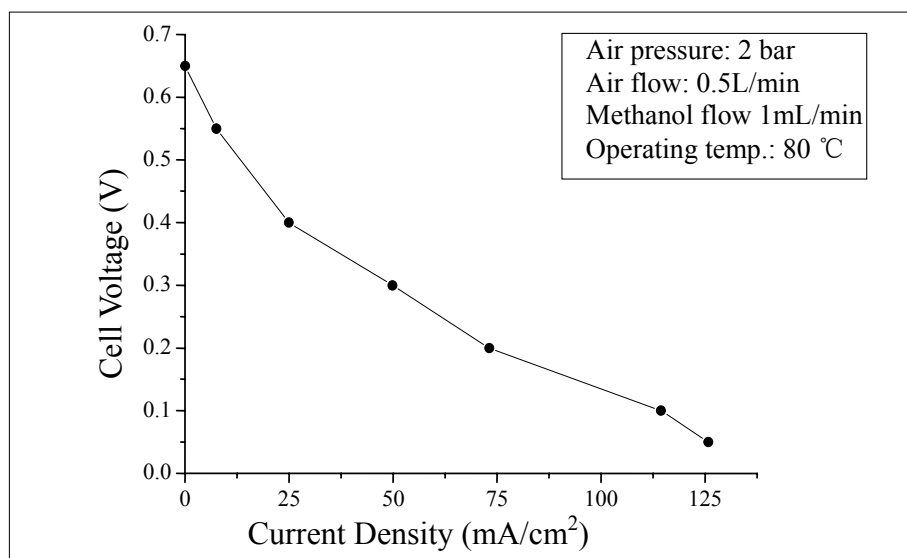


Figure 4.15: discharge curve of a single DMFC

After DMFC testing, SEM micrographs were taken of the MEA. Figure 4.16 is a typical SEM picture of the cross section of MEA, showing a gap between the membrane and electrode on the SEM picture. No doubt, if the gap was presented in the DMFC, it can be reduced the catalyst utilizing efficiency due to loss of DMFC reaction area. This problem can limit the performance of DMFC. It is believed to the combination of the SPEEK with the electrode was not strong via normal hot pressing method for Nafion[®] membrane. The effect of hot pressing in MEA on DMFC performance equipped with SPEEK/ZP composite membranes will be investigated in the future work.

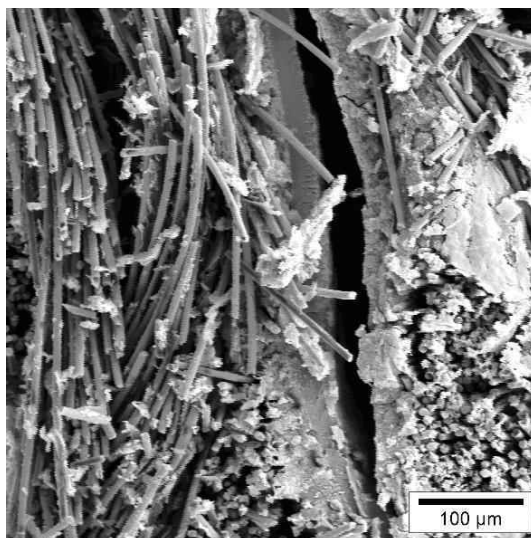


Figure 4.16: SEM of cross-section of MEA

4.4. Summary

A series of composite SPEEK/ZP membrane were synthesized and studied. The composite membranes were prepared by incorporating varying content of ZP into SPEEK with DS = 0.79. The conductivity of the SPEEK/ZP composite membranes was increased with the incorporation of increased ZP content. The high water uptake at high temperature was reduced by incorporated ZP (see Figure 4.8). The methanol permeability of SPEEK/ZP with low incorporated content ZP was reduced 28.5% compared to the SPEEK membrane. The composite membranes show a very good capability of maintaining conductivity at 100 °C.

These SPEEK/ZP (low wt%) composite membranes shown many advantages:

1. Simple synthesizing procedures;
2. Reasonable proton conductivity (it is close to Nafion recasting membrane);

3. Increased proton conductivity comparing with that of SPEEK membranes;
4. Reduction of the high water uptake value at higher temperature;
5. Largely reduced 28% methanol permeability with incorporated low ZP content (5 wt%);
6. Good thermal stability and good mechanical properties;
7. Promising cell performance in DMFCs;
8. The membranes are substantially cheaper than the perfluorinated based membranes;
9. Good stability demonstrated in maintaining conductivity at high temperature.

These results show that the SPEEK/ZP (low wt%) composite membrane holds promise when used in DMFC applications, especially the low methanol permeability and the promising DMFC performance which makes this membrane worthy of further study, e.g. the development of more suitable electrodes and electrode-membrane assemblies in the future.

CHAPTER 5

Preparation and Characterization of Nafion/ZP composite membranes

5.1. Introduction

DMFCs using proton exchange membrane polymer electrolyte offer the potential for high-energy efficiency and zero emissions when compared to internal combustion engines ^[5, 169, 170]. Perfluoro-ionomer membranes possess many advantages over other types of membranes. The best-known proton exchange membrane for application in fuel cells is Nafion[®] membrane, it has excellent chemical, mechanical and thermal stability and high protonic conductivity in its hydrated state.

However, the crossover of methanol through the electrolyte membrane in DMFCs and the lack of a stable intermediate temperature proton exchange membrane still restricts their performance and application. The methanol crossover to the cathode not only reduces fuel efficiency but also increases the overpotential of the cathode, resulting in lower cell performance. Operating a DMFC at elevated temperatures reduces the adsorption of CO onto the platinum electro-catalyst and improves the kinetics of methanol oxidation at the anode ^[171]. Meanwhile, it is expected to minimize problems due to electrode flooding and to lower the methanol crossover because of lower gas permeability of the polymer electrolyte at elevated temperature.

Unfortunately, Nafion[®] membrane is a poor barrier to methanol crossover ^[172]. In addition, the proton conduction mechanism of the perfluorosulfonic acid membrane relies on the presence of water; but there is a dramatic decrease of water uptake, proton conductivity at high temperature (above the boiling point of water) and consequently fuel cell performance will decrease.

So finding new proton conductive membranes with low methanol permeability and operating at elevated temperatures has attracted considerable attention. To still take advantage of Nafion[®] positive properties, strategies adopted include the incorporation of inorganic compounds with the aim of modifying Nafion[®] to simultaneously reduce the methanol permeability while preserving the water content and the high proton conductivity at high temperature. Of particular interest has been the incorporating of some conducting inorganic materials into the membranes, like zirconium phosphates ^[173–175] and phosphonates ^[176].

In this study, with the object to improve the proton conductivity of the perfluorosulfonic acid based membrane with low methanol cross-over for high temperature operation, a series of Nafion/ZP composite membranes were prepared and studied.

The Nafion/ZP composite membranes exhibit an increased ability to maintain proton conductivity at high temperature, and the methanol crossover is lower than that of Nafion. The observed characteristics of these composite membranes allow

them to be used as candidate electrolytes for the high temperature operation of the DMFCs.

5.2. Experimental

5.2.1. Preparation of ZP

The procedure is the same as described in Chapter 4 (see page 64).

5.2.2. Preparation of composite membranes

The composite membranes were prepared using 15 % Nafion[®] solution as the basic material. In each case, a membrane precursor solution containing Nafion[®] solution, additive (ZrO₂ nano-particles, ZP) was prepared. The detail was as follows: a 1:1 15% Nafion[®] solution/DMAc were mixed; the appropriate amount of additive, i.e. ZrO₂ nano-particles and ZP were added to the Nafion/DMAc solution and stirred at room temperature for 2 hours, then ultrasonizing for 30 minutes. The resulting solution was poured onto a piece of flat glass, and placed into an oven at 80°C for 12 h to remove solvent, and finally heated up to 160 °C for 30 min. The membranes were then removed by peeling off from the glass plate. Before measuring the proton conductivity, all membranes were kept at deionized water for 12 h.

5.2.3. Characterization of the membranes

5.2.3.1. X-Ray Diffraction (*XRD*)

The procedure is the same as described in Chapter 4 (see page 67).

5.2.3.2. *Water uptake.*

The procedure is the same as described in Chapter 3 (see page 44).

5.2.3.3. *Methanol permeability measurements*

The procedure is the same as described in Chapter 3 (see page 46).

5.2.3.4. *Thermo-gravimetry analysis (TGA)*

The procedure is the same as described in Chapter 3 (see page 43).

5.2.3.5. *Proton conductivity*

The procedure is the same as described in Chapter 3 (see page 45).

5.2.3.6. *Morphology by SEM*

The procedure is the same as described in Chapter 4 (see page 68).

5.3. Results and discussion

5.3.1. Study by XRD

Figure 5.1 is the crystallogram of the ZrO_2 , ZP and Nafion/ZP composite membranes analyzed by X-ray diffractometry. From the X-ray diffraction pattern, they show very similar reflections. This shows that there is no crystalline change of mixing ZP within the membranes.

Although the crystalline structure of the ZP did not change even after phosphorizing ZrO_2 as described in chapter 4, the results of the FTIR evaluation (see chapter 4) prove that the chemical structure did change after phosphorization.

So, the new chemical structure could have formed on the surface layer of the ZrO_2 nano-particles. Therefore, because Nafion[®] is amorphous, all the X-ray diffraction patterns of Nafion/ZP will be displayed as ZrO_2 .

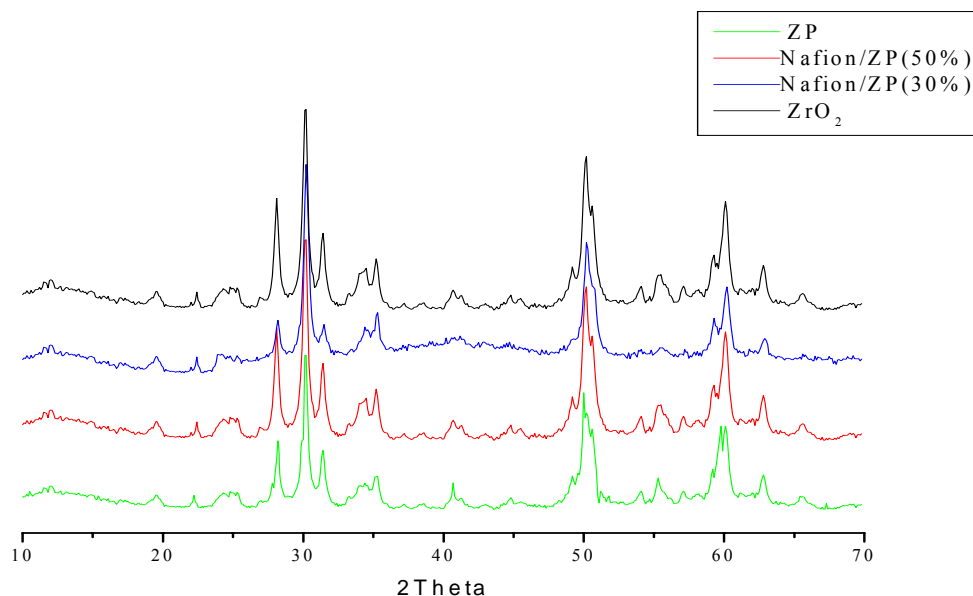


Figure 5.1: XRD patterns of ZrO₂ and various Nafion/ZP composite membranes

5.3.2. Scanning electron microscopy

The morphology of the composite Nafion/ZP membrane has been investigated by SEM. Micrographs of 30% ZP and 50% ZP of Nafion/ZP membranes are presented in Figure 5.2. The membrane containing 30% ZP shows that ZP particles are highly dispersed in Nafion[®] and no agglomeration was observed on the surface of the membrane. When the amount of ZP reaches 50%, some particulars appear in the micrographs picture and start to spread all over the surface. In the 70 % ZP Nafion/ZP membrane, many inorganic particles were observed.

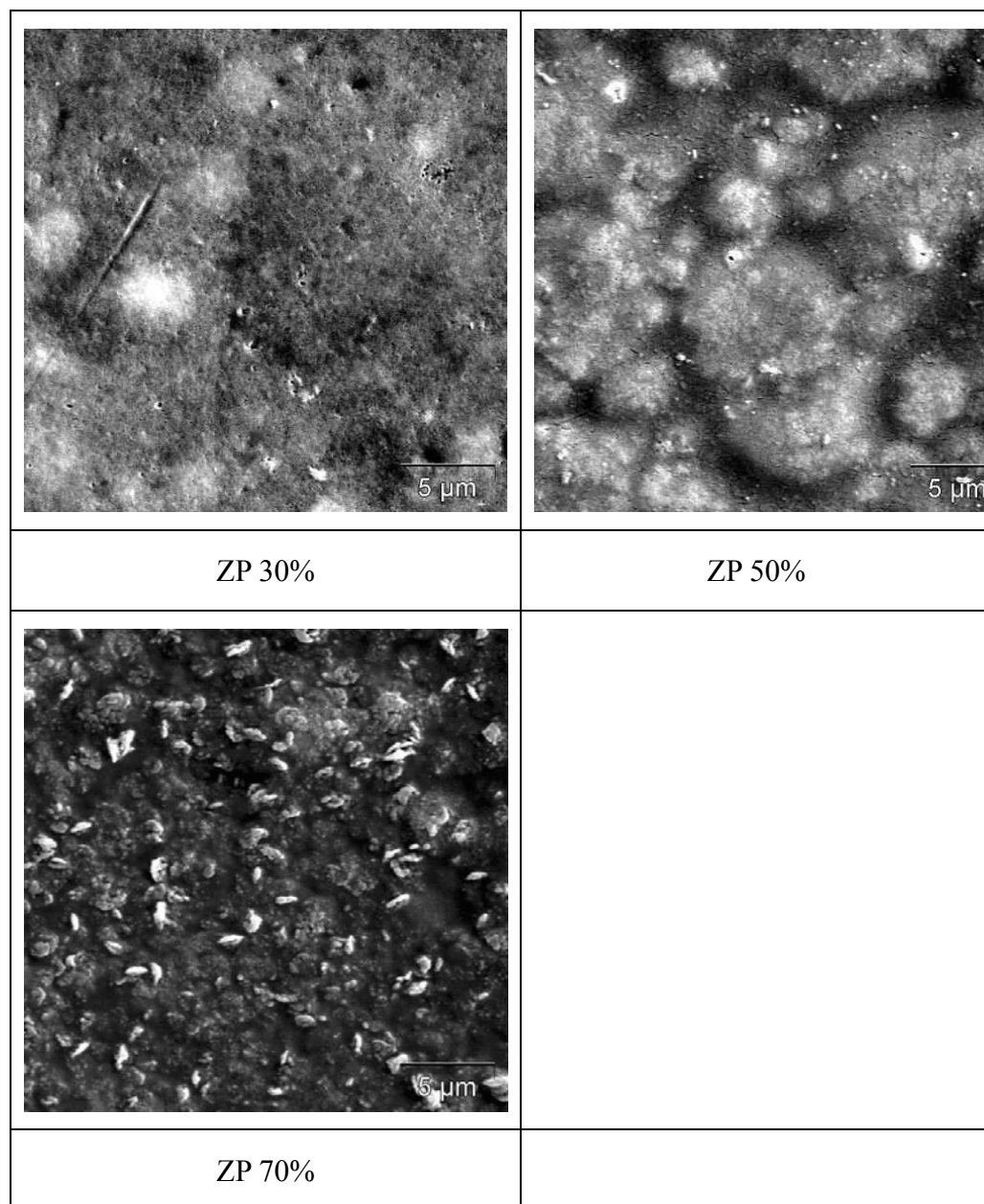


Figure 5.2: SEM of composite membranes

5.3.3. Water uptake

The water uptake for Nafion[®] and various Nafion/ZP composite membranes as a function of water temperature at 100% relative humidity, are presented in Figure 5.3. Compared to pure Nafion membrane, the water uptake is reduced in the composite membranes, especially in the high temperature range, and the water uptake reduces with increasing ZP in composite membranes over the range from 25 °C to 100 °C. The data suggests that the incorporated ZP can reduce the water uptake. One reason for the reduced water uptake is that the ZP nano-particles replace some of the water as pore fillers and the sorbed water appear only on the surface of the ZP nano-particles. Another reason might be that the incorporated ZP nano-particles by clustering in the pore of the physical strength of Nafion[®], contribute to increasing the physical strength of the structure. Since the incorporated ZP particles can still absorb water, water uptake will also increase with a rise in temperature.

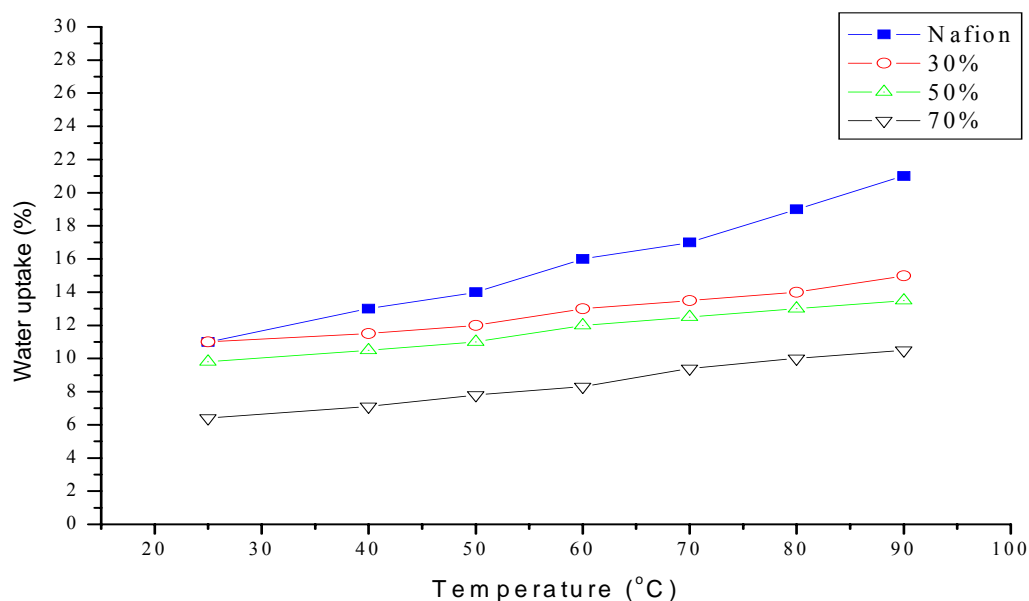


Figure 5.3: Water uptake of composite membranes as a function of temperature

5.3.4. Proton conductivity

All the membranes were immersed in deionized water for hydration before the conductivity measurement. The proton conductivity of Nafion/ZP membrane as a function of the ZP content in the membrane at room temperature and 100% relative humidity is presented in Figure 5.4. The conductivity increases with the amount of ZP and reaches a value of 0.029 S/cm for Nafion/ZP (70% ZP) membrane. This result shows that the ZP content can improve the proton conductivity effectively.

Comparing the water uptake results of Figure 5.3 with the corresponding proton

conductivity of Figure 5.4, the results accordantly prove that the incorporated ZP nano-particles improve the physical structure of the membrane, and reduce the water uptake of the membrane. As ZP is a surface conductor, ZP increases the proton conductivity of the membrane.

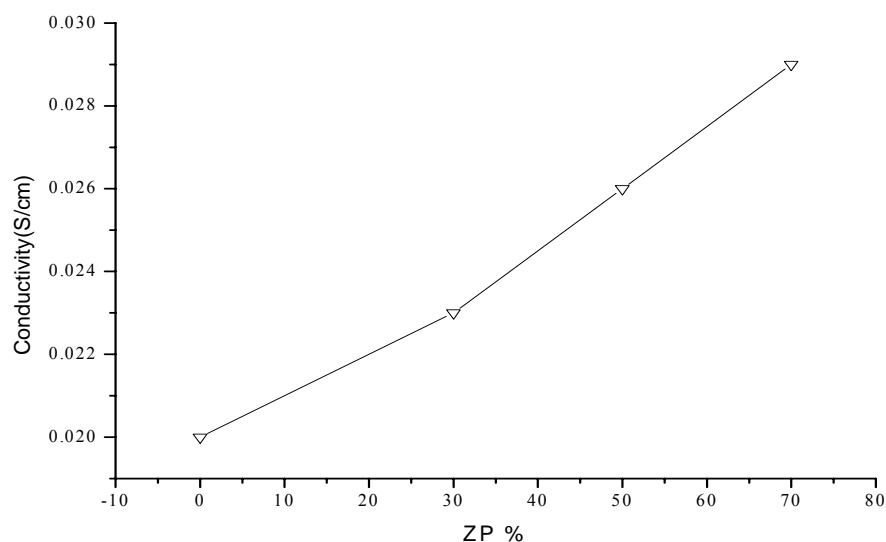


Figure 5.4: Conductivity of Nafion/ZP membranes at room temperature and 100% humidity

The conductivity of the Nafion[®] and Nafion/ZP composite membranes were measured at temperatures ranging from 20 °C to 120°C. The influence a proton conductivity of ZP content and temperature are presented in Figure 5.5. From this result, it can be seen that the incorporation of ZP increased the proton conductivity

compared to Nafion[®]. When the temperature is over 90 °C, the Nafion[®] quickly loses the conductivity due to dehydration. For all three Nafion/ZP composite membranes, the introduction of ZP into Nafion[®] matrices improves the stable conductivity at high temperature. It is natural that the proton conductivity is a thermally stimulated process and a rise with increasing temperature is expected. The conductivity of all membranes decreasing at high temperature is because dehydration of the membrane occurs. However, the rate of decreasing conductivity of composite membranes is much lower than that of Nafion[®]. The reason might be due to the good water retention of ZP in Nafion[®] at high temperatures (as shown in Figure 5.3).

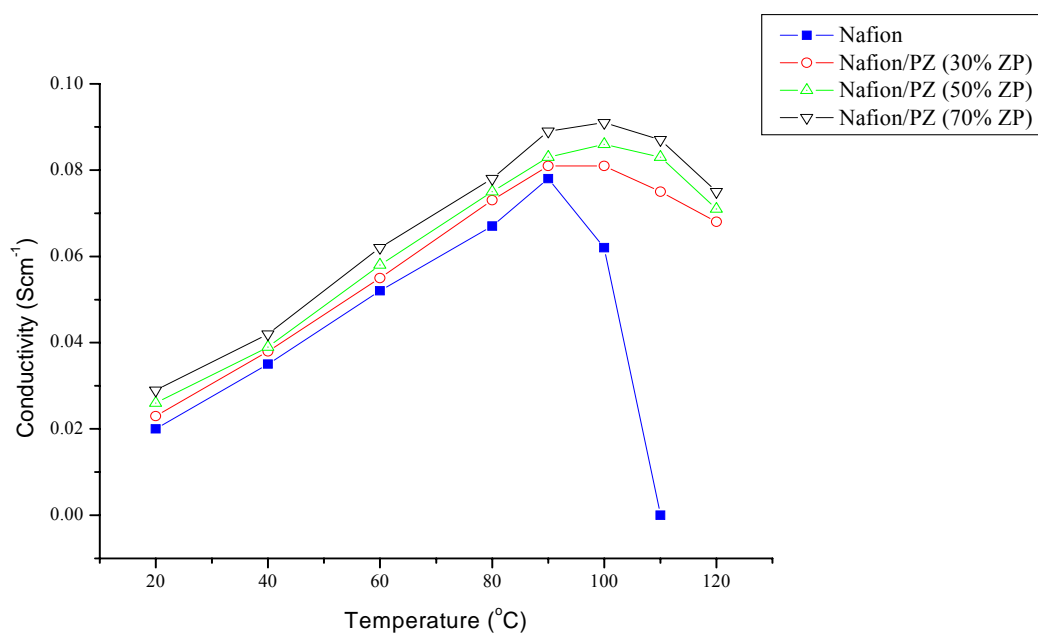


Figure 5.5:

Effect of different ZP content on the conductivity as a function of temperature

5.3.5. Methanol permeability

The permeability of methanol (1 M solution) through the Nafion/ZP composite membrane was investigated as a function of ZP weight content. The methanol permeability of pure Nafion[®] membrane is $1.4 \times 10^{-6} \text{ cm}^2/\text{S}$. For the composite membranes incorporating ZP the methanol permeability decreased to $8.3 \times 10^{-7} \text{ cm}^2/\text{S}$ in case of ZP 30 composite membrane. However, the methanol permeability that increased with increasing ZP content to a value of $1.7 \times 10^{-6} \text{ cm}^2/\text{S}$ for the Nafion/ZP (70 wt% ZP) membrane, which is higher than Nafion[®] (as shown in Figure 5.6). According to these results, incorporating small amounts of ZP into Nafion[®] can reduce the methanol permeability of the membrane. With small amounts of ZP introduced into the composite membrane, the nano-sized hydrophilic ZP particles very easily combine with Nafion[®]. A part of the channels in Nafion[®] will be filtered, blocked and narrowed by these nano-sized particles resulting in lower methanol permeability. From the SEM examination of the composite membrane, however, it is shown that the agglomeration of nano-sized ZP particles occurred in composite membranes with a high ZP content. As to the reason for a high methanol permeability, it is surmised that there isn't enough Nafion[®] as binder to bond all ZP nano-particles which result in the form a lot of channels within the membrane, and that these inorganic ZP channels lead to high permeability.

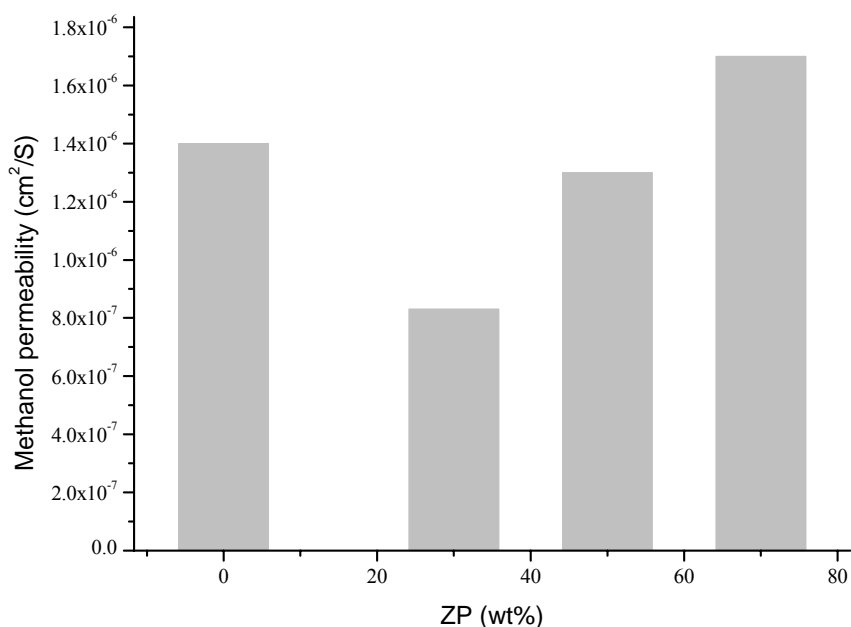
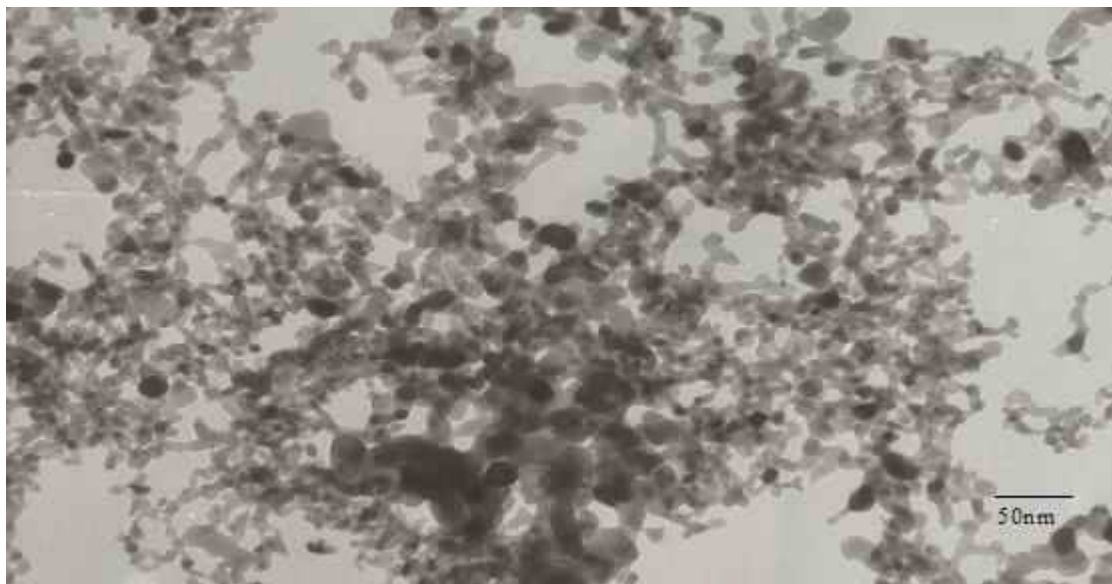


Figure 5.6: The methanol permeability of Nafion and Nafion/ZP composite membranes

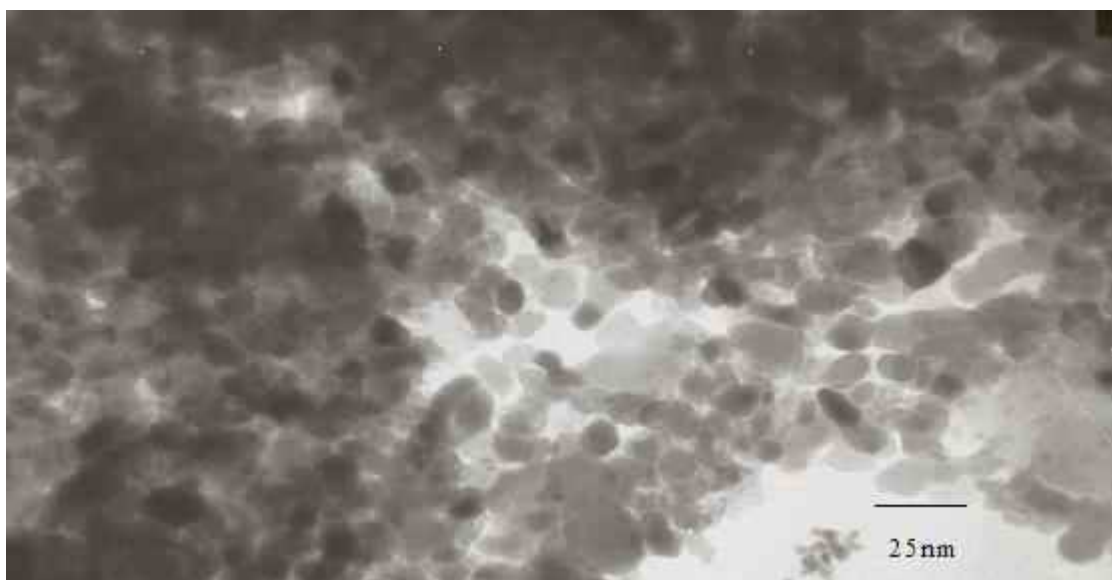
TEM of nano-sized ZrO_2 and ZP are presented in Figure 5.7. TEM of nano-sized ZrO_2 shows that the particle size of ZrO_2 is about 10 nm and the particle size distribution is uniform. The phosphorization did not change the bulk structure of nano-sized ZrO_2 particle because the XRD of nano-sized ZrO_2 and Nafion/ZP composite membrane shown the same structure. So the phosphorization blurs the boundary of particles due to zirconium phosphate form on the surface layer of ZrO_2 after phosphorization. The proton conductivity of Nafion/nano-sized ZrO_2 and Nafion/ZP (both of them containing 50% Nafion) was also measured, which were $1.2 \times 10^{-2} \text{ S/cm}$ and $2.6 \times 10^{-2} \text{ S/cm}$, respectively. The phosphorization results in an

enhancement in proton conductivity due to the surface structure being changed by phosphorization. Nafion/zirconium phosphate membrane (containing 50% Nafion[®]) was also prepared, and its measured proton conductivity is 1.8×10^{-2} S/cm, which is lower than the corresponding Nafion/ZP membrane. Compared to Nafion/zirconium phosphate membrane, the ZP possesses a high surface area due to the smaller particle size, and the phosphorization endows the ZP with hydrophilic sites, i.e. PO₄ groups on its surface. This is the reason why the proton conductivity of ZP is higher than that of Nafion/zirconium phosphate membrane. The high surface area of ZP and hydrophilic sites provide abundant vehicles for proton transport in the composite membrane.

The results show that the ZP is an excellent surface conducting inorganic material for improving the properties of the proton exchange membranes; it is an alternative conduction inorganic material compared with other references mentioned materials, like zirconium phosphates^[173–175] and phosphonates^[176]. It is suggested to be applied in further studies.



TEM analysis of ZrO_2 nano-particles before phosphorization



TEM results of ZrO_2 nano-particle after phosphorization

Figure 5.7: TEM of nano-sized ZrO_2 and ZP

5.4. Summary

In this chapter, a series of composite membranes have been prepared by incorporating ZP particles in Nafion[®]. These membranes exhibited a rather high conductivity of 2.9×10^{-2} S/cm at room temperature and reached a maximum 8.3×10^{-2} S/cm at 100 °C for Nafion/ZP(70%) membrane. The composite membrane incorporated a low amount of ZP showed lower methanol crossover compared to Nafion[®]. Additionally ZP increased the water retention of composite membranes resulting in an enhancement in conductivity at high temperature. The membranes are easy to prepare. Their high proton conductivity and low methanol cross over qualify composite membranes for consideration for use in DMFCs.

The Nafion/ZP composite membranes exhibit increased ability to maintaining proton conductivity above 90 °C. Considering this advantage, they can be used as candidate proton exchange membranes for the high temperature operation of the DMFCs.

CHAPTER 6

Conclusions and recommendations

6.1. Conclusions

In chapter 3 of this study, SPEEK membrane with DS ranging from 0.3 to 0.82 has shown conductivity values from 5.6×10^{-3} to 2.5×10^{-2} S/cm at room temperature. The conductivity of SPEEK membranes and the water uptake were increased with increasing DS. The methanol permeability of SPEEK membrane was also increased with increasing DS, but the highest was still 10 times lower than that of Nafion[®]. The extremely high water uptake of SPEEK membrane with high DS reduces the strength of the membranes, and the membranes become brittle when drying out. SPEEK with DS = 0.79 was chosen as the alternative material for synthesizing SPEEK/ZP composite membrane.

Chapter 4 presented a remarkable achievement in this study —the development of a new organic-inorganic SPEEK/ZP composite proton exchange membrane for DMFC application. A series of SPEEK/ZP composite membranes were prepared by incorporating ZP into the prepared SPEEK polymer with DS = 0.79. The ZP was synthesized by a phosphorization of nano-sized ZrO₂. The incorporated ZP increased the proton conductivity of the membranes. The SPEEK/ZP composite membranes with incorporate 40 wt% ZP content, reached 1.97×10^{-2} S cm⁻¹ proton conductivity at room temperature and maintained thermal and chemical stability. This proton

conductivity is comparable to that of Nafion[®] recast membrane. A study of the water uptake of the SPEEK/ZP composite membrane has shown reduced water uptake compared to that of pure SPEEK membrane at 80 °C. The methanol permeability of the membrane with a small mass of ZP content is reduced to 28.5% compared to that of the pure SPEEK membrane and 12 times lower than that of Nafion[®]. In a single-cell DMFC test, SPEEK/ZP composite membrane demonstrated promising performance.

Due to their low-cost, higher conductivity, suitable water uptake and low methanol permeability, SPEEK/ZP composite membranes are considered for use in DMFCs as alternatives to Nafion[®].

At last in chapter 5, a series of Nafion/ZP composite membranes were prepared by incorporating ZP in Nafion[®]. These membranes exhibited a rather high conductivity of 2.9×10^{-2} S/cm at room temperature and reached a maximum 9.1×10^{-2} S/cm at 100 °C for Nafion/ZP(70wt%) membrane. The composite membrane with low incorporated ZP content showed lower methanol permeability compared to Nafion[®]. Increased ZP content reduced the water retention, but enhanced the proton conductivity, especially at high temperature. The membranes are easy to prepare. Their high proton conductivity and maintained at high temperature, reduced methanol permeability compared to Nafion[®] qualify these composite membranes for consideration for use in DMFCs.

The most frequently used analytical methods to characterize membranes and basic

materials are TGA, SEM, FTIR etc. These methods provide information about the physical and chemical properties.

6.2. Recommendations

We need to improve the quality of the interface between the SPEEK/ZP composite membrane and the electrodes. The performance of the DMFC using prepared SPEEK/ZP composite membrane can be improved if this problem is solved. The development of more suitable electrodes and electrode-membrane assemblies is in progress.

There is a need to test the lifetime of the composite membranes in actual DMFC application. Further modification of the membranes via appropriate methods might be needed in order to enhance the stability and proton conductivity of the membrane.

REFERENCES

- [1]. <http://www.humboldt.edu/~serc/gifs/fuelcellani.gif>, 22 October (2003).
- [2]. Fraunhofer magazine special issue “Fuel cell-the versatile energy supply Feb, 2004.
- [3]. “Performance Modeling of Direct Methanol Fuel Cells”, Journal of the Electrochemical Society, 150(6):A811-A825, 2003.
- [4]. W.G. Grot, “Perfluorinated ion exchange polymers and their use in research and industry”, Macromolecules. Symposia 82 (1994) 161–172.
- [5]. S. Surampudi, S.R. Narayanan, E. Vamos, H. Frank, G. Halpert, A. LaConti, J. Kosek, G.K. Surya Prakash, G.A. Olah, “Advances in direct oxidation methanol fuel cells”, J. Power Sources 47 (1994) 377–385.
- [6]. A. Küver and W. Vielstich, J. Power Sources 74 (1998) 211-218.
- [7]. M.K. Ravikumar and A.K. Shukla, J. Electrochem. Soc. 143 (1996) 2601-2606.
- [8]. K. Scott, W.M. Taama, P. Argyropoulos, K. Sundmacher, J. Power Sources 83 (1999) 204-216.
- [9]. J. Cruickshank and K. Scott, J. Power Sources 70 (1998) 40-47.
- [10]. V.M. Barragán and A. Heinzl, J. Power Sources 104 (2002) 66-72.
- [11]. C. Pu, W. Huang, K.L. Ley, E.S. Smotkin, J. Electrochem. Soc. 142 (1995) L119-L120.
- [12]. President George Bush from the White House Lawn, February 25, 2002.
- [13]. E. Wakefield, “History of the electric Automobile, Battery-Only Powered Cars”, 1st ed. (1994), Society of Automobile Engineers, Inc., Warrendale, PA, USA, ISBN 1-56091-299-5.
- [14]. Zalbowitz, M., S. Thomas, “Fuel Cells: Green Power”, Department of Energy 1999. Appelby, A., Scientific American 1999, 74-79.
- [15]. A. Appleby, F. Foulkes, “Fuel Cell Handbook”, Van Nostrand Reinhold, New York, New York, USA (1989), 762 pages, ISBN 00-442-3126-6.
- [16]. “Fuel Cell Handbook, 5th Edition”, Report prepared by EG&G Services, Parsons, Inc. and Science Applications International Corporation under contract no. DE-AM26-99FT40575 for the U.S. Department of Energy, National Energy

- Technology Laboratory, October 2000.
- [17]. R.W. Glazebrook, *J. Power Sources* 7 (1982) 215-256.
- [18]. M.J. Schatter, in *Fuel Cells*, G.J. Young (Ed.), Vol. 2, Reinhold, New York, 1983, p. 290.
- [19]. D. Rastler, "Fuel Cells for a Distributed Power Market", presentation at the Seventh Grove Fuel Cell Symposium, 11 – 13 September 2001, London, UK.
- [20]. www.h2fuelcells.org/commentary1_3.html - 45k, 13 November (2003).
- [21]. Brown, A., *Chemical Engineering Progress*, 98(2), 2002,12-14.
- [22]. www.rmi.org/sitepages/pid556.php - 17k, 13 November (2003).
- [23]. www.nfrcr.uci.edu/fcresources/FCexplained/FC_Types.htm, 13 November (2003).
- [24]. James Burnham, "The Business of Fuel Cells", Issue 1 February 2002.
- [25]. Wolf Vielstich, "Electrochemical Energy Conversion – Methanol Fuel Cell as Example", *J. Braz. Chem. Soc.*, Vol. 14, No. 4, 2003, 503-509.
- [26]. U. Stimming, L. Carrette, K. Andreas Friedrich. "Fuel cells: Principles, types, fuels, and applications". *ChemPhysChem*, 1 (2002)162-193.
- [27]. L. Carrette, K.A. Friedrich, U. Stimming, "Fuel Cells" 1 (2001) 5-39.
- [28]. K.V. Kordesch and G.R. Simader, *Chem. Rev.* 95 (1995) 191-207.
- [29]. www.gkss.de/Einrichtung/Chemie/fuelcell/fuel_cell/dmfc.jpg 22 October (2003).
- [30]. www.voltaicpower.com/FuelCell/Types.htm - 8k, 13 November (2003).
- [31]. J.Larminie, A. Dicks, "Fuel Cell System Explained", Wiley, West Sussex, 2000.
- [32]. Stefan Geiger and David Jollie, "Fuel Cell Market Survey: Military Applications", *Fuel Cell Today*, 1 April (2004).
- [33]. R.J. Nichols and A. Bewick, *Electrochim. Acta* 33 (1988) 1691-1694.
- [34]. B. Bedan, F. Hahn, S. Juanto, C. Lamy, J.-M. Léger, *J. Electroanal. Chem.* 225 (1987) 215-225.
- [35]. T. Iwasita-Vielstich, in *Advances in Electrochemical Science and Engineering*, H. Gerischer, C.W. Tobias (Eds.), 1st edn., VCH, Weinheim, 1990, p. 127-170.
- [36]. M. Watanabe and S. Motoo, *J. Electroanal. Chem.* 60 (1975) 259-266.
- [37]. Dr. Ferdinand Panik, Daimler Chrysler Fuel Cell Project Head, Following

- Cross-Country Trek of Methanol-Fueled NECAR 5, June 4, 2002.
- [38]. L. Carrette, K.A. Friedrich and U. Stimming, "Fuel cells – Fundamentals and Applications", 1, 1, (2001), 5-39.
- [39]. Helen L. Maynard and Jeremy P. Meyers. Miniature fuel cells for portable power: Design considerations and challenges. *Journal of Vacuum Science & Technology B*, 20 2000,1287-1297.
- [40]. X Ren, M S Wilson, S.Gottesfeld, "High Performance Direct Methanol Polymer Electrolyte Fuel Cell". *J. Electrochem. Soc.*. 1996, 143: L 12-L15.
- [41]. Z. Poltarzewski, W. Wieczorek, J. Przulski and V. Antonucci, "Novel proton conducting composite electrolytes for application in methanol fuel cells", *Solid State Ionics* 119 (1999) 301-304.
- [42]. www.rmi.org/sitepages/pid556.php - 17k, 13 November (2003).
- [43]. S. F. Baxter, V.S. Battaglia and R.E. White, "Methanol Fuel Cell Anode", *Journal of the Electrochemical Society*, 146, 2, (1999), 437-447.
- [44]. A. Steck, C. Stone, in: O. Savadogo, P.R. Roberge (Eds.), *Proceedings of the 2nd International Symposium on New Materials for Fuel Cell and Modern Battery Systems, Development of BAM Membranes for Fuel Cell Applications*, Montreal, Canada, 6–10 July 1997, p. 792.
- [45]. A. Kuver, I. Vogel, W. Vielstich, "Distinct performance evaluation of a direct methanol fuel cell. A new method using a dynamic hydrogen reference electrode", *J. Power Sources* 52 (1994) 77.
- [46]. S.D. Mikhailenko, S.M.J. Zaidi, S. Kaliaguine, "Development of zeolite based proton conductive membranes for use in direct methanol fuel cells", Report submitted to Natural Resources Canada, Ottawa, 1997.
- [47]. J. Przulski, W. Wieczorek, S. Glowinkowski, "Novel proton polymer ionic conductors", *Electrochim. Acta* 37 (1992) 1733.
- [48]. J.T. Wang, S. Wasmus, R.F. Savinell, "Real-time mass spectrometric study of the methanol crossover in a direct methanol fuel cell", *J. Electrochem. Soc.* 143 (1996) 1233.
- [49]. A.J. Appleby, "Recent developments and application of the polymer fuel cell", *Philos. Trans. R. Soc. Lond.* A354 (1996) 1681.
- [50]. J. Jiang, A.Kucernak, "Electro-oxidation of Small Organic Molecules on Mesoporous Precious Metal Catalysts. Part 1: CO and Methanol on Platinum,

- Journal of Electroanalytical Chemistry, 533 (2002) 153 – 165.
- [51]. B.S. Pivovar, Y. Wang, E.L. Cussler, “Pervaporation membranes in direct methanol fuel cells”, *J. Membr. Sci.* 154 (1999) 155–162.
- [52]. M.P. Hogarth, G.A. Hards, “Direct methanol fuel cells, technological advances and further requirements”, *Platinum Met. Rev.* 40 (4) (1996) 150.
- [53]. S. Gunter and K. Kordesch. *Fuel Cells and their Application*. VCH, Weinheim, 1996.
- [54]. A. John Collins. “Development of Electrocatalyst Materials for Direct Methanol Fuel Cells Energy”, Marie Curie Fellowship Conference Profactor GmbH, Steyr, Austria, May (2001) 16 – 19.
- [55]. S. Slade, S.A. Campbell, et al, “Ionic Conductivity of an extracted Nafion 1100 EW series of membranes” *Journal of the Electrochemical Society*, 149, 12, (2002), A1556-A1564.
- [56]. M. Laporta, M. Pegoraro, and I. Zanderighi. “Perfluorosulfonated membrane (Nafion): FT-IR study of the state of water with increasing humidity.” *Physical Chemistry Chemical Physics* 1, (1999) 4619-4628.
- [57]. A. Weber, Z. and J. Newman. “Transport in polymer-electrolyte membranes.” *Journal of The Electrochemical Society* 150, (2003) A1008-A1015.
- [58]. Zawodzinski, T. A, Springer, T. E., Davey, J., Jestel, R., Lopez, C., Valerio, J. and S. Gottesfeld. “A Comparative Study of Water Uptake By and Transport Through Ionomeric Fuel Cell Membranes.” *Journal of The Electrochemical Society* 140, (1993) 1981- 1985.
- [59]. Tsou, Y.M., M. C. Kimble and R. E. White. “Hydrogen Diffusion, Solubility, and Water Uptake in Dow’s Short-Side-Chain Perfluorocarbon Membranes.” *Journal of The Electrochemical Society* 139, (1992) 1913.
- [60]. Inzelt, G., Pineri, M., Schultze, J. W. and M. A. Vorotyntsev. “Electron and proton conducting polymers: recent developments and prospects.” *Electrochimica Acta* 45, (2000) 2403-2421.
- [61]. Yoshida, N. Ishisaki, T., Watakabe, A. and M. Yoshitake. “Characterization of Flemion membranes for PEFC.” *Electrochimica Acta* 43, (1998) 3749–3754.
- [62]. X. D. Din, and E. E. Michaelides. “Transport of water and protons through micropores.” *AICHE Journal* 44, (1998) 35-47.
- [63]. j. Ding, Q. Tang and S. Holdcroft. “Morphologically Controlled Proton-

- Conducting Membranes Using Graft Polymers Possessing Block Copolymer Graft Chains.” *Australian Journal of Chemistry* 55, (2002) 461-466.
- [64]. M. Baldauf, W. Preidel, “Status of the development of direct methanol fuel cell”, *J. Power Sources* 84 (1999) 161.
- [65]. B. Tazi, O. Savadogo, “New cation exchange membranes based on Nafion, silicotungstic acid and thiophene”, *J. New Mater. Electrochem. Syst.*, submitted for publication.
- [66]. J.A. Kolde, B. Bahar, M.S. Wilson, T.A. Zawodzinski, S. Gottesfeld, in: S. Gottesfeld, G. Halpert, A. Landgrebe (Eds.), *Proceedings of the 1st International Symposium on Proton Conducting Membrane Fuel Cells, The Electrochemical Society Proceedings, Advanced Composite Polymer Electrolyte Fuel Cell Membranes*, Vol. 95-23, 1995, pp. 193–201.
- [67]. B. Bahar, A.R. Hobson, J.A. Kolde, D. Zuckerbrod, Ultra-thin integral composite membrane, US Patent 5,547,551 (1996).
- [68]. G.G. Scherer, Polymer membranes for fuel cells, *Ber. Bunsenges. Phys. Chem.* 94 (1990) 1008–1014.
- [69]. B. Gupta, F.N. Büchi, G.G. Scherer, Materials research aspects of organic solid proton conductors, *Solid State Ionics* 61 (1993) 213–218.
- [70]. F. Sundholm, New polymer electrolytes for low temperature fuel cells, in: *Proceedings of the 9th International Conference on Solid State Protonic Conductors SSPC’98, Extended Abstracts’ Book*, Bled, Slovenia, 17–21 August 1998, pp. 155–158.
- [71]. A. Steck, Membrane materials in fuel cells, in *Proceedings of the First International Symposium on New Materials for Fuel Cell Systems 1*, O.Savadogo, P.R. Roberge, T.N. Veziroglu (Eds.), Montréal, Quebec, Canada, July 9-13, 1995, p.74.
- [72]. J. Wei, C. Stone, A. Steck, US Patent 5,422,411 (1995).
- [73]. J. Wei, C. Stone, A.E. Steck, Trifluorostyrene and substituted trifluorostyrene copolymeric compositions and ion-exchange membranes formed therefrom, Ballard Power Systems, WO 95/08581, 30 March 1995.
- [74]. B.C. Johnson, I. Yilgor, C. Tran, M. Iqbal, J.P. Wightman, D.R. Llyod, J.E. McGrath, *J. Polym. Sci.* 22 (1984) 721-737.
- [75]. R. Nolte, K. Ledjeff, M. Bauer, R. Mülhaupt, Partially sulfonated poly (arylene

- ether sulfone) — a versatile proton conducting membrane material for modern energy conversion technologies, *J. Membr. Sci.* 83 (1993) 211–220.
- [76]. A. Nabe, E. Staude, G. Belfort, Surface modification of polysulfone ultrafiltration membranes and fouling by BSA solutions, *J. Membr. Sci.* 133 (1997) 57–72.
- [77]. C. Arnold, R.A. Assink, Development of sulfonated polysulfone membranes for redox flow batteries, *J. Membr. Sci.* 38 (1987) 71–83.
- [78]. G. Pozniak, M. Bryjak, W. Trochimczuk, Sulfonated polysulfone membranes with antifouling activity, *Die Angewandte Makromolekulare Chemie* 233 (1995) 23–31.
- [79]. J. Kerres, W. Cui, S. Reichle, New sulfonated engineering polymers via the metalation route. I. Sulfonated poly (ethersulfone) PSU Udel® via metalation–sulfination–oxidation, *J. Polym. Sci.: Part A: Polym. Chem.* 34 (1996) 2421–2438.
- [80]. W. Preidel, M. Baldauf, U. Gebhardt, J. Kerres, A. Ullrich, G. Eigenberger, in *Extended Abstract of the 3rd International Symposium on New Materials for Electrochemical Systems*, Montréal, Canada, 4-8 July, 1999, p. 233-234.
- [81]. J. Kerres, A. Ullrich, T. Häring, M. Baldauf, U. Gebhardt, W. Preidel, *J. New Mater. Electrochem. Systems* 3 (2000) 229-239.
- [82]. M. Walker, K.-M. Baurngdrtner, M. Kaiser, et al., *J. Appl. Polym. Sci.* 74 (1999) 67-73.
- [83]. L. Jörissen, J. Kerres, V. Gogel, A. Ullrich, Th. Häring, in *Proceedings of the 11th Annual Conference of the North American Membrane Society, NAMS2000*, Boulder, CO, USA, 23-27 May, 2000.
- [84]. J. Kerres, W. Zhang, L. Jorissen, V. Gogel, Application of different types of polyaryl-blend-membranes in DMFC, *J. New Mater. Electrochem. Syst.* 5 (2) (2002) 97–107.
- [85]. B. Bauer, D.J. Jones, J. Roziere, L. Tchicaya, G. Alberti, M. Casciola, L. Massinelli, A. Peraio, S. Besse, E. Ramunni, *J. New Mat. Electrochem. Sys.* 3 (2000) 93.
- [86]. S.M.J. Zaidi, S.D. Mikhailenko, G.P. Robertson, M.D. Guiver, S. Kaliaguine, Proton conducting composite membranes from polyether ether ketone and heteropolyacids for fuel cell applications, *J. Membr. Sci.* 173 (2000) 17–34.
- [87]. C.M. Burns, X. Feng, Sulfonation of poly(ether ether ketone) (PEEK): kinetic

- study and characterization, *J. Appl. Polym. Sci.* 82 (2001) 2651.
- [88]. Kreuer, K. D. "On the development of proton conducting materials for technological applications." *Solid State Ionics* 97, 1-15 (1997).
- [89]. C. Bailly, D.J. Williams, F.E. Krantz, W.J. Macknight, The sodium salts of sulfonated poly(aryl ether ether ketone) (PEEK): Preparation and characterization, *Polymer* 28 (1987) 1009.
- [90]. F. Helmer-Metzmann et al., EP 0 574 791 A2, Hoechst AG, 1993.
- [91]. G. Hubner and E. Roduner, *J. Mater. Chem.* 9 (1999) 409-418.
- [92]. K.D Kreuer, *J. Membr. Sci.* 185 (2001) 29-39.
- [93]. S. Sherman. US Patent 4, (1986) 595,708.
- [94]. S. Konagaya, M. Tokai, *J. Appl. Polym. Sci.* 76 (2000) 913.
- [95]. N. Gunduz, J.E. McFraith. *Poly. Preprints* 41 (2000) 182.
- [96]. Y. Woo, S.Y. Oh, Y.S. Kang, B. Jung, *J. Membr. Sci.* 220 (2003) 31.
- [97]. S. Faure, N. Cornet, G. Gebel, R. Mercier, M. Pineri, B. Sillion, in *Proceeding of the Second International Symposium on New Materials for Fuel Cell and Modern Battery Systems*, O. Savadogo, P.R. Roberge (Eds.), Montréal, Canada, July 6-10, 1997, p. 818.
- [98]. G. Gebel, P. Aldebert, M. Pineri, *Polymer* ,34 (1993) 333-339.
- [99]. E.J. Powers, G.A. Serad, History and development of polybenzimidazoles, in: R.B. Seymour, G.S. Kirschenbaum (Eds.), *High Performance Polymers: Their Origin and Development*, Elsevier, Amsterdam, 1986, p. 355.
- [100]. S.R. Samms, S. Wasmus, R.F. Savinell, Thermal stability of proton conducting acid doped polybenzimidazole in simulated fuel cell environments, *J. Electrochem. Soc.* 143 (1996) 1225.
- [101]. H. Vogel, C.S. Marvel, "Polybenzimidazoles, new thermally stable polymers", *J. Polym. Sci.* 50 (1961) 511.
- [102]. R. Bouchet, E. Siebert, "Proton conduction in acid doped polybenzimidazole", *Solid State Ionics* 118 (1999) 287.
- [103]. X. Glipa, M. El Haddad, D.J. Jones, J. Rozière, "Synthesis and characterisation of sulfonated polybenzimidazole: a highly conducting proton exchange polymer", *Solid State Ionics* 97(1997) 323.

- [104]. J.S. Wainright, R.F. Savinell, M.H. Litt, in Proceedings of the Second International Symposium on New Materials for Fuel Cell and Modern Battery Systems, O. Savadogo, P.R. Roberge (Eds.), Montréal, Canada, July 6-10, 1997, p. 808-817.
- [105]. B. Xing, O. Savadogo, The effect of acid doping on the conductivity of polybenzimidazole (PBI), *J. New. Mater. Electrochem. Syst.* 2 (1999) 95.
- [106]. J.T. Wang, R.F. Savinell, J. Wainright, M. Litt, H. Yu, *Electrochim. Acta* 41 (1996) 193-197.
- [107]. X. Glipa, B. Bonnet, B. Mula, D.J. Jones, J. Rozière, Investigation of the conduction properties of phosphoric and sulfuric acid doped polybenzimidazole, *J. Mater. Chem.* 9 (1999) 3045.
- [108]. M. Gieselman, J.R. Reynolds, Water-soluble polybenzimidazole-based polyelectrolytes, *Macromolecules* 25 (1992) 4832.
- [109]. B. Xing, O. Savadogo, Hydrogen/oxygen polymer electrolyte membrane fuel cells (PEMFCs) based on alkaline-doped polybenzimidazole (PBI), *Electrochem. Commun.* 2 (2000) 697.
- [110]. D. Hoel, E. Grunwald, "High protonic conduction of polybenzimidazole films", *J. Phys. Chem.* 81 (1977) 2135.
- [111]. S.M. Aharoni, M.H. Litt, "Synthesis and some properties of poly(2,5-trimethylenebenzimidazole) and poly(2,5-trimethylenebenzimidazole hydrochloride)", *J. Polym. Sci., Polym. Chem. Edn.* 12 (1974) 639.
- [112]. J.S. Wainright, J.-T. Wang, R.F. Savinell, M. Litt, H. Moaddel, C. Rogers, "Acid doped polybenzimidazoles, a new polymer electrolyte", *Proc. Electrochem. Soc.* 94 (1994) 255.
- [113]. J.S. Wainright, R.F. Savinell, M.H. Litt, "Acid doped polybenzimidazole as a polymer electrolyte for methanol fuel cells, in: O. Savadogo, P.R. Roberge (Eds.), Proceedings of the Second International Symposium on New Materials for Fuel Cells and Modern Battery Systems", Montreal, Canada, 6-10 July 1997, p. 808.
- [114]. P.M. Preston, D.M. Smith, G. Tennant, "Benzimidazoles and Congeneric Tricyclic Compounds," Part I, Wiley, New York, 1981.
- [115]. M.J. Sansone, N-substituted polybenzimidazole polymer, US Patent 4,898,917 (1990).
- [116]. C.A. Linkous, H.R. Anderson, R.W. Kopitzke, G.L. Nelson, "Development of

- new proton exchange membrane electrolytes for water electrolysis at higher temperatures”, *Int. J. Hydrogen Energy* 23 (1998) 525.
- [117]. J. Kerres, W. Cui, R. Disson, W. Neubrand, ‘Development and characterization of cross-linked ionomer membranes based upon sulfinated and sulfonated PSU. 1. Cross-linked PSU blend membranes by disproportionation of sulfinic acid groups”, *J. Membr. Sci.* 139 (1998) 211–225.
- [118]. J. Kerres, A. Ullrich, F. Meier, T. Häring, *Solid State Ionics* 125 (1999) 243-249.
- [119]. [132] L. Jörissen, V. Gogel, J. Kerres, J. Garche, *J. Power Sources* 105 (2002) 267-273.
- [120]. S.-P.S. Yen, S.R. Narayanan, G. Halpert, E. Graham, A.Yavrouian, US Patent 5,795,496 (1998).
- [121]. D.J. Jones and J. Rozière, *J. Membr. Sci.* 185 (2001) 41-58.
- [122]. B. Bonnet, D.J. Jones, J. Rozière, L. Tchicaya, G. Alberti, M. Casciola, L. Massinelli, D. Bauer, A. Peraio, E. Ramunni, *J. New Mater. Electrochem. Systems* 3 (2000) 87-92.
- [123]. S.R. Narayanan, A. Kindler, B. Jeffries-Nakamura, W. Chun, H. Frank, M. Smart, T.I. Valdez, S. Surampudi, G. Halpert, J. Kosek, C. Cropley, in *Proceedings of 11th Annual Battery Conference on Applications and Advances*, Long Beach, Calif., Jan. 9-12, 1996, p. 113-122.
- [124]. K.A. Mauritz, Organic–inorganic hybrid materials: perfluorinated ionomers as sol–gel polymerization templates for inorganic alkoxides, *Mater. Sci. Eng. C* 6 (1998) 121–133.
- [125]. K.A. Mauritz, I.D. Stefanithis, S.V. Davis, et al., “Microstructural evolution of a silicon oxide phase in a perfluorosulfonic acid ionomer by an in situ sol–gel reaction”, *J. Appl. Polym. Sci.* 55 (1995) 181–190.
- [126]. W. Apichatachutapan, R.B. Moore, K.A. Mauritz, “Asymmetric Nafion/(zirconium oxide) hybrid membranes via in situ sol–gel chemistry”, *J. Appl. Polym. Sci.* 62 (1996) 417–426.
- [127]. D.A. Siuzdak, K.A. Mauritz, Surlyn® [silicon oxide] hybrid materials. 2. Physical properties characterization, *J. Polym. Sci. Part B: Polym. Phys.* 37 (1999) 143–154.
- [128]. J. Ganthier-Luneau, A. Denoyelle, J.Y. Sanchez, C. Poinignon, “Organic–inorganic protonic polymer electrolytes as membrane for

- low-temperature fuel cell”, *Electrochim. Acta* 37 (1992) 1615.
- [129]. Kreuer, K. D. “On the development of proton conducting polymer membranes for hydrogen and methanol fuel cells.” *Journal of Membrane Science* 185, 29-39 (2000).
- [130]. Gierke, T. D., G. E. Munn and F. C. Wilson. “The morphology in Nafion Perfluorinated Membrane Products, as Determined by Wide- and Small-Angle X-Ray Studies.” *Journal of Polymer Science: Polymer Physics Edition* 19, 1687-1704 (1981).
- [131]. Gierke, T. D. and W. Y. Hsu. “Ion-Transport and Clustering in Nafion Perfluorinated Membranes.” *Journal of Membrane Science* 13, 307-326 (1983).
- [132]. Gierke, T. D. and W. Y. Hsu. “Elastic Theory for Ionic Clustering in Perfluorinated Ionomers.” *Macromolecules* 15, 101-105 (1982).
- [133]. Gierke, T. D., G. E. Munn and F. C. Wilson. “Morphology of Perfluorosulfonated Membrane Products.” *ACS Symposium Series* 180, 195-216 (1982).
- [134]. J. Bockris, S. Srinivasan, “Fuel Cells, Their Electrochemistry, 1st Ed.”, McGraw-Hill, New York, USA 1969, 659 pages.
- [135]. B. Lafitte, L.E. Karlsson, P. Jannasch, “Sulfophenylation of polysulfones for proton-conducting fuel cell membranes”, *Macromol. Rapid Commun.* 23 (2002) 896.
- [136]. M. Ulbricht, M. Riedel, U. Marx, Novel photochemical surface functionalization of polysulfone ultrafiltration membranes for covalent immobilization of biomolecules, *J. Membr. Sci.* 120 (1996) 239–259.
- [137]. .H. Fang, X.X. Guo, S. Harada, T. Watari, K. Tanaka, H. Kita, K. Okamoto, *Macromolecules* 35 (2002) 9022.
- [138]. C. Manea, M. Mulder, *J. Membr. Sci.* 206 (2002) 443 (Sp. Iss. SI).
- [139]. M. Rikukawa, K. Sanui, *Prog. Polym. Sci.* 25 (2000) 1463.
- [140]. K.D. Kreuer, *J. Membr. Sci.* 185 (2001) 29 (Sp. Iss. SI).
- [141]. S.M.J. Zaidi, S.D. Mikhailenko, G.P. Robertson, M.D. Guiver, S. Kaliaguine, *J. Membr. Sci.* 173 (2000) 17.
- [142]. B. Bauer, D.J. Jones, J. Roziere, L. Tchicaya, G. Alberti, M. Casciola, L. Massinelli, A. Peraio, S. Besse, E. Ramunni, *J. New Mat. Electrochem. Sys.* 3

- (2000) 93.
- [143]. S.P. Nunes, B. Ruffmann, E. Rikowski, S. Vetter, K. Richau, *J. Membr. Sci.* 203 (2002) 215.
- [144]. K.D. Kreuer, *Solid State Ionics* 97 (1997) 1.
- [145]. K.D. Kreuer, M. Ise, A. Fuchs, J. Maier, *J. Phys. IV* 10 (2000) 279.
- [146]. L. Li, Xu, Y.X. Wang, "Study on the preparation and properties of sulfonated polyether ether ketone membrane", *Acta Polym. Sin.* (3) (2003) 452.
- [147]. R. Y. M. Huang, P.H. Shao, C.M. Burns, X. Feng, "Sulfonation of Poly(ether ether ketone) (PEEK): kinetic study and characterization", *J. Appl. Polym. Sci.* 82 (2001) 2651.
- [148]. V. Tricoli, N. Carretta, M. Bartolozzi, "A comparative investigation of proton and methanol transport in fluorinated ionomeric membranes", *J. Electrochem. Soc.* 147 No4, (2000), 1286-1290.
- [149]. B. S. Pivovar, Y. Wang, E. L. Cusseler, "Pervaporation membranes in direct methanol fuel cells", *J. Membrane Science*, 154, (1999), 155-162.
- [150]. X. Jin, M.T. Bishop, T.S. Ellis, F.E. Karasz, "A sulphonated poly(aryl ether ether ketone)", *Br. Polym. J.* 17 (1985) 4.
- [151]. M.T. Bishop, F.E. Karasz, P.S. Russo, K.H. Langley, "Solubility and properties of a poly(aryl ether ketone) in strong acids", *Macromolecules* 18 (1985) 86.
- [152]. O. Nakamura, I. Ogino, "Electrical conductivities of some hydrates of dodecamolybdophosphoric acid and dodecatungstophosphoric acid and their mixed crystals", *Mater. Res. Bull.* 17 (1982) 231.
- [153]. D. Daoust, J. Devaux, P. Godard, A. Jonas, R. Legras, in: H. Kausch (Ed.), "Advanced Thermoplastic Composites—Characterization and Processing", Carl Hanser, Munich, 1992, Chapter 1.
- [154]. T. Ogawa, C.S. Marvel, "Polyaromatic ether-ketones ether-ketonesulfones having various hydrophilic groups", *J. Polym. Sci. A* 23 (1985) 1231.
- [155]. J. Devaux, D. Delimoy, D. Daoust, R. Legras, J.P. Mercier, C. Strazielle, E. Nield, "On the molecular weight determination of a poly(aryl ether ether ketone) (PEEK)", *Polymer* 26 (1985).
- [156]. D. Daoust, J. Devaux, P. Godard, "Mechanism kinetics of poly(ether ether ketone) (PEEK) sulfonation in concentrated sulfuric acid at room temperature. Part 1.

- Qualitative comparison between polymer and monomer model compound sulfonation”, *Polym. Int.* 50 (2001) 917.
- [157]. N. Shibuya, R.S. Porter, “A kinetic study of PEEK sulfonation in concentrated sulfuric acid by ultraviolet-visible spectroscopy”, *Polymer* 35 (1994) 3237.
- [158]. M.I. Litter, C.S. Marvel, *J. Polym. Sci., Polym. Chem. Edn.* 29 (1990) 239.
- [159]. A. Clearfield and J.A. Stynes, “The preparation of crystalline zirconium phosphate and some observations on its ion exchange behavior”, *Journal of Inorganic Nuclear Chemistry*, 26, (1994), 117-119.
- [160]. F. Helmer-Metamann, F. Osan, A. Schneller, H. Ritter, K. Ledjeff, R. Nolte, R. Thorwirth, US Patent 5 438 082 (1995).
- [161]. [164] Costamagna P, Yang C, Bocarsly AB, Srinivasan S. *Electrochim. Acta* 2002; 47: 1023.
- [162]. Yang C, Costamagna P, Srinivasan S, Benziger J, Bocarsly AB. *J. Power Sources* 2001; 103: 1.
- [163]. Grot WG, Rajendran G. US Patent 5,919,583 (1999).
- [164]. G. Vaivars, T. Mokrani, N. Hendricks and V. Linkov. “Inorganic Zirconium Phosphate Based PEM for Fuel Cells”. In: *Abstr. of NEFP Workshop on “New Materials and Technologies for Low Temperature Fuel Cells.”* 27-28 September, 2001. Helsinki.
- [165]. Nobanathi Wendy Maxakato “Preparation and characterization of inorganic proton conducting membranes based on zirconium phosphate for application in direct methanol fuel cell (DMFC)” Thesis (M. Sc. (Dept. of Chemistry, Faculty of Natural Science))--University of the Western Cape, 2003.
- [166]. A. Lewandowski, K. Skorapake, J. Malinska, *Solid State Ionics* 133 (2000) 265.
- [167]. P. Colomban, A. Novak, “Nature of the protonic species and the gel-crystal transition hydrated zirconium phosphate”, *Journal of Molecular Structure*, 198, (1989), 277-295.
- [168]. B. Bondars, G. Heidemane, J. Grabis, K. Laschke, H. Boyesen, J. Schneider, F. Frey, *J. Mater. Sci.* 30 (1995) 1621-1625.
- [169]. B.C.H. Steele, A. Hertz, *Materials for fuel-cell technologies*, *Nature* 414 (2001) 345.

- [170]. A.K. Shukla, P. A. Christensen, A. Hamnett, M. P. Hogarth, "A vapour-feed direct-methanol fuel cell with proton-exchange membrane electrolyte", *J. Power, Sources* 55 (1995) 87.
- [171]. P. Staiti, F. Lufrano, A.S. Arico, E. Passalacqua and V. Antonucci, "Sulfonated polybenzimidazole membranes-preparation and physico-chemical characterization". *J. Membrane Science* 188 (2001) 71.
- [172]. Lei Li, Li Xu and Yuxin Wang, "Novel proton conducting composite membranes for direct methanol fuel cell", *Materials Letters* 57(2003) 1406.
- [173]. Y.J. Liu, M.G. Kanatzidis, *Chem. Mater.* 7 (1995) 1525.
- [174]. D.J. Jones, R. Elmejjad, J. Roziere, *ACS Symp. Ser.* 499 (1992) 220.
- [175]. [T.C. Chang, W.Y. Shen, S.Y. Ho, *Microporous Mater.* 4 (1995) 335.
- [176]. G. Huan, A.J. Jacobson, J.W. Johnson, D.P. Goshorn, *Chem. Mater.* 4 (1992) 661.